481

19960207 141

NASA CR-120973

LMSC-D309742

DEVELOPMENT OF MANUFACTURING PROCESS FOR LARGE-DIAMETER COMPOSITE MONOFILAMENTS BY PYROLYSIS OF RESIN-IMPREGNATED CARBON-FIBER BUNDLES

by W. G. Bradshaw, P. C. Pinoli, and A. E. Vidoz

LOCKHEED PALO ALTO RESEARCH LABORATORY

prepared for

NATIONAL AERONAUTICS AND SPACE ADMINISTRATION

NASA Lewis Research Center

Contract NAS 3-15552

NASA CR-120973
LMSC-D309742

DEVELOPMENT OF MANUFACTURING PROCESS FOR LARGE-DIAMETER COMPOSITE MONOFILAMENTS BY PYROLYSIS OF RESIN-IMPREGNATED CARBON-FIBER BUNDLES

by W. G. Bradshaw, P. C. Pinoli, and A. E. Vidoz

LOCKHEED PALO ALTO RESEARCH LABORATORY

prepared for

NATIONAL AERONAUTICS AND SPACE ADMINISTRATION

NASA Lewis Research Center
Contract NAS 3-15552

ABSTRACT

Large-diameter carbon-carbon-composite monofilaments were produced from the pyrolysis of organic precursor resins reinforced with high-strength carbon fibers. The mechanical properties were measured before and after pyrolysis and the results were correlated with the properties of the constituents. The composite resulting from the combination of Thornel 75 and GW-173 resin precursor produced the highest tensile strength. The importance of matching strain-to-failure of fibers and matrix to obtain all the potential reinforcement of fibers is discussed. Methods are described to reduce, within the carbonaceous matrix, pyrolysis flaws which tend to reduce the composite strength. Preliminary studies are described which demonstrated the feasibility of fiber-matrix copyrolysis to alleviate matrix cracking and provide an improved matrix-fiber interfacial bonding.

TABLE OF CONTENTS

LIST OF ILLUSTRATIONS

Figure		Page

LIST OF TABLES

Section 1

SUMMARY

The objective of this program was to develop a process for producing large-diameter carbon composite monofilaments by impregnation of multifiber bundles with a suitable organic resin and converting the resulting composite to all carbon by pyrolysis. Seven commercially available carbon fibers and four thermosetting resins were selected for evaluation. The fibers were originated from rayon, polyacrylonitrile, and pitch precursors; the resins were phenol-formaldehyde, modified phenol-formaldehyde, and furfuryl alcohol.

All candidate fibers were exposed to pyrolysis gases evolved from each of the four candidate resins. Degradation of the fiber tensile strength upon gas exposure ranged from 2.4 to 42.5 percent, with the rayon based fibers exhibiting the highest resistance to attack.

The mechanical properties of the candidate matrices were measured on specimens prepared by casting and curing 3-mm-diameter rods subsequently pyrolyzed to monolithic carbon rod.

The highest candidate matrix tensile strength was obtained for the glass-like carbon derived from GW-173, $1.46 \times 10^8 N/m^2$ (2.13×10^4 psi). The material has a 0.41 percent strain-to-failure. An impregnation process consisting of the immersion of fibers in a 70 percent methanol-GW-173 solution was found to be the best method to coat the fiber bundles uniformly. The best carbon composite monofilament strength was obtained for the system Thornel 75– GW-173 ($1.34 \times 10^9 N/m^2 - 1.95 \times 10^5$ psi).

All composite monofilaments produced by pyrolysis of a carbon fiber embedded in organic resins were found to contain pyrolysis cracks and voids within the matrix which prevented full utilization of fiber strength.

Preliminary studies have demonstrated the feasibility of composite processing by co-pyrolysis. In this technique both fibers and matrix are pyrolyzed simultaneously. This fabrication method has produced composites with excellent fiber-matrix interface and no pyrolysis cracks.

Section 2

INTRODUCTION

The successful development of advanced air-breathing engines requires oxidation-resistant materials with higher specific modulus and strength than now available. This demand for new materials can be met by reinforcing oxidation-resistant alloys with stiff and strong filaments. The resulting composites will inherit the oxidation resistance or toughness of the matrix as well as the stiffness and strength of the reinforcement. From the standpoint of these specific mechanical properties as well as their retention at high temperatures, carbon and graphite fibers offer competitive or superior properties with respect to such reinforcing agents as boron or glasses (Figure 1).

The use of carbon or graphite fibers in metal matrices, however, has been limited by the rapid reactions that take place between the matrix metal and the very small (micro-size) carbon filaments during fabrication or service of the material. At the temperatures involved in the fabrication of these composites, the carbon filaments either react with the metallic constituents of the matrix to form carbides or are dissolved in the interaction (Refs. 1, 2). Diffusion barriers or protective coatings for the filaments are therefore necessary to limit or prevent these deleterious effects. However, to uniformly coat tows of such small filaments is a difficult process and, because of the extremely high surface area to be protected, will substantially increase the cross section of the filaments. This results in a decrease of the effective volume fraction of the reinforcement to levels that makes the composite of little or no advantage with respect to conventional materials.

Consequently, the approach of producing a large-diameter carbon-carbon composite monofilament has been suggested. A way to manufacture such a monofilament module is by impregnating high-strength, high-modulus carbon fiber bundles with suitable precursor resins and pyrolyzing the resultant product. These monofilament modules will have low surface area and should have low porosity. A reinforcement monofilament of such characteristics will be easier to protect by a diffusion barrier coating. Also, in the absence of such coatings, it will be less subject to degradation by the attack of the metallic matrix because of the smaller surface area exposed. The difficulties encountered in the manufacture of such a monofilament module have been failure to control fiber-matrix ratios, nonuniformity along the fiber length, matrix porosity, and an apparent degradation in the reinforcement tensile strength (Ref. 3).

To a great extent, nonuniformity and matrix porosity can be optimized by development of optimum prepregging, curing, and pyrolysis cycles. For example, rapidly cured thermosetting resin tends to promote the entrapment of volatiles and undoubtedly causes the formation of voids, cracks, and blisters (Ref. 4). Both curing and pyrolysis have to be carried out at low enough heat rates to permit the escape of volatiles and degradation gases without causing distortion or rupture of the residual carbon network (Refs. 5, 6, 7).

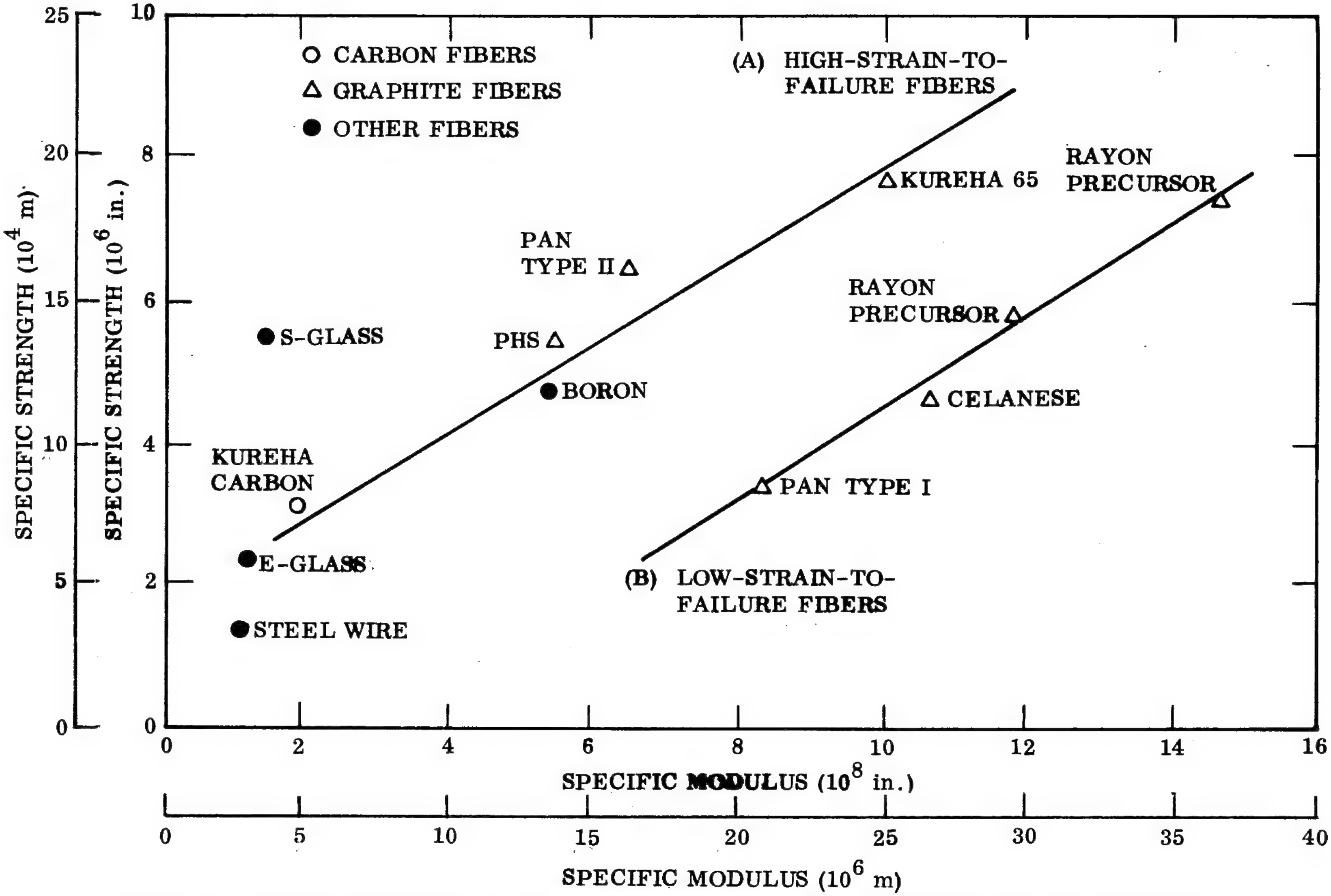

Figure 1. - Specific Strength as a Function of Specific Modulus of Various Fibrous Materials

Failure to achieve theoretical properties in the composite monofilament may be due to lack of adequate wetting during the prepregging phase, degradation of fiber properties by attack of pyrolysis gases, and a mismatch between the strain-to-failure of the fiber and matrix (Ref. 8). Wetting the fiber surface can be enhanced by appropriate prepregging techniques (Ref. 9). Possible degradation of the fiber properties by exposure to gases during pyrolysis must be known before the selection of the composite systems, since it may drastically reduce the reinforcing effect.

A critical factor in designing a carbon-carbon composite system (having both brittle matrix and fibers) is the matching of the strain-to-failure of the fiber and the matrix. Both fiber and matrix have to deform simultaneously under the influence of the applied stress. Failure of the composite will occur at the strain at which either fiber or matrix reaches its maximum attainable strain. Since the strain-to-failure of most pyrolyzed organic resins is less than 0.5 percent, to achieve maximum reinforcement efficiency only those fibers having high elastic modulus and similar low strain-to-failures should be employed with existent conventional precursor resins, such as phenol-formaldehydes or furfuryl alcohol (Refs. 10, 11).

The use of high strain-to-failure fibers should be restricted to more graphitizing resins or advanced precursor concepts that, upon pyrolysis, may yield higher strain-to-failures. Previous studies in our laboratory have shown that with these concepts it is possible to produce composite monofilaments with very high strength and modulus (Refs. 12, 13). These studies indicated excellent fiber strength retention in glassy carbon precursor resins after pyrolysis to 1273°K. Further advancement in monofilament properties can be expected with improvements in selection of fiber-matrix combinations and in fiber-surface treatments, and with refinement of fiber prepregging and pyrolysis methods (Refs. 14, 15, 16, 17).

The objective of the work described here was to develop a process for the manufacture of large-diameter high-strength, high-modulus, carbon-base monofilaments. The proposed approach was to use commercially available small-diameter carbon-base fiber bundles or tapes, impregnate them with suitable precursor resins, and pyrolyze them to produce a carbon-composite monofilament of low porosity and surface area. The monofilaments should have a surface of low porosity for ultimate use as a reinforcement of metal-matrix composites in air-breathing engines.

The ultimate goal was a composite monofilament, 0.05 to 0.25 mm (2 to 10 mils) in diameter, that is spoolable, with a tensile strength of $4.13 \times 10^9 N/m^2$ (600,000 psi) and an elastic modulus of $4.13 \times 10^{10} N/m^2$ (60×10^6 psi) or greater. However, since at present the tensile strength of commercial fibers is not much better than $2.06 \times 10^9 N/cm$ (300,000 psi), an interim objective was to demonstrate the feasibility of producing composite monofilaments with a strength of $1.36 \times 10^9 N/m^2$ (200,000 psi) and a modulus of 2.06 to $4.13 \times 10^{10} N/m^2$ (30 to 60×10^6 psi). Although a circular cross section was desirable, composite monofilaments of slightly different geometry were developed in this work in order to use state-of-the-art fiber configurations. Although the ultimate goal was to develop continuous spoolable monofilaments, it was anticipated that initial feasibility studies were to be carried out using fibers in batch studies. Consequently, initial lengths were as short as 23 to 35 mm (8 to 12 in).

The first stage of this program was the selection of compatible fiber/precursor matrix systems. This selection was carried out after a complete evaluation of the mechanical properties of candidate components. Fibers in the as-received condition and after exposure to pyrolysis gases, and specimens of precursor resins after pyrolysis, were tested. In addition, other characteristics of the pyrolyzed resins were determined which influence their interaction with fibers in the composite form.

Following a careful evaluation of these results, the systems to be tried were selected and composite monofilaments were fabricated and tested. During the final stages of the program an advanced concept for composite monofilament fabrication was evaluated. It consists of the copyrolysis of oxidized PAN fibers, heat-treated to several temperatures with a matrix composed of a modified phenol-formaldehyde precursor. In the following sections the procedures and results are presented and discussed.

Section 3

EXPERIMENTAL RESULTS

3.1 EXPERIMENTAL PROCEDURES

The aims of this program were: to evaluate available fibers and matrices, to utilize several processing techniques, to characterize the composite monofilaments. The experimental procedures for each of these tasks is discussed separately.

3.1.1 Matrices

Candidate matrix precursor resins were studied to determine strain-to-failure, char yield, dimensional change, ease of fabrication, and reaction by products evolved during pyrolysis. To accomplish this, 3-mm-diameter rods were prepared by casting the precursor resin into glass or tygon tubing. These rods were oven cured to 350° K and then removed, post-cured, and pyrolyzed in a slotted holder to prevent warpage. The heat treatment cycle consisted of: (1) a 1.7 to 2.6×10^5-sec (2- to 3-day) cure cycle to 350° K in air; (2) a 4.3×10^5-sec (5-day) post-cure cycle in vacuum from 350° K to 450° K; and (3) 6.0×10^5-sec (7-day) pyrolysis cycle to 1273°K. Measurements of diameter, length, and weight were made after the rods were processed to the as-cast condition and post-cured condition, and after pyrolysis to 1273°K. Char yield and volume changes were calculated from the formulas

$$\text{Char yield, \%} = \frac{W_2}{W_1} \times 100$$

$$\text{Volume change, \%} = \frac{V_1 - V_2}{V_1} \times 100$$

where

W_1 = initial resin weight
W_2 = weight of pyrolyzed resin
V_1 = volume in the initial condition (as cured)
V_2 = volume after pyrolysis

Density measurements were made per ASTM D-792 method A (water displacement).

The tensile strength and strain-to-failure were measured on the rod stock after pyrolysis to 1273°K. The rod stock specimens were epoxy-bonded to half-circle grooved steel end tabs to provide for uniform load transfer from grips to specimen. The end tabs were predrilled to accept a 3-mm (1/8-in.) diameter end pin for alignment. A gage length of 2.54×10^{-2} m (1 in.) was used, and tests were carried out at a cross-heat speed of 2.12×10^{-5} m/sec (0.05 in./min). Strain-to-failure measurements were made using a Wiedemann-Baldwin microformer extensometer. Spots of epoxy were placed on the specimen at each knife point to prevent specimen damage and ensure coupling of the extensometer to the specimen.

The decomposition of candidate resins during pyrolysis was analyzed by differential thermal analysis (DTA) and gas chromatography analysis (GCA). DTA thermograms were obtained on an R. L. Stone differential thermal analyzer. Samples were crushed and mixed to about 10 percent by weight in anhydrous alumina. The DTA was operated at a heating rate of 0.42° K/sec (25°C/min) from ambient to about 1173°K, with helium as the carrier gas. After each pyrolysis the run was repeated on the identical spent sample, and the baseline so obtained was used to find the location of the endotherms and exotherms.

Gas chromatography of the gaseous pyrolysis samples was performed on an FM Model 810 gas chromatograph in conjunction with an Infotronics digital readout system. CO, CO_2, and CH_4 were obtained with helium as carrier gas. CO and CH_4 were separated on a molecular sieve column at 373°K (100°C); the CO_2 was separated on a Porapak column. Hydrogen was separated on the molecular sieve column at 373°K (100°C) using nitrogen as carrier gas. Higher boiling constituents such as phenols were not identified separately, but were reported as residuals. The detection made was by thermal conductivity throughput.

3.1.2 Fibers

Candidate fibers were analyzed by determining the effect of exposure to pyrolysis gases evolved by candidate matrix resins, and by comparing fiber strain-to-failure with pyrolyzed matrix strain-to-failure. Candidate fibers and a slug of precursor matrix resin were inserted into graphite tubes fitted with tight end caps. A 1-mm-diameter hole was drilled through each end cap to prevent a pressure differential. Eight tubes were prepared in this manner and inserted into a large tube furnace having a hot zone 0.71 m (28 in.) long. Calibration and temperature profiling showed that at 1273°K (1000°C) the thermal gradients were less than ±13°K (13° C). This furnace was equipped with an automatic programmer controller power system with provisions for vacuum or inert gas operation, and was sufficiently large to accept all eight graphite tubes simultaneously. The cycle used simulated our anticipated pyrolysis cycle, which was a rough vacuum from room temperature to 653°K followed by a slow argon purge to 1273°K. The total pyrolysis cycle time was 2.6×10^5 sec (3 days).

Tensile testing of fibers before and after exposure to matrix pyrolysis gases was done in the following way. The carbon fiber rovings or tows were vacuum-impregnated with epoxy resin made from the following components:

- ERL 2472 — 100 parts
- Methyl nadic dianhydride — 90 parts
- Benzyl dimethylamine — 15 parts

The fiber bundles, 0.355 m (14 in.) long, were impregnated with the epoxy anhydride resin by immersing the bundle in the resin and subjecting the container to full vacuum. After the mixture was outgassed, the bundles were removed from the resin bath and oven-cured under tension for 720 sec at 394° K (121° C) and 720 sec at 450° K (177° C). For testing purposes, a tensile specimen 0.127 m (5 in.) long with an 0.0254-m (1-in.) gage length was prepared by epoxy-bonding the specimen to pin-loaded tab ends. The tests were carried out on an Instron Universal Test Machine at a cross-head speed of 2.12×10^{-5} m/sec (0.05 in./min).

3.1.3 Processing Techniques

Processing studies were conducted to obtain a uniform void-free coating of resin around each filament and bundle of carbon fibers. Techniques investigated were resin hot-melt, compression molding, vacuum impregnation, resistance fiber heating, and solvent addition to the resin.

3.1.4 Composite Monofilaments

Composite monofilaments were analyzed before and after pyrolysis to 1273°K to determine fiber and matrix cross-sectional area, tensile strength, and matrix continuity. Matrix and fiber cross-sectional area were determined in the following manner:

$$A_f = \frac{W_f}{\rho_f} \quad ; \quad A_m = \frac{W_c - W_f}{\rho_m}$$

where

A_f = cross-sectional area of fiber
A_m = cross-sectional area of matrix
W_f = weight per cm of fiber
W_c = weight per cm of composite
ρ_m = specific gravity of matrix

Cross-sectional area and matrix continuity were determined by optical and scanning electron microscopy (SEM). This latter technique was used also to characterize composite monofilament fracture surfaces.

Specific gravity of the bare fibers and matrix were determined on a Beckman air comparison pycnometer by helium displacement.

Specimen configuration and procedure for determining tensile strength were identical to the bare fiber tensile measurements for direct comparison of results; i.e., tests were carried out using steel end tabs and a gage length of 2.54×10^{-2} m(1 in.) and a cross-head speed of 2.12×10^{-5} m/sec (0.05 in./min). Tensile strength was calculated and reported in two ways – one based on fiber cross-sectional area only, and one based on total area.

3.2 MATERIALS SELECTION

The composite monofilament constituents were selected on the basis of compatibility of fibers and matrices. To ascertain this compatibility it was necessary to evaluate both matrices and fibers and to know how the interactions taking place during pyrolysis affected the properties of the constituents.

For the initial screening, nine potential resin candidates (Table I) were recommended as possible choices, but early in the screening program, candidate resin systems were rapidly narrowed to four. P-polyparaphenylene was eliminated because of its high cost and difficult processability. Polybenzimideazole was eliminated because of its difficult processability and because a subsequent study (Ref. 18) has shown that, even in the form of a drawn graphitic fiber, the strain-to-failure ranges from 0.25 to 0.37 percent. B-modified GW-173 was not evaluated because graphitization can be accomplished only by high-temperature heat treatment (> 2723°K). Since EC-201 and SC-1008 are both standard phenol-formaldehydes, it was decided to run screening tests on SC-1008, which is readily available commercially. Pitch-modified EC-201 was eliminated for the following reasons:

- The resin system contained so much volatile material that it could not successfully be processed to monolithic rods for the evaluation of char yield and strain-to-failure.
- A newly released study (Ref. 19) indicated that in carbon, with pitch as a matrix precursor, improvement in matrix strain-to-failure was not as great as anticipated. In uniaxial composites of VYB-70 in pitch, the strain-to-failure ranged from 0.07 to 0.13 percent in the as-pyrolyzed condition and from 0.10 to 0.40 percent in the graphitized condition. Improvement in properties was also dependent on the nature of the fiber and on the presence of discrete flaws such as voids.

TABLE I. - POTENTIAL RESIN CANDIDATE SYSTEMS

Candidate Resins	% Char Yield, 1273° K	Laminate Density, 1273° K	Reason for Choice
(1) GW-173[(a)]	62	–	Low volatiles content. Good results in preliminary feasibility study.
(2) A-2[(a)]	62	–	Low volatiles content. Nominally forms a high-strength form of glass-like carbon (Ref. 7).
(3) SC-1008	54.5	–	Reference: standard phenol-formaldehyde.
(4) EC-201	58.7	1.17	Reference: standard phenol-formaldehyde.
(5) Varcum (Furfuryl Alcohol)	61.15 (Ref. 4)	–	Low viscosity. Fast curing characteristics.
(6) Pitch modified EC-201	56–59.5	1.12–1.16	Development of selected graphitization and anisotropy in the matrix in pyrolyzed composites (Ref. 12).
(7) B-modified GW-173	–	1.12	Development of graphitization in matrix. Promotion of fiber-matrix bonding (Ref. 12).
(8) Polybenzimidazole (PBI)	74.5	1.11	High char yield, reportedly as high as 90%.
(9) P-Parapolyphenylene	81.0	1.04	High char yield. Tendency to cause graphitization of matrix (Ref. 12).

a - Modified phenol-formaldehydes which form glass-like carbons.

In an attempt to understand the matrix degradation process, thermogravimetric analysis (TGA), differential thermal analysis (DTA), and gas chromatograph analysis (GCA) were run on the four candidate matrix precursors.

DTA shows that with all specimens there is a pronounced endotherm between 473 and 673° K, which relates to bond breakage and vaporization of volatile species. All samples, except the Varcum, exhibit a pronounced secondary endotherm. Further studies on the temperature of water formation were designed to give insight into degradation phenomena.

Results of the GCA and TGA analysis are summarized in Table II. In all cases the volume fraction of H_2 and CH_4 increases with pyrolysis temperature and the volume fraction of CO_2 and phenols decreases with pyrolysis temperature. In general, such a distribution is in agreement with thermodynamic data. During pyrolysis, the four candidate matrix resins released different amounts of water vapor with the percent of water increasing in the following order: A-2 $<$ GW-173 $<$ SC-1008 $<$ Varcum.

A thermodynamic computer analysis was run to determine the effect of equilibrium composition of various gas compositions when they remain in contact with hot carbon. At lower temperatures, more methane, carbon dioxide, and water vapor would be expected from the Sabatier reaction. At higher temperatures the water-gas reaction dominates, and equilibrium conditions are such that CO and H_2 predominate as the gaseous species. A typical plot of the predominant species as a function of temperature is given in Figure 2 for a starting composition of 0% H_2, 25% CH_4, 25% CO_2, 25% CO, and 25% H_2O. Similar results are obtained when the starting compositions are varied as in Table III; that is, no matter what the starting composition, the predominant high-temperature species are CO and H_2 if equilibrium conditions are maintained.

The equilibrium mole fraction of solid carbon is given in Table III. Carbon fractions listed in parentheses are those in which the amount of carbon is increased, i.e., could be expected to deposit carbon. For example, when water vapor is absent (condition 5), equilibria are such that carbon would be deposited. However, in most cases where water vapor is present, carbon would be attacked.

Properties of the four candidate matrices surviving the complete screening analysis are summarized in Table IV and Figure 3. Of the four candidates, GW-173 has the best overall characteristics. It is listed as the first choice for matrix precursor because of its high char yield, low volume shrinkage, good strain-to-failure, and good processability.

The SC-1008 had a mix of good and bad characteristics; it showed excellent processing characteristics and a high char yield (65.1 ± 8.5 percent), but it varied, depending upon the method of solvent removal. The volume shrinkage was low (41.3 percent) and the strain-to-failure was good (0.36 to 0.44 percent), but the low density (1.20 to 1.33) confirms a large amount of porosity due to trapped solvent. Furfuryl alcohol (Varcum) also had a mixture of good and bad properties. Although it showed excellent processing characteristics, char yield was low (56.85 percent), volume shrinkage

TABLE II. - RESULTS OF THERMOGRAVIMETRIC AND GAS CHROMATOGRAPHIC ANALYSIS

Resin	Temperature		Vol % of Gaseous Products					Percent by Weight			
	°C	°K	H_2	CH4	CO_2	CO	Phenols	H_2O	Tar	Solid Residue	Estimated Gaseous Product
GW-173	400	673	0.12	6.16	9.3	36.0	48.4	–	–	–	–
	600	873	12.9	27.5	7.55	26.5	25.6	–	–	–	–
	800	1073	41.5	29.3	0.43	15.4	13.4	12.8	25	59.7	2.5
SC-1008	400	673	← No Gas Prod. →					–	–	–	–
	600	873	30.3	29.0	0.45	13.45	26.8	–	–	–	–
	800	1073	41.8	7.14	0.03	4.65	46.4	14.5	19.0	61.6	4.9
Varcum (Furfuryl Alcohol)	400	673	0.7	8.35	10.63	55.2	25.17				
	600	873	9.7	23.5	3.5	43.7	19.65				
	800	1073	30.7	9.7	5.8	11.0	42.85	16.6	37.8	41.7	3.9
A-2	400	673	2.34	2.12	15.8	32.6	47.14				
	600	873	18.35	35.5	4.28	21.0	21.0				
	800	1073	39.3	21.3	1.13	11.7	26.6	9.1	27.8	61.2	1.9

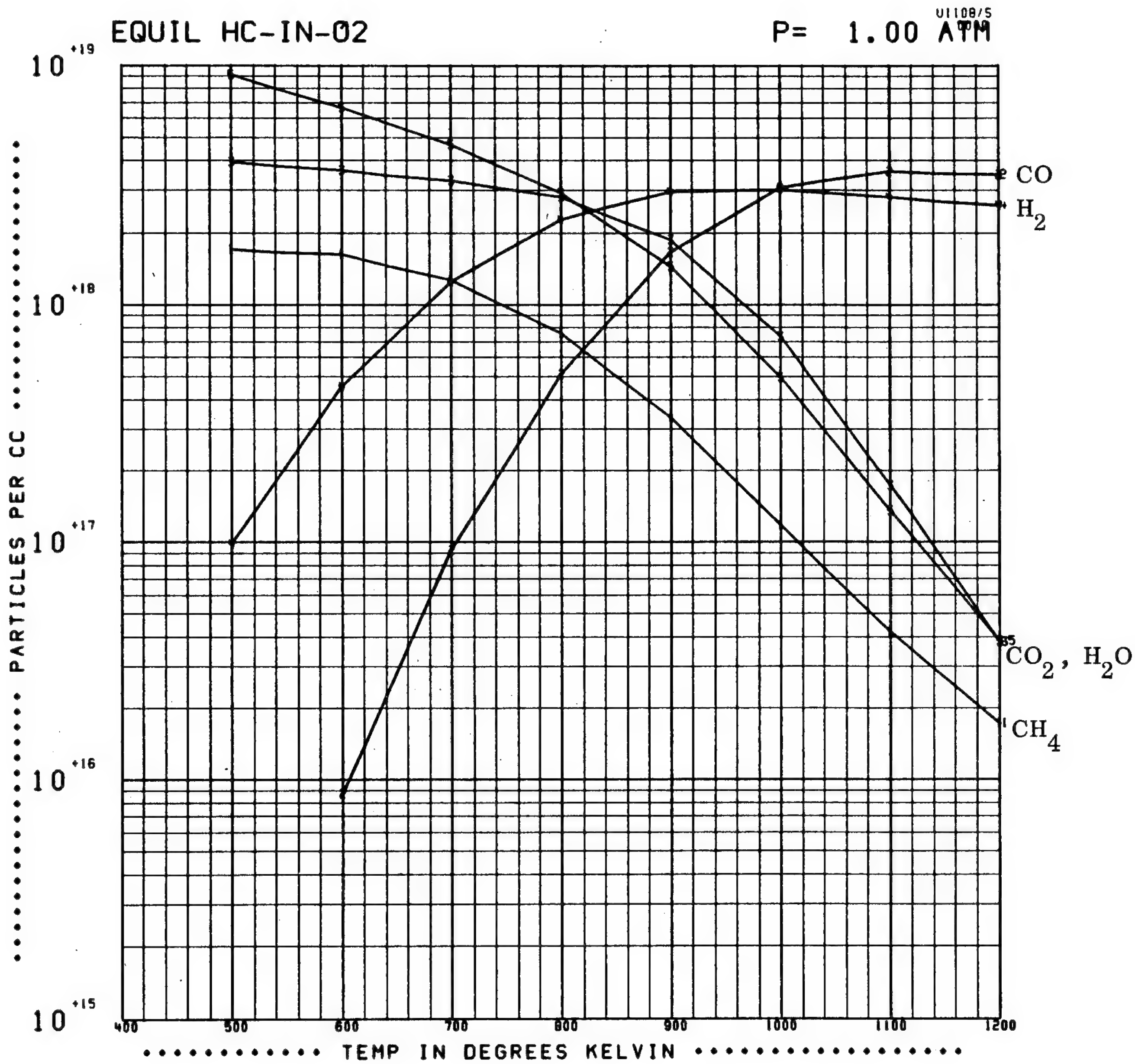

Figure 2. - Equilibrium Diagram of Interaction Between Carbon and Pyrolysis Species (Starting Composition: 0 Percent H_2, 25 Percent CH_4, 25 Percent CO_2, 25 Percent CO, 25 Percent H_2O)

TABLE III. - RESULTS OF EQUILIBRIUM STUDY

BASIS: 1 MOLE GAS } STARTING MIXTURE
2 MOLES SOLID CARBON

Case	Starting Gaseous Composition					Total Starting Atomic Fraction			Equilibrium Mole Fraction of Solid Carbon (°K)								
	H_2	CH_4	CO_2	CO	H_2O	H	C	O	Starting	500	600	700	800	900	1000	1100	1200
1	0	0.25	0.25	0.25	0.25	.284	.525	.191	.382	(.461)*	(.452)	(.446)	(.439)	(.417)	.376	.346	.337
2	0.25	0.25	0	0.25	0.25	.364	.455	.181	.400	.389	.380	.375	.370	.351	.312	.285	.277
3	0	0	0.50	0	0.50	.200	.500	.300	.400	.388	.382	.375	.363	.330	.269	.221	.206
4	0.5	0	0	0	0.50	.445	.445	.110	.445	.370	.366	.369	.375	.371	.352	.338	.335
5	0.5	0.25	0	0.25	0	.296	.665	.039	.422	(.607)	(.608)	(.614)	(.624)	(.630)	(.627)	(.625)	(.625)
6	0	0.50	0	0	0.50	.500	.417	.083	.333	.324	.325	.332	(.346)	(.351)	(.342)	(.334)	(.333)

*Carbon Deposition Indicated by Parenthesis

TABLE IV. - SUMMARY OF MATRIX PRECURSOR PROPERTIES AFTER PYROLYSIS TO 1273°K

Characteristic	Type of Resin			
	GW-173	SC-1008	Varcum (Furfuryl Alcohol)	A-2
Processability	Good	Excellent	Excellent	Poor
Char Yield From Post-Cure (450°K) to Pyrolysis (1273°K)	68.9[(a)] 66.9[(b)] 67.9 Av.	71.2[(a)] 59.0[(b)] 65.1 Av.	56.85	57.1
Percent Volume Change to 1273°K	42.5[(a)] 43.0[(b)] 42.75 Av.	– 41.3	52.3	51.5
Density (kg/m^3)	1.49	1.30[(a)] 1.33[(b)]	1.51	1.50
Tensile Strength				
$N/m^2 \times 10^7$	13.0 – 16.2	9.6 – 12.1	6.3 – 8.9	7.9 – 14.9
psi $\times 10^3$	18.9 – 23.7	14.0 – 17.6	9.1 – 12.8	11.5 – 21.6
Strain-to-Failure (percent)	0.36 – 0.49	0.36 – 0.44	0.24 – 0.29	0.25 – 0.44
	0.41 ± 0.06	0.26 ± 0.04	0.32 – 0.02	0.34 – 0.2
Elastic Modulus				
$N/m^2 \times 10^{10}$	3.3 – 4.1	3.2 – 3.4	2.7 – 2.75	3.2 – 3.7
psi $\times 10^6$	4.8 – 6.0	4.7 – 5.0	3.9 – 4.0	4.6 – 5.3

a- First test series.
b- Second test series.

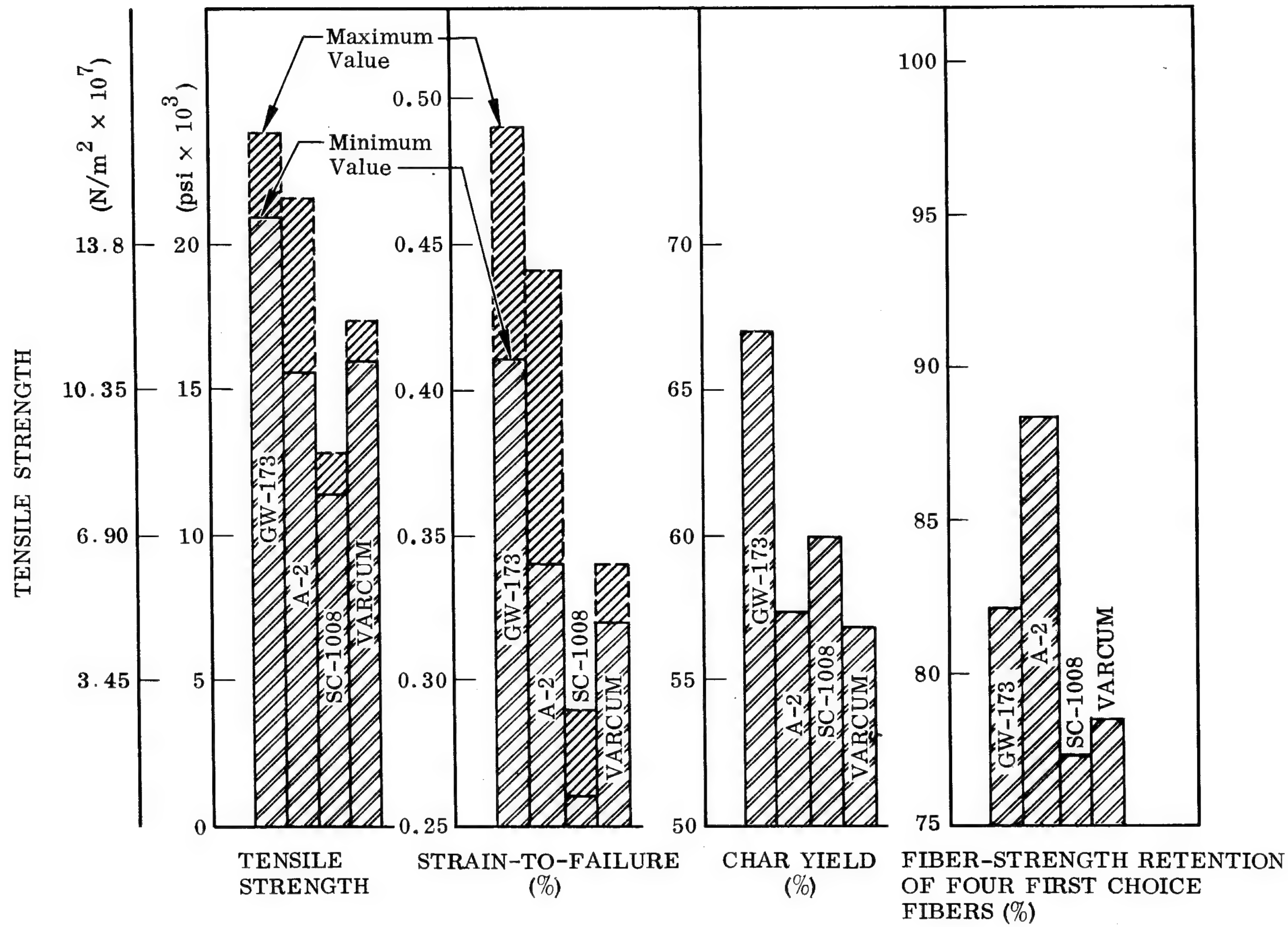

Figure 3. - Comparison of Matrix Properties Pyrolyzed to 1273°K (1000°C)

was high (52.3 percent), and its strain-to-failure was low (0.24 to 0.29 percent). SC-1008 was ranked better than furfuryl alcohol because of its higher char yield, lower volume shrinkage, and better strain-to-failure characteristics. A-2, an LMSC-developed resin, had poor processability, low char yield, (57.1 percent), high volume shrinkage (51.5 percent), and a high spread in mechanical properties. The strain-to-failure ranged from 0.25 to 0.44 percent.

3.3 FIBER SELECTION

For the initial screening it was decided to evaluate the 9 fibers described in Table V. The first two fibers Hitco 50 and Thornel 75, are produced from rayon fiber, have a crenulated cross section, and come as a two-ply yarn with relatively low degree of twist. Thornel 400 is oval in cross section and has a very slight twist to facilitate ease of handling. Most of the fibers generated from polyacrylonitrile are round in cross section and are available in the form of tows (Ref. 20). The FTIC fiber has the particular advantage of a small number of filaments per end; so these are available as small bundles. GY-70, produced from modified acrylonitrile, has an unusual dogbone cross-section shape. The Kureha fibers are generated from pitch, have a round cross section, and have a high degree of twist.

The criteria for fiber selection were the fiber tensile strength before and after exposure to matrix pyrolysis gases, and the fiber strain-to-failure. Tensile strengths of the fibers in the as-received condition and after exposure to pyrolysis gases from four resin-matrix candidates are summarized in Table VI, along with vendor (or nominal) tensile strength data. It can be seen that the as-received values are not necessarily those supplied by the vendor. This is particularly true of data obtained on the Celanese GY-70 and on the KGF-200 fibers. The low values obtained with the Celanese may be related to the fact that this was fairly old material. Also it was found by metallography (late in the test program) that these fibers were coated with a foreign substance, which microprobe analysis indicated was a compound rich in Zn and Cl_2.

The effect of pyrolysis gases on rayon-based fibers is summarized in Table VII. The glassy-carbon precursor resin, GW-173, appears to cause the least degradation (7.8 percent). For rayon-base fibers, the average degradation for all four types of matrices is 15.5 percent.

For fibers generated from PAN (Table VIII), the degradation is least severe with A-2 resin (13.7 percent); but the average degradation with all resins is 19.7 percent. For fibers generated from pitch, the lowest attack is from pyrolysis gases generated from Varcum (furfuryl alcohol) (Table IX). The average attack is about 16 percent.

The nominal strain-to-failure values also are shown comparatively in Figure 4. The fibers which most closely match matrix strain-to-failure characteristics of 0.3 to 0.6 percent are Hitco 50, Thornel 75, FTIC, Modmor I, GY-70, and KHF-40. The strain-to failure of Modmor II is slightly high, and that of Thornel 400 and KCF-200 is much too high.

TABLE V. – DESCRIPTION OF CANDIDATE FILAMENTS

Designation	Precursor	Fiber Cross Section		Form	Nominal No. of Filaments	Nominal Twist TPI	Nominal Density, gm/cm^3
		Shape	Measured Diameter, μ				
Hitco 50	Rayon	Crenulated	6.0	2-ply yarn	1440	1.5	1.72
Thornel 75	Rayon	Crenulated	5.4	2-ply yarn	1440	1.5	1.82
Thornel 400	Pan	Ovoid	8.35	1-ply yarn	1000	0.4	1.78
FTIC-2000	Pan	Round	7.0	Tow	2000	0	1.80
Modmor I	Pan	Round	7.65	Tow	10000	Nil	2.0
Modmor II	Pan	Round	8.2	Tow	10000	Nil	1.8
GY-70	Modified Pan	Dogbone	8.55	Tow	400	—	1.96
Kureha 200	Pitch	Round	12.3	3-ply yarn	—	7	1.6
Kureha 40	Pitch	Round	8.55	3-ply yarn	—	7	1.75

TABLE VI. - COMPARISON OF NINE FIBER CANDIDATES

Type of Fiber	Function[a]	Nominal		As-Received		After Exposure to Pyrolysis Gases							
						GW-173		A-2		Furfuryl Alcohol		SC-1008	
		psi × 10^5	$(N/m^2) \times 10^8$	psi × 10^5	$(N/m^2) \times 10^8$	psi × 10^5	$(N/m^2) \times 10^8$	psi × 10^5	$(N/m^2) \times 10^8$	psi × 10^5	$(N/m^2) \times 10^8$	psi × 10^5	$(N/m^2) \times 10^8$
Hitco 50	$\bar{x}$	3.10	21.4	3.13	21.6	3.10	20.4	2.77	19.1	2.71	18.7	2.69	18.55
	σ			0.39	2.7	0.24	2.8	0.23	1.6	0.25	1.7	0.20	1.4
	$\sigma/\sqrt{n}$			0.12	1.2	0.10	0.70	0.13	0.90	0.10	0.70	0.08	0.55
Thornel 75	$\bar{x}$	3.80	26.2	3.92	27.0	3.48	24.0	3.46	23.8	3.20	22.0	3.00	20.6
	σ			0.37	2.6	0.17	1.17	0.52	3.62	0.63	4.35	0.24	1.64
	$\sigma/\sqrt{n}$			0.13	0.90	0.07	0.48	0.07	1.63	0.26	1.77	0.10	0.67
Thornel 400	$\bar{x}$	4.25	29.3	4.25	28.6	4.15	28.6	3.92	27.0	3.87	26.7	3.89	26.8
	σ			0.28	1.93	0.48	3.3	0.25	1.7	0.28	1.9	0.56	3.9
	$\sigma/\sqrt{n}$			0.12	0.83	0.20	1.4	0.10	0.7	0.13	1.2	0.23	1.6
Modmor I	$\bar{x}$	2.75	19.0	2.89	19.9	2.41	16.6	2.35	16.2	2.11	14.5	2.15	14.8
	σ			0.18	1.2	0.54	3.7	0.14	1.0	0.84	3.7	0.58	4.0
	$\sigma/\sqrt{n}$			0.08	0.6	0.22	1.5	0.06	0.4	0.24	1.7	0.26	1.8
Modmor II	$\bar{x}$	3.0	20.7	3.73	25.7	3.52	24.3	3.34	23.0	3.10	21.4	3.07	21.2
	σ			0.57	3.9	0.45	3.1	0.39	2.6	0.39	2.7	0.51	3.5
	$\sigma/\sqrt{n}$			0.25	1.7	0.18	1.2	1.5	1.0	0.16	1.1	0.21	1.4
FTIC-2000	$\bar{x}$	3.40	23.4	3.51	24.2	2.18	15.0	3.19	22.0	2.49	17.2	2.51	17.3
	σ			0.45	3.1	0.62	4.3	0.28	1.9	0.50	3.4	0.25	1.7
	$\sigma/\sqrt{n}$			0.18	1.2	0.25	1.7	0.12	0.8	0.20	1.4	0.10	0.7
GY-70	$\bar{x}$	3.10	21.4	2.22	15.3	1.95	13.4	1.79	12.3	1.82	12.5	1.93	13.3
	σ			0.20	1.4	0.12	0.8	0.19	1.32	0.45	3.12	0.47	2.29
	$\sigma/\sqrt{n}$			0.08	0.6	0.05	0.3	0.08	0.54	0.18	1.28	0.14	0.95
KGF-200	$\bar{x}$	1.50	10.3	1.04	7.17	1.01	6.96	0.94	6.48	1.06	7.31	0.96	6.62
	σ			0.05	0.34	0.10	0.70	0.09	0.62	0.13	0.90	0.10	0.70
	$\sigma/\sqrt{n}$			0.02	0.14	0.04	0.28	0.04	0.28	0.05	0.34	0.04	0.28
KHF-40	$\bar{x}$	2.25	15.5	2.24	15.4	1.42	9.78	1.69	11.6	1.70	11.7	1.66	11.4
	σ			0.16	1.1	0.41	4.08	0.20	1.38	0.25	1.72	0.33	2.3
	$\sigma/\sqrt{n}$			0.07	0.5	0.24	1.66	0.09	0.61	0.11	0.77	0.15	1.02

a - $\bar{x}$ = average. σ = standard deviation. $\sigma/\sqrt{n}$ = standard error = standard deviation/$\sqrt{\text{number of tests}}$.

TABLE VII. - EFFECT OF MATRIX PYROLYSIS GASES ON RAYON-BASED FIBERS

Matrix / Fiber	% Reduction in Tensile Strength After Exposure, T → 1273°K						
	GW-173	A-2	Varcum	SC-1008	Range	Avg[(a)]	Avg[(b)]
Thornel 25	11.5	–	18.9	25.6	11.5–25.6	18.7 ± 7.0	18.7 ± 7.0
Hitco 50	0.9	11.6	13.4	13.9	0.9–13.9	9.95 ± 5.9	9.4 ± 7.4
Thornel 75	11.1	11.9	18.5	23.7	11.1–18.5	17.8 ± 6.3	17.8 ± 6.3
Avg	7.8	11.75	16.9	21.1	0.9–25.6	15.5 ± 4.8	15.3 ± 5.1
σ	6.1	2.1	2.5	6.3			

a - All candidate matrix precursors.

b - Average of GW-173, Varcum, and SC-1008 only.

TABLE VIII. - EFFECT OF MATRIX PYROLYSIS GASES ON PAN-BASED FIBERS

Matrix / Fiber	% Reduction in Tensile Strength After Exposure, T → 1273°K						
	GW-173	A-2	Varcum	SC-1008	Range	Avg[a]	Avg[b]
Thornel 400	2.4	7.85	9.25	6.15	2.4 - 9.25	6.4	5.9
FTIC-2000	42.5	9.1	29.0	28.5	9.1 - 42.5	27.3	33.3
FTIC-3000	41.5	27.1	30.4	21.8	21.8 - 41.5	30.2	31.2
Modmor I	16.6	18.6	27.2	25.6	16.6 - 27.2	22.0	23.1
Modmor II	6.2	10.1	16.7	17.5	6.2 - 17.5	12.6	13.5
GY-70	19.6	12.3	18.3	13.1	12.3 - 19.6	17.0	17.0
Avg	21.8	13.7	22.5	19.9	2.4 - 42.5	19.7	20.7
σ	16.5	7.3	8.0	8.4		7.7	10.6

a - All candidate matrix precursors.

b - GW-173, Varcum, and SC-1008 only.

TABLE IX. - EFFECT OF MATRIX PYROLYSIS GASES ON PITCH-TYPE FIBERS

Matrix / Fiber	% Reduction in Tensile Strength After Exposure, T → 1273°K						
	GW-173	A-2	Varcum	SC-1008	Range	Avg[(a)]	Avg[(b)]
KCF-100	Neg.	Neg.	Neg.	Neg.	Neg.	Neg.	Neg.
KGF-200	2.65	18.9	Neg.	7.55	2.65 - 18.9	7.3	5.1
KHF-40	36.4	18.2	17.5	26.0	17.5 - 36.4	24.5	26.6
Avg	19.5	18.5	5.8	16.8	0 - 36.4	15.9	15.8

a - All candidate matrix precursors.

b - Avg of GW-173, Varcum, and SC-1008 only.

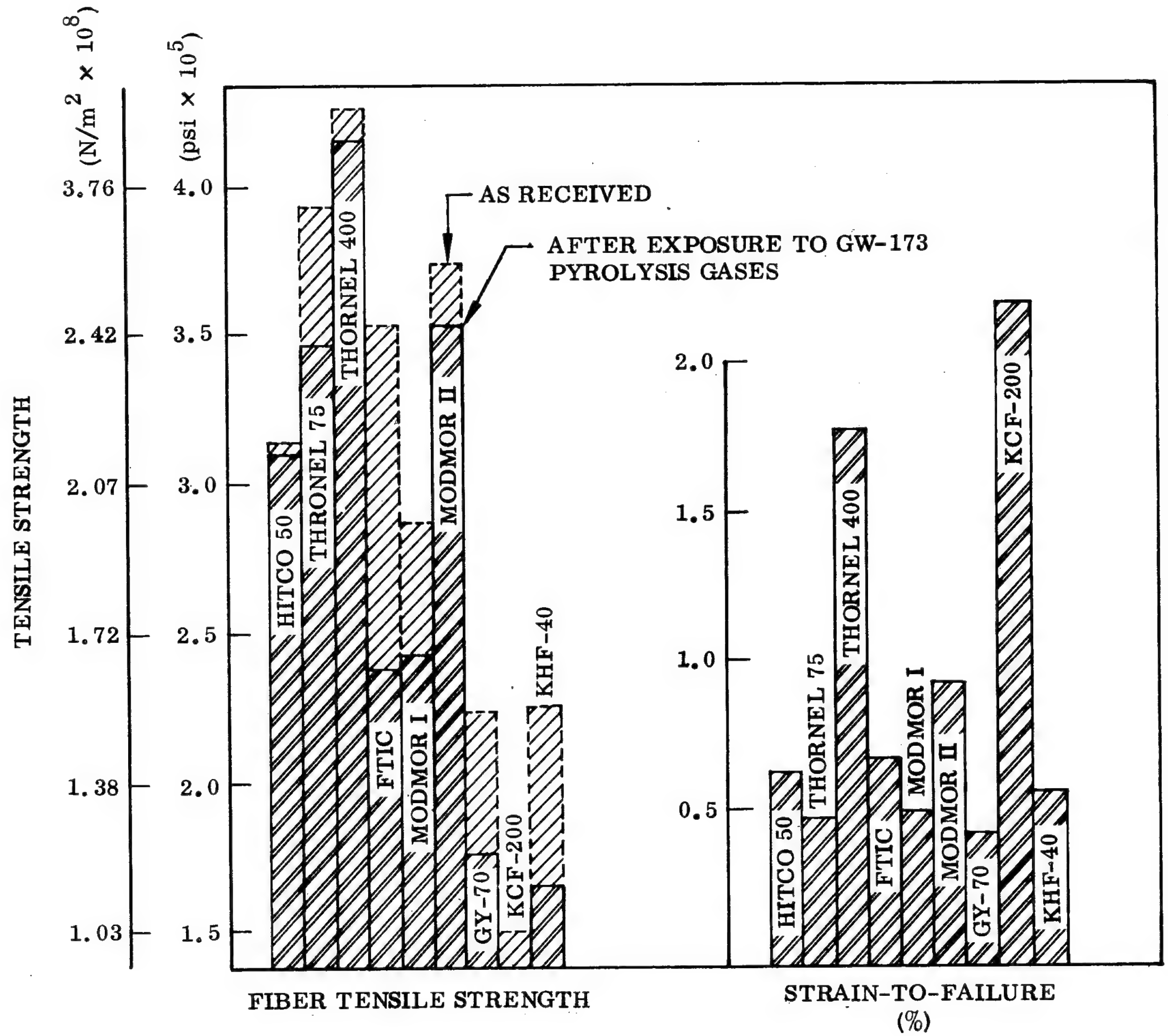

Figure 4. - Comparison of Nine Fiber Candidates

Ranking of individual fiber types along with other properties is summarized in Table X. Tensile strengths and reductions in strength values were determined in this test series; tensile modulus and strain-to-failure are quoted from vendor data. The three most critical properties are fiber tensile strength before and after exposure to pyrolysis gases, and fiber strain-to-failure. Fiber tensile strength should be at least $1.62 \times 10^9 N/m^2$ (250×10^5 psi) and the strain-to-failure should be about 0.5 percent to match matrix characteristics.

Thornel 75 was rated first because of its high tensile strength even after exposure to GW-173, coupled with a strain-to-failure that matches that of the pyrolyzed matrix. Hitco 50 was rated second, having slightly lower tensile strength and modulus, together with a higher strain-to-failure. Kureha 500, with a reported tensile strength of 3.44×10^9 N/m^2 (5×10^5 psi) and a strain-to-failure of 0.5 percent appeared most promising but had to be dropped because of its unavailability. The other pitch-base fibers, KGF-200 and KHF-40, showed little promise because of their low tensile strength, particularly after exposure to pyrolysis gases. Fibers generated from PAN or modified PAN show less promise than those generated from rayon. On the basis of available data, Modmor I and FTIC-2000 show the most promise for PAN-based fibers although Mormor I is marginal in tensile strength, after exposure to pyrolysis gases.

As a result of these tests, seven fibers were selected for further evaluation and screening by impregnation with the best matrix precursor resins – GW-173 and SC-1008 – and furfuryl alcohol, followed by pyrolysis and monofilament evaluation. Those selected are the two rayon-base fibers (Thornel 75 and Hitco 50) and the PAN based fibers (FTIC-2000 and Modmor I). Modmor II and Thornel 400 were included as typical fibers for testing the hypothesis that the maximum tensile properties cannot be utilized with a fiber having a strain-to-failure greater than that of the matrix. Kureha KHF-40 was considered marginal; KGF-200 was eliminated from further testing; and GY-70 was suggested for further evaluation only because a newer batch might have better properties. Kureha 500 was eliminated because of its unavailability.

3.4 IMPREGNATION OPTIMIZATION STUDIES

The objective of this study was to produce fiber/resin matrix composite monofilaments with minimum matrix volume fraction contingent with a void-free and uniform matrix. Preliminary screening of the three candidate matrix precursor resins indicated that Varcum (furfuryl alcohol) was an acceptable pregging resin, and that SC-1008 with the addition of 25-percent methanol (by volume) produced an acceptable composite. The relatively high viscosity of GW-173 (200 poise), however, prevented complete wetting of the fiber bundle and produced composites with excessive matrix content. Four methods were evaluated to analyze the general problems associated with all resin systems and develop a method which would produce specimens with GW-173 resin for direct comparison with the other two candidate resins.

The methods evaluated were; matched die molding, resistance heated hot melt, continuous process, and batch process.

TABLE X. - SUMMARY OF FIBER SELECTION CRITERIA

Type of Fiber	Tensile Strength[(a)]		Strain-to-Failure, percent	Reduction in Strength, percent	Elastic Modulus[(b)]	Precursor	Rating
	As-Received	After Exposure to Pyrolysis Gases					
Hitco 50	21.6 (3.13)	21.4 – 18.5 (3.10 – 2.69)	0.62	0.9 – 13.9	34 (50)	Rayon	2
Thornel 75	27.0 (3.92)	24.0 (3.48)	0.5	11.1 – 18.5	54 (79)	Rayon	1
Thornel 400	29.3 (4.25)	28.6 – 26.8 (4.15 – 3.87)	1.42	2.4 – 9.25	21 (30)	PAN	6
Modmor I	19.9 (2.89)	16.6 – 14.5 (2.41 – 2.11)	0.50	16.6 – 27.2	34 – 41 (50 – 60)	PAN	3
Modmor II	25.7 (3.73)	24.3 – 21.2 (3.52 – 3.07)	0.93	6.2 – 17.5	24 – 28 (35 – 40)	PAN	5
FTIC-2000	24.2 (3.51)	22.0–17.3 (3.19–2.51	0.66	9.1 – 42.5	34 – 38 (50 – 55)	Modified PAN	4
Kureha 500	34.5 (5.0)	31.0, est. (4.5, est.)	0.5	10.0 est.	70 (100)	Pitch	7
GY-70	15.3 (2.22)	13.4 (1.95)	0.42	12.2 – 19.6	52 (75)	Modified PAN	9
KGF-200	7.17 (1.04)	7.31 – 6.96 (1.06 – 0.94)	1.5	2.65 – 18.9	–	Pitch	10
KHF-40	15.4 (2.24)	–	0.56	17.5 – 36.4	28 (40)	Pitch	8

a - The first value or set of values listed is in (newtons/meter^2) $\times 10^8$; the values in parentheses are in psi $\times 10^5$.

b - The first value or set of values listed is in (newtons/meter^2) $\times 10^{10}$; the values in parentheses are in psi $\times 10^6$.

3.4.1 Matched-Die Molding Process

In this process, 0.61-m (24 in.) lengths of carbon yarn were impregnated horizontally in a trough containing 70-percent GW-173 in methyl ethyl ketone and were dried vertically under tension for 5.8×10^5 sec (16 hr) at room temperature and for 3,600 sec (1 hr) at 344° K (160° F). The impregnated yarns were then placed in a matched-die mold and cured for 1.08×10^4 sec (3 hr) at 367° K (200° F) and for 3.6×10^3 sec (1 hr) each at 380° K (225° F), 303° K (250° F), 408° K (275° F), 422° K (300° F), 436° K (325° F), and 453° K (350° F). The resultant yarn composites were examined by optical microscopy and were found resin-rich and poor in resin distribution (Fig. 5). Fiber-matrix wetting appeared good except for isolated regions. It appeared that the mold was oversize. Nevertheless, even if the groove size were correct, it is apparent that uniform resin distribution is achievable only in length but not in cross section. Both HMG 50 and Thornel 75 gave similar results.

3.4.2 Resistance-Heated Hot Melt

This technique consisted of resistance-heating the fiber while it was immersed in GW-173 resin, without added solvent. The objective of this study was to eliminate beading and voids caused by the entrapment of excess volatiles in the fiber bundle and to improve fiber-matrix bonding by causing the development of the resin cure to proceed from the fiber-matrix interface. In this process, the precursor resin was heated sufficiently (approximately to 317°K) to lower the viscosity to 20 ns/m^2. Alligator clamps were attached to each end of a 0.23-m-long fiber bundle. Voltage to the bundle was controlled through a 115-V Variac and monitored by a voltage test meter. For large bundles such as Modmor I, 3 to 6 V were applied, and for small bundles such as Thornel 75, 15 to 23 V were applied. The bundles were immersed in the resin and resistance-heated for 180 sec, then removed and held in a vertical position for 60 sec to allow excess resin to flow off. The temperature of resin on the fiber bundle was not allowed to exceed 350° K. Final cure was the standard procedure of 7.2×10^3 sec (2 hr) at 350° K and 7.2×10^3 sec at 450°K.

This technique produced good infiltration; however, the high resin viscosity prevented sufficient resin run-off prior to cure. The addition of solvent to the resin reduced the viscosity but the solvent volatilized during fiber heating producing a foamy matrix. This technique, in conjunction with the continuous process, would be worthy of consideration for a high-production process; for this program, however, the reduction to practice was considered to cost too much time and effort.

3.4.3 Continuous Impregnation

Figure 6 describes the technique employed to prepreg candidate fibers with GW-173 matrix resin. The line speed was controlled by a variable-speed motor driving the take-up spool. Constant fiber tension was maintained by a magnetic brake on the feed spool. Table XI summarized experimental results with HMG-50 to optimize processing conditions and compares results with Thornel 75-S. An optimum line speed of 17×10^{-4}m/sec (4 in./min) yielded prepregged monofilament with no resin beads.

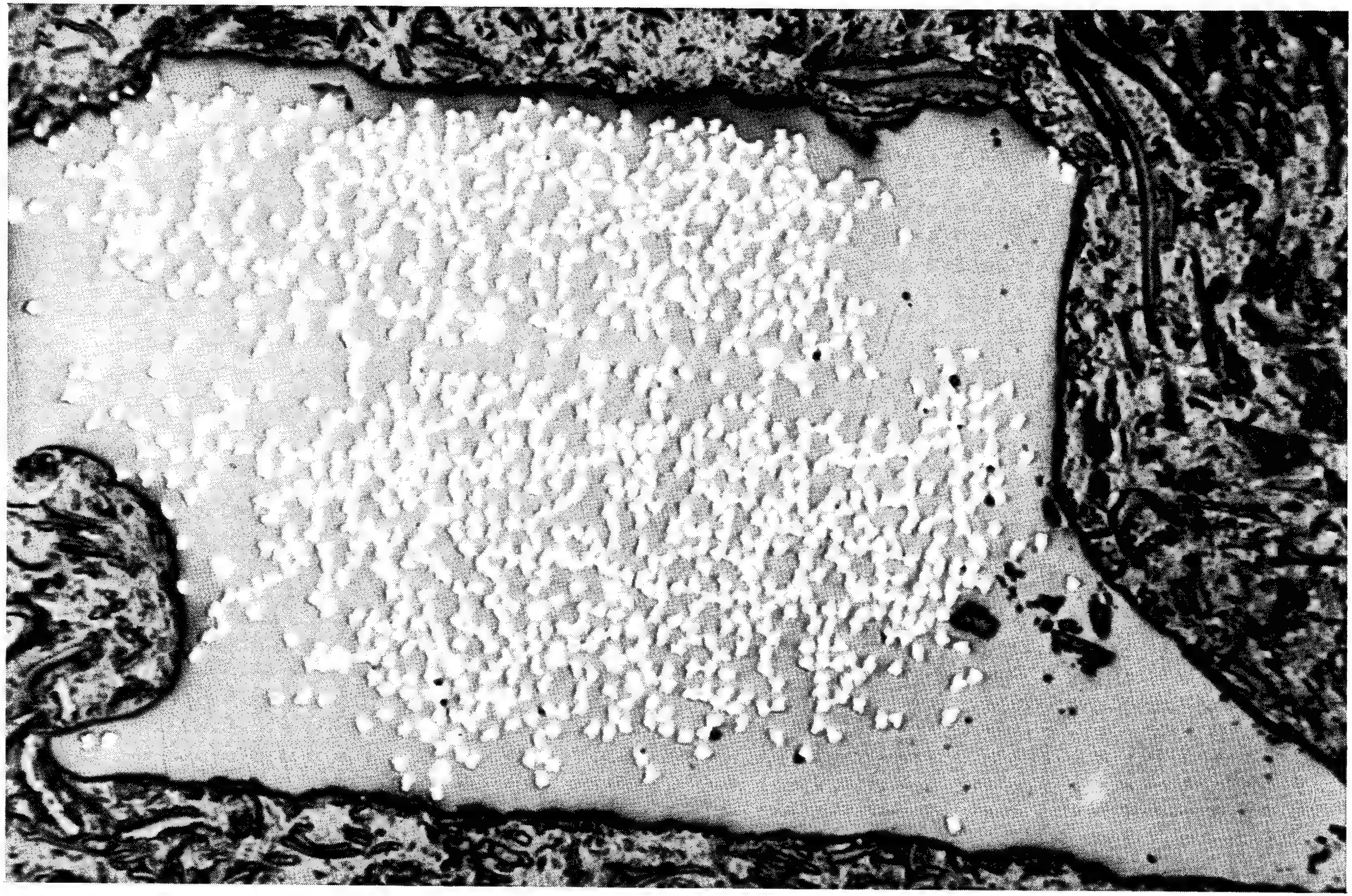

Figure 5. - Cross Section of Hitco 50 Prepregged Monofilament, Produced by Matched-Die Molding

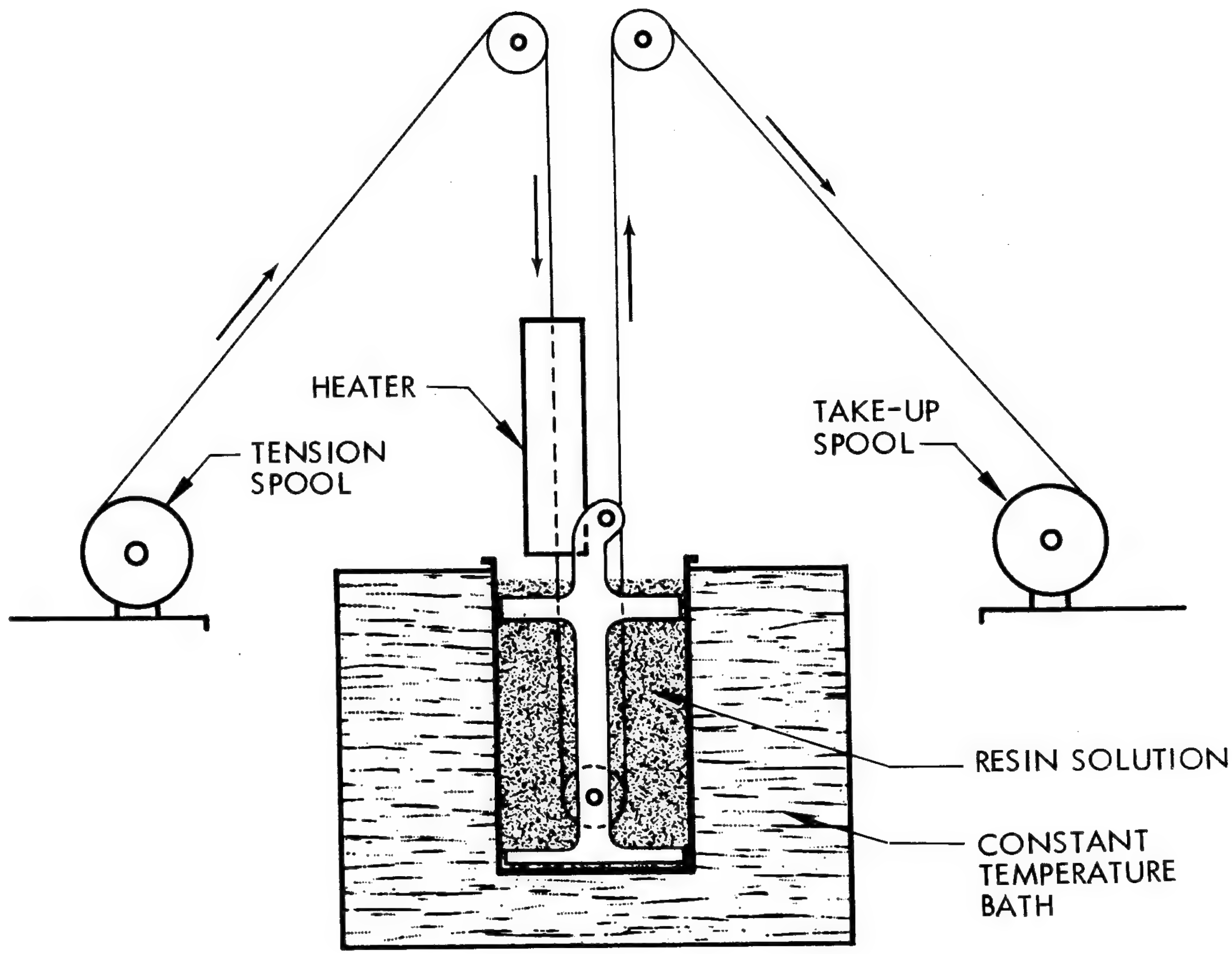

Figure 6. - Continuous Impregnation of Carbon Yarn

TABLE XI. - RESULTS OF CONTINUOUS IMPREGNATION PROCESS

Run No.	Carbon Yarn	Resin Solvent Concentration, w/o[a]	Line Speed		Resin Bath Temperature		Dry Yarn Preheat Treatment	Resin Content of Prepreg, w/o	Remarks
			$m/sec \times 10^{-4}$	in./min	°K	°F			
1	HMG-50	60	8.5	2	311	100	No	43.0	Few beads
2	HMG-50	70	8.5	2	311	100	No	48.8	Many beads
3	HMG-50	70	8.5	2	328	130	No	36.0	Low resin pickup
4	HMG-50	60	25	6	311	100	No	43.8	Many beads
5	HMG-50	70	25	6	328	130	Yes	46.8	Many beads
6	HMG-50	70	17	4	328	130	Yes	45.8	No beads
7	Thornel 75	70	17	4	328	130	Yes	58.9	No beads

a – Remainder of solution was resin.

Resin pickup for Thornel 75-S was 59 percent, compared with 46 percent for HMG-50. Metallographic analysis (Figure 5) showed a poor fiber distribution and excess of resin particularly in the outside periphery of the composite.

The following major problems were found to be associated with this process:

- Processing parameters such as line speed, resin/solvent concentration, preheat temperature, bath dwell time, fiber tension, and cure time must be developed for each carbon fiber.
- Fiber damage and frayed ends are difficult to eliminate at roller contact points.
- Considerable time and costly fiber would be consumed in producing material for evaluation.

3.4.4 Batch Process

This method of impregnating the fiber bundle involved the following operations:

1. Cut candidate fibers to a length of 0.36 m (14 in.)
2. Apply 1.77×10^{-2} m (0.5-in.) masking tape to each filament end to prevent filament fraying.
3. Attach 1×10^{-2} kg weight (10.635×10^{-3} m nut) with paper clip to one end for tension.
4. Submerge weighted bundles vertically in a solvent solution of the candidate resin for a minimum of 300 sec .
5. Air-dry pregged specimens for a minimum of 300 sec.
6. Cure weighted specimen vertically in oven.

Initial studies indicated that a solution of 30 percent by volume of GW-173 in methyl alcohol was acceptable for preliminary evaluation. With this approach, initial prepregging and curing were performed on Hitco 50, Thornel 75, Modmor I, Thornel 400, and Celanese GY-70. Good bundle penetration and wetting were obtained with Hitco 50, Thornel 75, and Thornel 400. Good localized wetting was obtained with Modmor I, but there were areas of poor fiber bundle penetration. Poor fiber bundle penetration was obtained with Celanese GY-70. This fiber has not shown good properties with respect to tensile strength before and after exposure to matrix pyrolysis gases.

A typical scanning electron micrograph of a fractured surface of Thornel 75 shows good fiber distribution and relatively uniform external module dimensions (Figure 7). The fiber-to-matrix bonding appears to be good (Figure 8). Hitco 50 is shown in cross section in Figure 9. The micrograph indicates no surplus resin. Optical metallography (Table XII) indicates a low volume fraction of resin of about 0.34; i.e., the composite is low in resin concentration. The lack of debonding at the interface between fibers and matrix indicates that the wetting of the fiber bundle is good (Figure 10). There are also no internal voids. Wetting of the Thornel 75 also was good (Figure 11). There is considerable variation of individual filament size. The estimated volume fraction resin was 0.20 (Table XII). Bundle impregnation, monofilament uniformity, and distribution of fiber and resin were good for Thornel 400 (Figure 12). Wetting of the individual fibrils was also good (Fig. 13). Individual filaments are ellipsoid in shape, have small

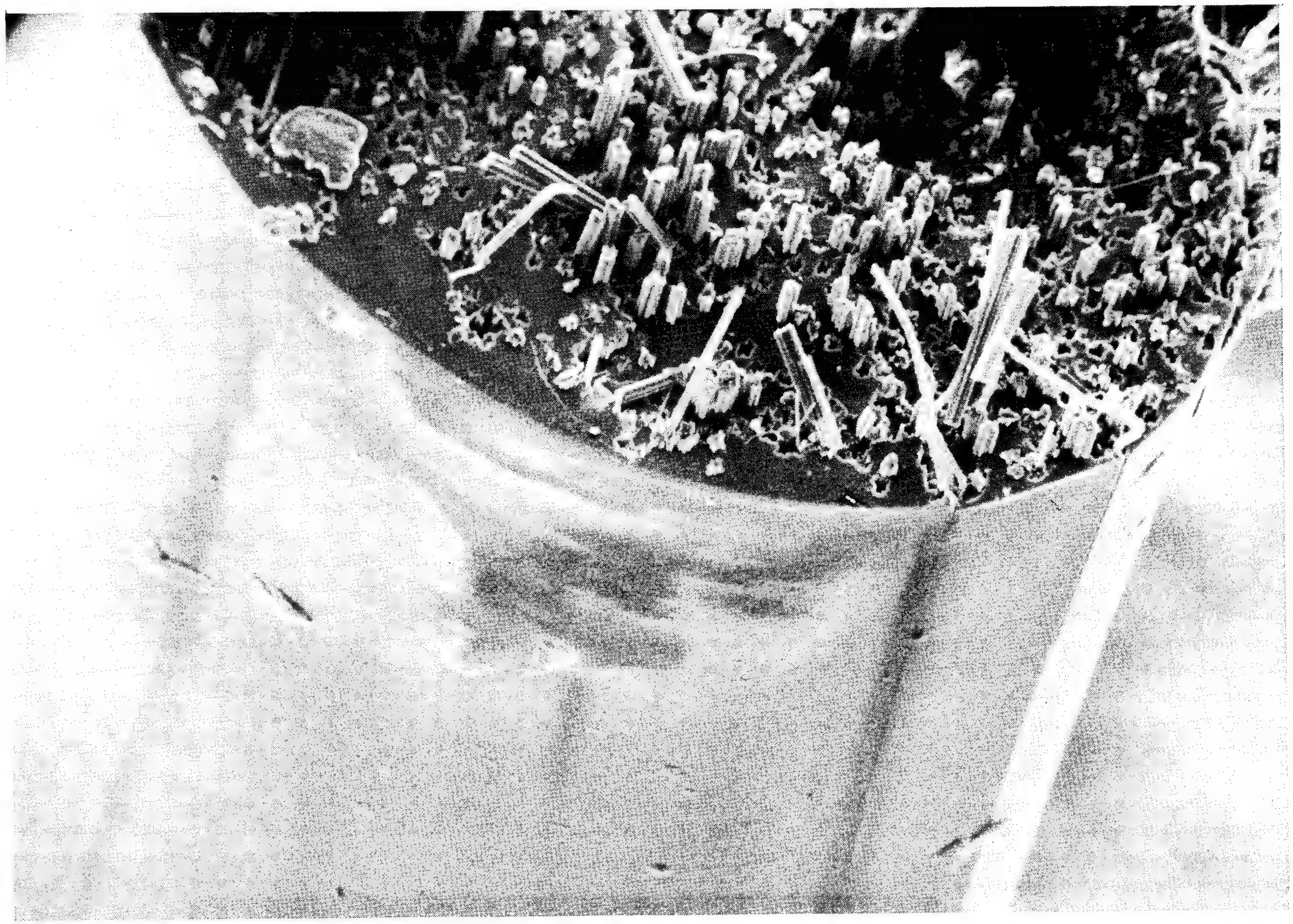

Figure 7. - Scanning Electron Micrograph of Thornel 75 in GW-173 Matrix, 400×

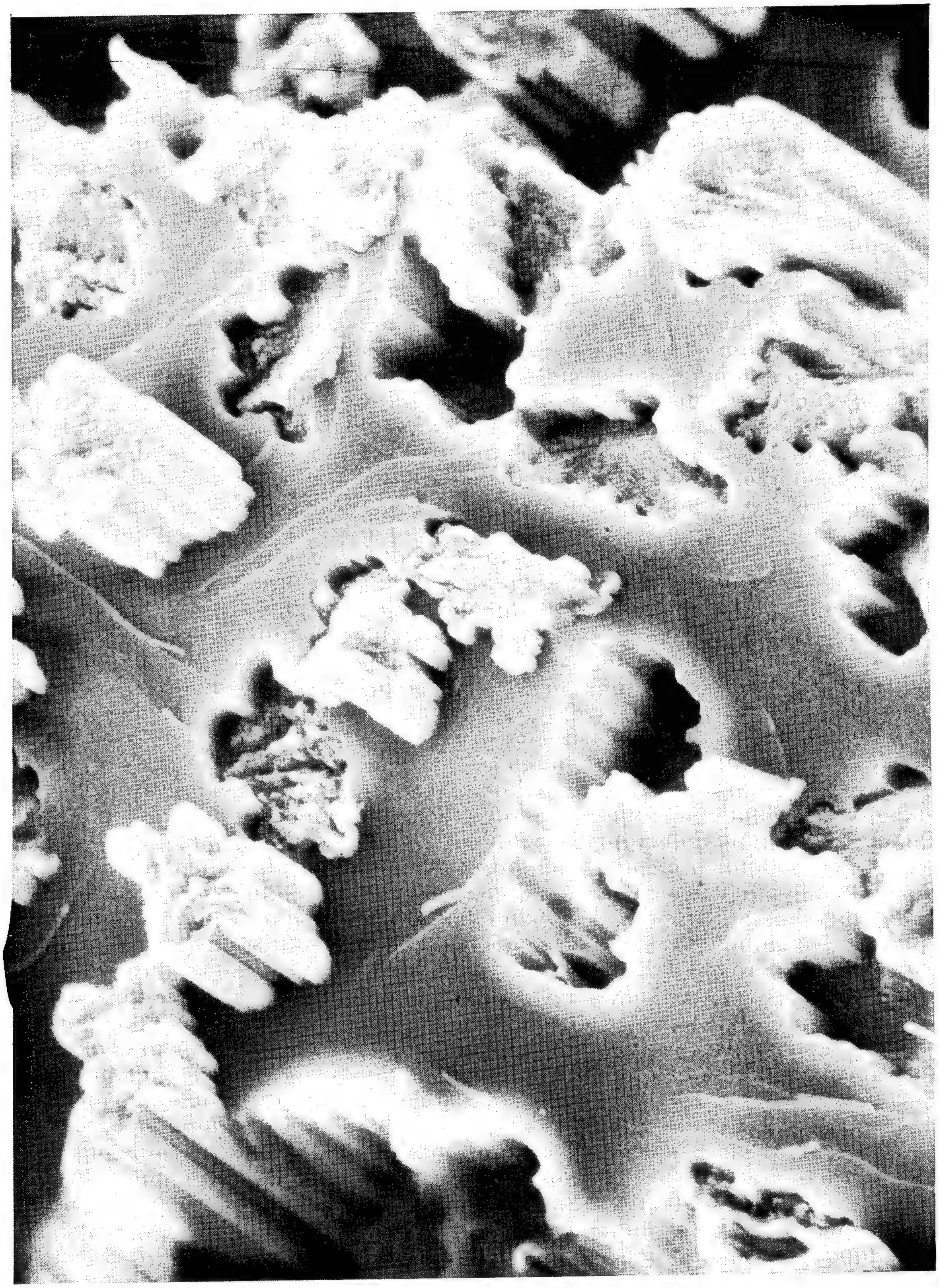

Figure 8. - Fracture Surface of Thornel 75 in GW-173 Matrix, 1400×

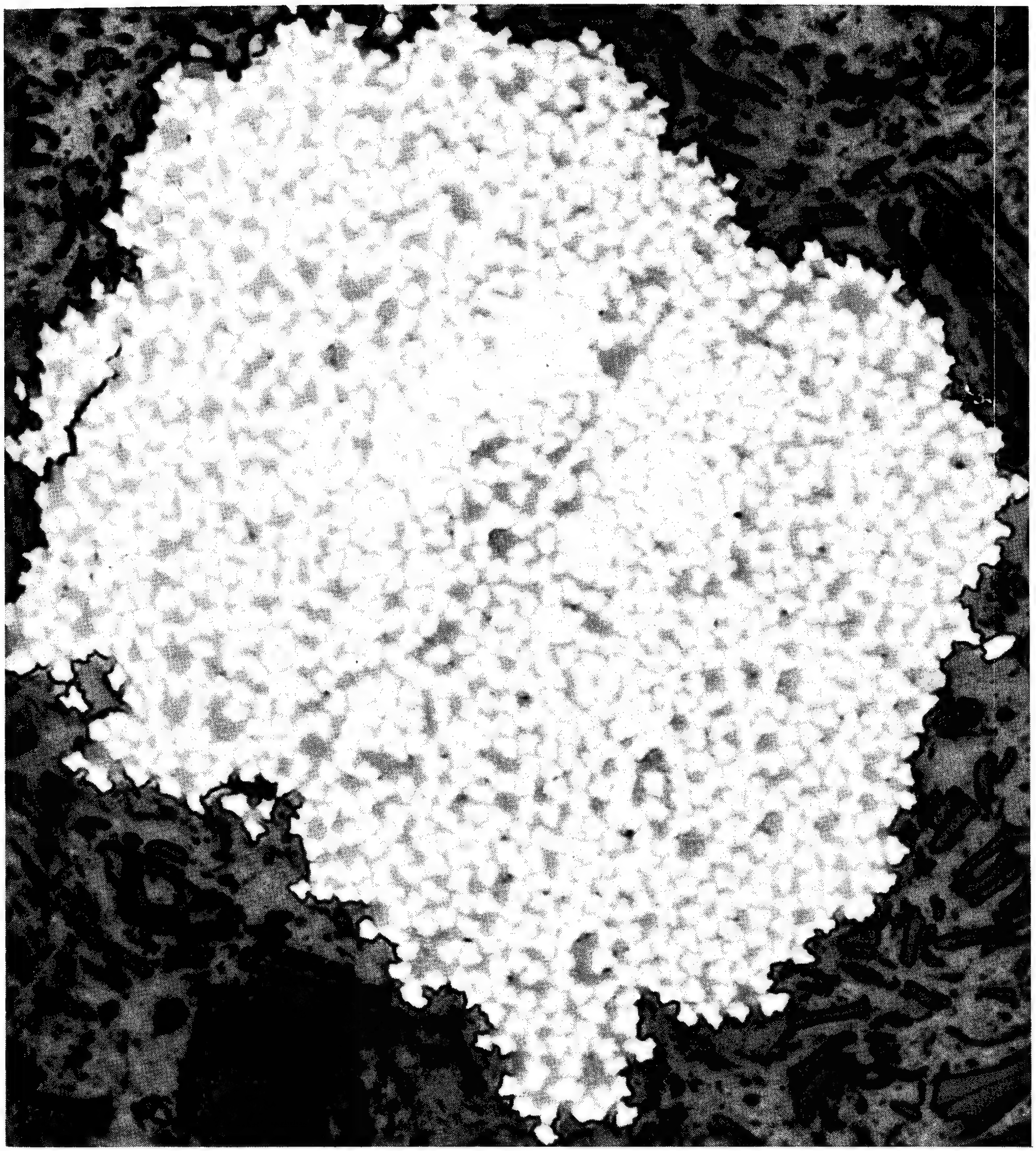

Figure 9. - Cross Section of Hitco 50 Prepregged Monofilament Produced by Vertical Impregnation in GW-173 Solution, 500×

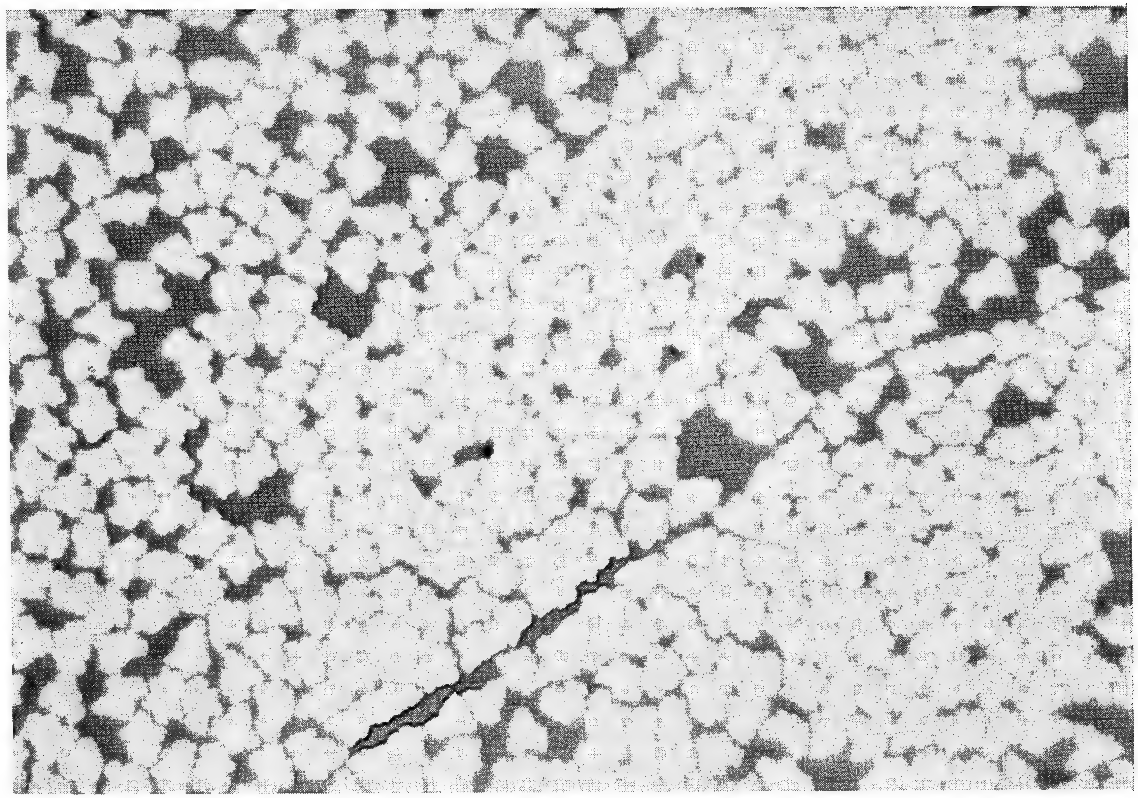

Figure 10. - Cross Section of Hitco 50/GW-173 Prepregged Monofilament Module Produced by Batch Process, 1000×

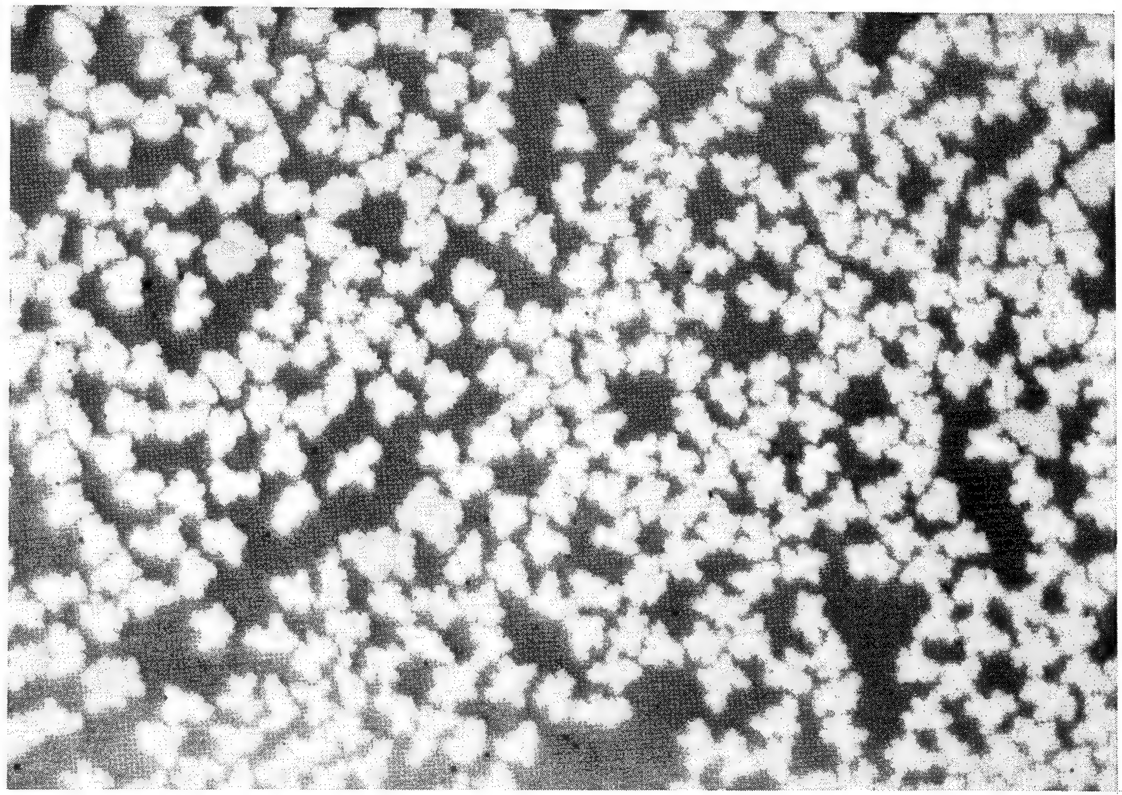

Figure 11. - Cross Section of Thornel 75/GW-173 Prepregged Monofilament Module Produced by Batch Process, 1000×

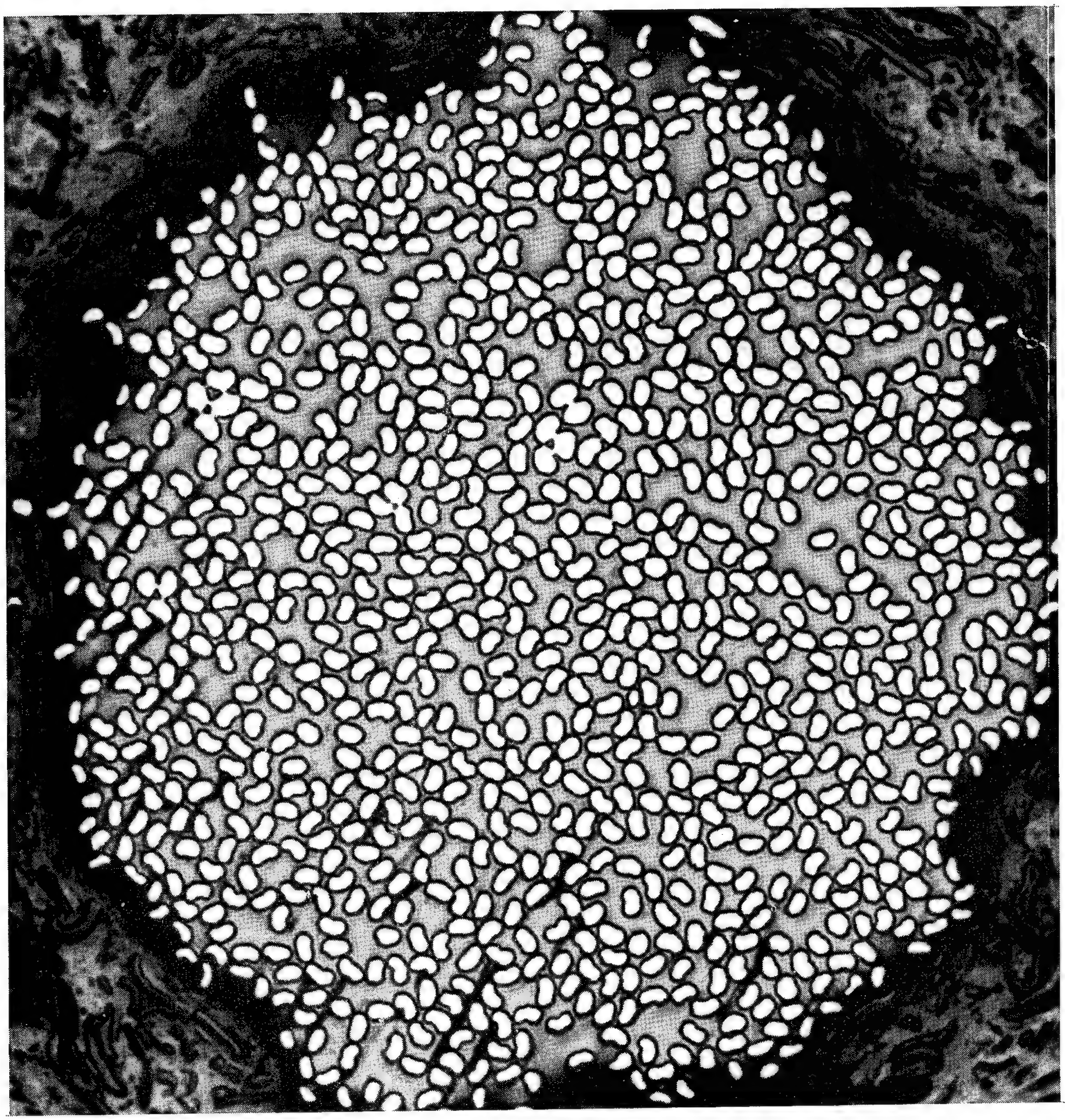

Figure 12. - Cross Section of Thornel 400/GW-173 Prepregged Monofilament Module Produced by Batch Process, 400×

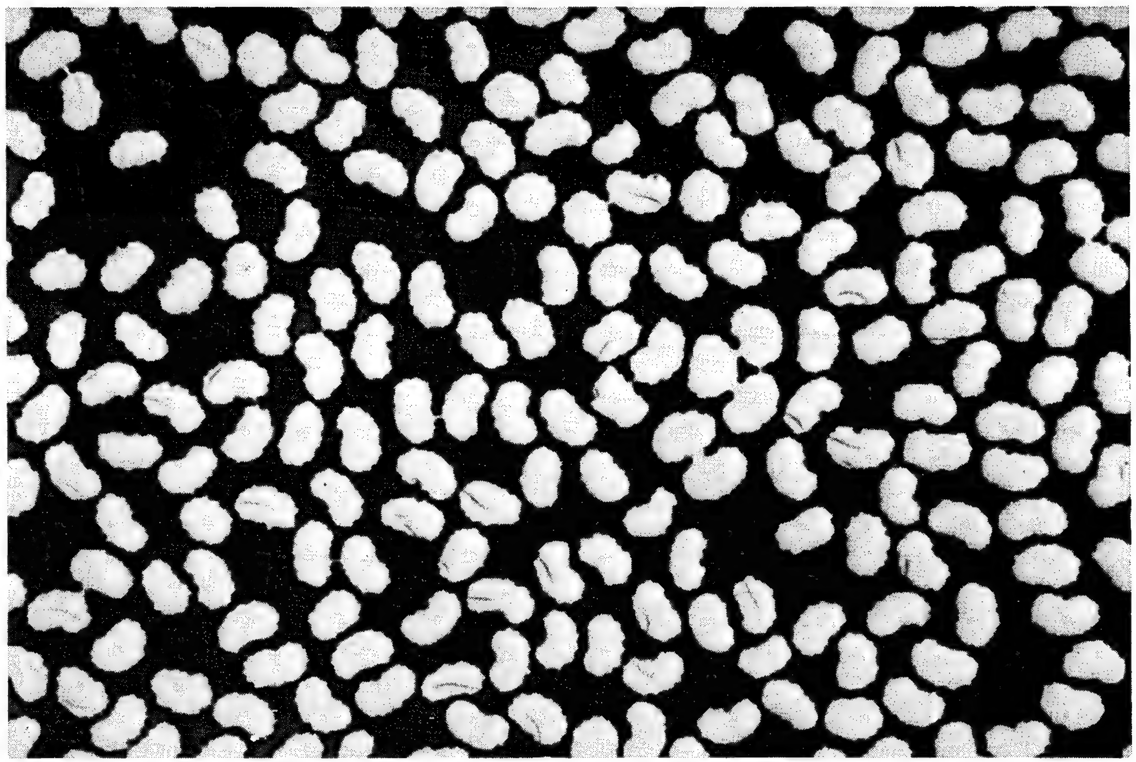

Figure 13. - Cross Section of Thornel 400/GW-173 Prepregged Monofilament Module Produced by Batch Process, 1000×

TABLE XII. - FIBER-RESIN RATIO ESTIMATED FROM OPTICAL MICROSCOPY FOR VERTICAL PREPREG OPERATION

Carbon-Preg Module	Volume Fraction			Weight Fraction	
	Fiber	Resin	Void	Fiber	Resin
Hitco 50	0.66	0.34	0	0.73	0.27
Thornel 75	0.80	0.20	0	0.84	0.16
Thornel 400	0.57	0.43	0	0.61	0.39
Modmor I	0.47	0.53	—	0.59	0.41
GY-70	0.56	0.21	0.23	0.80	0.22

cracks, and in some areas from two to three individual fibrils are self-bonded together in a "pseudopod" connection between the fibers. The resin concentration was estimated as 43 percent.

With the Modmor I fiber, the bundle was not completely impregnated, but fiber-matrix wetting appeared to be good (Figure 14). The estimated resin concentration was 53 percent. Large fiber bundles such as Modmor I were found to lose fiber collimation after removal from the resin solution. When cured, these specimens tended to be nonuniform in cross section, with frayed sections and a nonuniform resin concentration. To minimize these problems, the large fiber bundles were screeded after removal from the resin solution. A short 6×10^{-3} m piece of tygon tubing with a 1×10^{-3} m internal diameter was pulled down the fiber length to remove excess resin and collimate the filaments. This technique produced more uniform cross section, resin concentration, and fiber collimation, with a minimum of filament degradation.

The Celanese fiber, which has not been a prime candidate because of its poor mechanical properties, was not well impregnated with matrix precursor resin. In regions where the resin had penetrated, only partial wetting between filament and matrix occurred (Figure 15), as shown by the large void regions which appear black.

The initial results with this technique were acceptable; however, additional data concerning solvent concentration with GW-173 were required to optimize the procedure. Thornel 75 fiber was chosen for this study. Resin pickup and matrix/fiber ratios were measured for 60-, 70-, 75-, and 80-percent solvent solutions and are summarized in Table XIII. These results indicate that resin pickup is a function of GW-173 resin ageing. With the fresh solution, the resin pickup increased with decreasing solvent concentration. The resin pickup with the surface-treated Thornel 75-S (UC-307) was almost always less than with the untreated Thornel 75 (PVA).

The composite tensile properties in the as-cured condition are summarized in Table XIV, (five tests were run to obtain the average reported values). The highest tensile values were obtained with the 60-percent-solvent/GW-173 resin. Results appear to be better with the surface-treated Thornel 75-S/resin system.

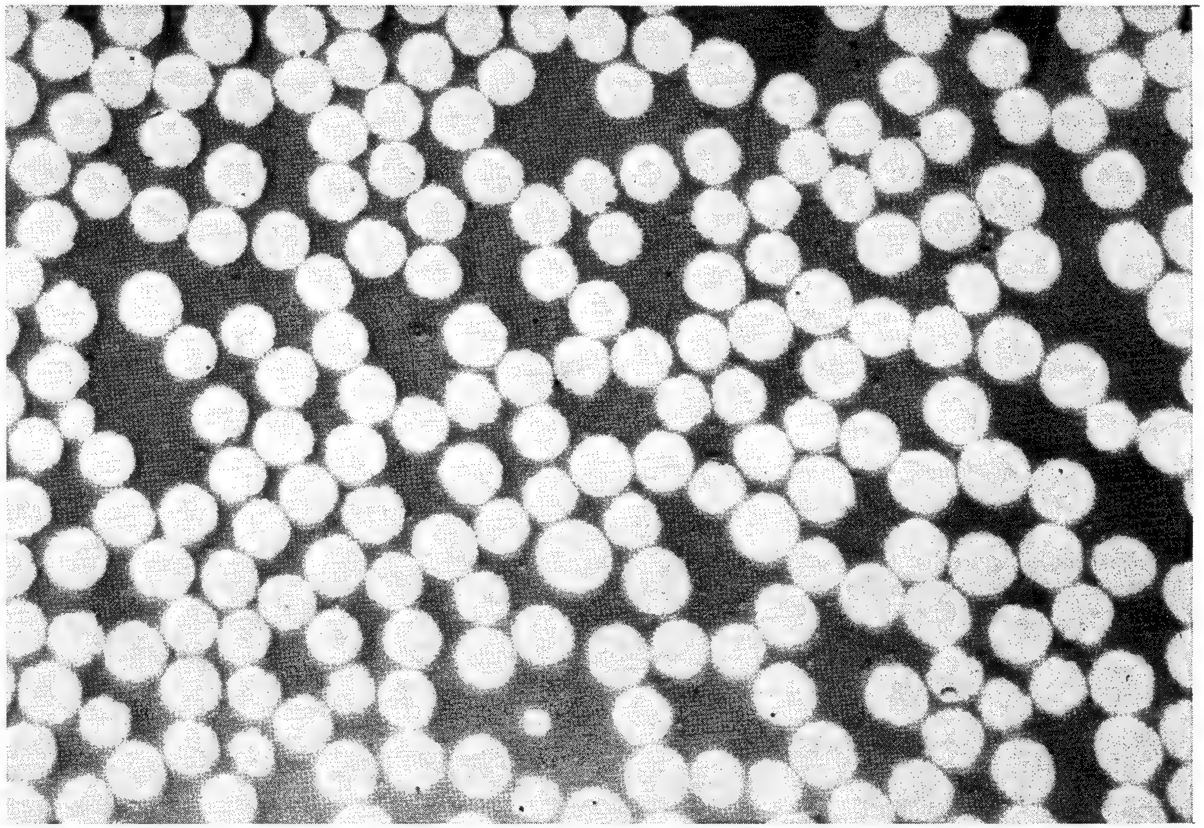

Figure 14. - Cross Section of Modmor I/GW-173 Prepregged Monofilament Module Produced by Batch Process, 1000×

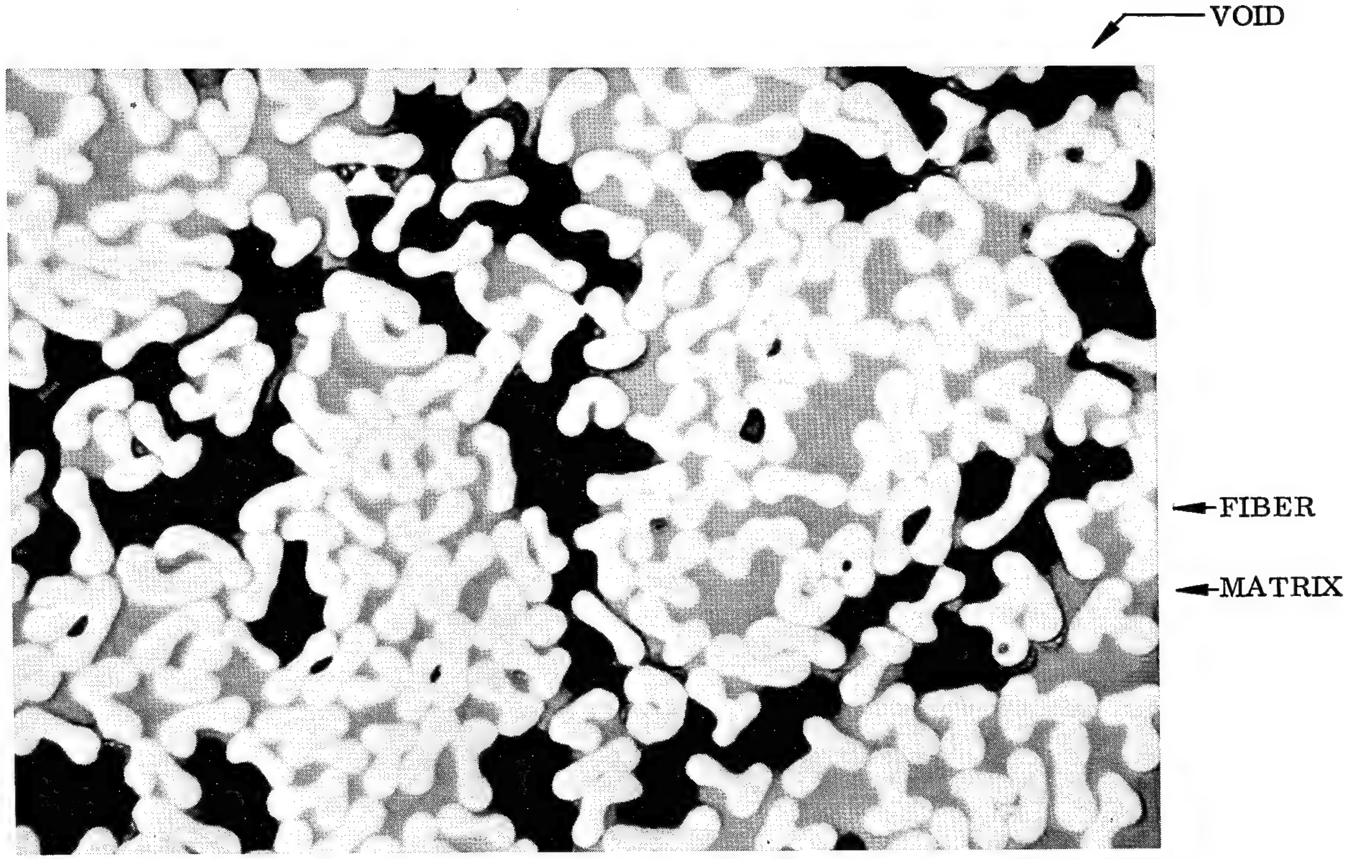

Figure 15. - Cross Section of GY-70/GW-173 Prepregged Monofilament Module Produced by Batch Process, 1000×

TABLE XIII. - RESIN PICKUP AS A FUNCTION OF SOLVENT CONTENT

(Thornel 75 of Two Different Types)

% Solvent	Fiber Type	Resin Pick-up		Matrix Area		Total Area		% Matrix	
		gm/in.	Kg/m	$in.^2 10^{-4}$	$m^2 10^{-8}$	$in.^2 10^{-4}$	$m^2 10^{-8}$	Vol	Wt.
60% [b]	PVA [a]	.00099	.0039	0.47	3.0	.95	6.1	50	68
	UC-307 [b]	.00071	.0028	0.34	2.2	.83	5.4	41	48
70% [b]	PVA	.00065	.0026	0.31	2.0	.79	5.1	39	45
	UC-307	.00054	.0022	0.26	1.6	.75	4.8	35	36
75% [b]	PVA	.00055	.0023	0.26	1.7	.74	4.8	35	39
	UC-307	.00046	.0018	0.22	1.4	.71	4.6	31	31
80% [b]	PVA	.00052	.0020	0.25	1.6	.73	4.7	34	36
	UC-307	.00033	.0013	0.16	1.0	.65	4.2	38	22
80% [c]	PVA	.00110	.0043	0.51	3.3	1.0	6.5	51	77

a - PVA — Thornel 75 coated with polyvinyl alcohol.
UC-307 — Thornel 75S coated with UC-307 proprietary resin.

b - Freshly prepared GW-173.

c - "old" GW-173.

TABLE XIV. - TENSILE PROPERTIES OF AS-CURED COMPOSITE MONOFILAMENT AS A FUNCTION OF RESIN SOLVENT CONTENT

% Solvent	Fiber Type	Function[a]	Tensile Force		Tensile Stress From Fiber Area		From Fiber + Matrix		Wt. % Matrix
			newtons	lbs	$N/m^2 \times 10^9$	$psi \times 10^5$	$N/m^2 \times 10^9$	$psi \times 10^5$	
60%[b]	Th 75 PVA	$\overline{x}$	81.5	18.3	2.61	3.79	1.32	1.91	68
		σ	—	0.7	0.10	0.15	0.05	0.75	—
60%[b]	Th 75S UC-307	$\overline{x}$	81.5	18.3	2.56	3.71	1.52	2.21	48
		σ	—	0.7	0.10	0.14	0.06	0.86	—
70%[b]	Th 75 PVA	$\overline{x}$	63.6	14.3	2.04	2.96	1.25	1.81	45
		σ	—	3.7	0.49	0.72	0.32	0.47	—
70%[b]	Th 75S UC-307	$\overline{x}$	69.0	15.5	2.16	3.14	1.42	2.06	36
		σ	—	3.4	0.48	0.48	0.31	0.45	—
75%[b]	Th 75 PVA	$\overline{x}$	45.9	10.3	1.40	2.13	0.96	1.39	39
		σ	8.9	2.0	0.69	4.15	0.19	0.27	—
75%[b]	Th 75S UC-307	$\overline{x}$	63.5	14.5	2.02	2.94	1.41	2.04	31
		σ	4.9	1.1	0.15	0.22	0.10	0.15	—
80%[b]	Th 75 PVA	$\overline{x}$	55.2	12.4	1.76	2.56	1.17	1.70	36
		σ	—	8.5	1.21	1.76	0.80	1.16	—
80%[b]	Th 75S UC-307	$\overline{x}$	49.9	11.2	1.56	2.27	1.19	1.72	22
		σ	—	6.5	0.91	1.32	0.69	1.00	
80%[c]	Th 75 PVA	$\overline{x}$	67.6	15.2	2.16	3.13	1.05	1.52	77

a - $\overline{x}$ = average value, σ = standard deviation.
b - freshly prepared GW-173
c - "aged" GW-173.

There was a significant spread in the data when 80-percent solvent was used. For example, for Thornel 75 (PVA) in 20-percent GW-173 the standard deviation is much higher, i.e., 1.21×10^9 N/m^2 (1.76×10^5 psi), than with other resin-solvent compositions, 0.10×10^9 N/m^2 (0.15×10^5 psi). This indicates a high degree of nonuniformity in impregnation. Visual examination of the cured fiber bundles showed that the samples which are low in resin are not well impregnated and tend to fray. The optimum concentration appears to be between 60 and 70 percent.

3.5 COMPOSITE MONOFILAMENT EVALUATION

3.5.1 Screening Studies

Seven candidate fibers and three matrix resins were evaluated to determine the optimum composite combination. Monofilament tensile strength and volume fraction of the candidates' constituents were measured before and after matrix pyrolysis to 1273°K. The results are summarized in Tables XV through XVIII.

GW-173 resin was used with 60- and 70-percent solvent concentration to determine the effect of changes in matrix volume fraction upon the tensile strength of the pyrolyzed monofilament. Results for each matrix resin precursor are as follows:

- GW-173 matrix precursor. In the preliminary studies the best composite monofilament mechanical properties were obtained with Thornel 75 in 70-percent-solvent/GW-173; the highest individual strength value was shown by Thornel 75 (UC-307) in 70-percent-solvent/GW-173, 1.32×10^9 N/m^2 (1.92×10^5 psi). The best average tensile strength, 1.08×10^9 N/m^2 (1.56×10^5 psi), was obtained with Thornel 75 (PVA) in 70-percent-solvent/GW-173 (see Tables XV and XVI). The strain-to-failure of such composite monofilament was 0.26 percent and the elastic modulus was 4.74×10^{11} N/m^2 (69.6×10^6 psi). Monofilament composite strength appears to be limited by the carbon matrix strain-to-failure. Pyrolysis cracking, which initiates at 673°K, appears to be one of the principal factors that degrades the matrix strain-to-failure and consequently the monofilament strength. [Subsequent process optimization studies (section 3.5.2) led to further improvement in composite tensile properties.]

- SC-1008 matrix precursor. Monofilament properties in a matrix generated from SC-1008 are given in Table XVII. The matrix volume fraction tends to be greater than that obtained with GW-173 and the tensile properties tend to be lower. The best strength values were obtained with Thornel 75 (PVA and UC-307). Maximum tensile strength values were 0.71×10^9 N/m^2 (1.03×10^5 psi) and 0.80×10^9 N/m^2 (1.17×10^5 psi), respectively. Very poor results were obtained with Mod I, FTIC-1000, and Thornel 400.

- Varcum (furfuryl alcohol) matrix precursor. Monofilament properties after cure and pyrolysis to 1273°K are given in Table XVIII. The matrix volume fraction is larger and the tensile strength is lower than those obtained with the other precursor resins. The maximum tensile stress, obtained with Mod II, was 0.72×10^9 N/m^2 (1.05×10^5 psi). Next highest values were obtained with Thornel 75 (PVA and UC-307). Poor strength values were obtained with Thornel 400, Mod I, FTIC-1000, and Celanese.

TABLE XV. - SCREENING OF CANDIDATE FIBERS WITH GW-173 IN 60-PERCENT SOLUTION

Fiber	Function[a]	Cured							Pyrolyzed							% of As-Cured Value
		% Matrix	Tensile Load		Tensile Stress				% Matrix	Tensile Load		Tensile Stress				
					From Fiber Area		From Fiber + Matrix					From Fiber Area		From Fiber + Matrix		
			N	lb	$n/m^2 \times 10^9$	$psi \times 10^5$	$n/m^2 \times 10^9$	$psi \times 10^5$		N	lb	$n/m^2 \times 10^9$	$psi \times 10^5$	$n/m^2 \times 10^9$	$psi \times 10^5$	
Thornel 75	$\bar{x}$	51.0	81.2	18.3	2.60	3.78	1.03	1.50	32.6	29.8	6.7	0.95	1.38	0.59	0.86	57.3
(PVA)	σ		1.8	0.4	0.06	0.08	0.02	0.03		11.1	2.5	0.35	0.51	0.22	0.32	
	Max		83.5	18.8	2.67	3.88	1.16	1.54		38.2	8.6	1.22	1.75	0.76	1.10	
Thornel 75	$\bar{x}$	38.6	89.0	20.0	2.79	4.05	1.50	2.18	27.8	40.0	9.0	1.26	1.83	0.86	1.25	57.3
(UC 307)	σ		4.6	1.4	0.20	0.28	0.10	0.15		4.8	1.1	0.15	0.22	0.10	0.15	
	Max		97.0	21.8	3.14	4.42	1.64	2.38		47.6	10.7	1.50	2.18	1.03	1.49	
HMG-50	$\bar{x}$	39.6	72.0	16.2	1.84	2.64	0.97	1.40	28.9	35.4	7.95	0.90	1.30	0.61	0.88	62.9
	σ		4.9	1.1	0.13	0.18	0.07	0.10		4.7	1.06	0.12	0.17	0.08	0.12	
	Max		76.5	17.2	1.95	2.80	1.05	1.53		39.6	8.9	1.01	1.46	0.68	0.99	
Mod I	$\bar{x}$	59.1	663	149	1.37	1.98	0.46	0.67	41.4	396	89.0	0.82	1.18	0.43	0.63	94.3
	σ		84	19	0.18	0.25	0.06	0.09		18	4.1	0.04	0.05	0.02	0.03	
	Max		765	174	1.60	2.12	0.54	0.78		418	94	0.87	1.25	0.46	0.67	
Mod II	$\bar{x}$	65.0	1245	280	2.52	3.57	0.70	1.02	46.5	510	115	1.01	1.47	0.50	0.73	71.2
	σ		111	25	0.22	0.33	0.06	0.09		98	22	0.19	0.28	0.10	0.14	
	Max		1430	322	2.80	4.10	0.77	1.12		635	143	1.26	1.83	0.63	0.91	
FTIC-1000	$\bar{x}$	49.9	57.4	12.9	0.77	1.12	0.33	0.48	38.2	37.8	8.5	0.50	0.73	0.29	0.42	87.5
	σ		12.0	2.7	0.16	0.23	0.07	0.10		9.8	2.2	0.13	0.19	0.08	0.11	
	Max		69.7	15.7	0.94	1.36	0.41	0.59		51.5	11.6	0.68	1.00	0.39	0.57	
Celanese	$\bar{x}$	37.3	34.2	7.7	1.54	2.24	0.99	1.43	20.9	7.7	1.74	0.34	0.50	0.28	0.40	28.0
GY-70	σ		2.6	0.60	0.12	0.18	0.08	0.11		4.9	1.1	0.22	0.32	0.24	0.35	
	Max		38.2	8.6	1.72	2.50	1.10	1.60		12.9	2.9	0.57	0.83	0.46	0.67	
Thornel 400	$\bar{x}$	37.8	149.5	33.6	3.27	4.75	1.80	2.61	28.0	24.6	5.5	0.53	0.77	0.36	0.53	20.2
	σ		4.0	0.9	0.09	0.13	0.05	0.07		2.2	0.5	0.05	0.07	0.04	0.05	
	Max		155	34.9	3.40	4.94	1.87	2.71		26.6	6.2	0.60	0.68	0.41	0.60	

(a) $\bar{x}$ = average, σ = standard deviation, Max = maximum value

TABLE XVI. - SCREENING OF CANDIDATE FIBERS WITH GW-173
IN 70-PERCENT SOLUTION

Fiber	Function[a]	Cured								Pyrolyzed								% of As-Cured Value
		% Matrix	Tensile Load		Tensile Stress				% Matrix	Tensile Load		Tensile Stress				
					From Fiber Area		From Fiber + Matrix					From Fiber Area		From Fiber + Matrix		
			N	lb	$n/m^2 \times 10^9$	$psi \times 10^5$	$n/m^2 \times 10^9$	$psi \times 10^5$		N	lb	$n/m^2 \times 10^9$	$psi \times 10^5$	$n/m^2 \times 10^9$	$psi \times 10^5$	
Thornel 75	$\bar{x}$	29.9	77.3	17.4	2.48	3.60	1.54	2.23	17.7	42.6	9.6	1.37	1.99	1.08	1.56	70.0
(PVA)	σ		3.1	0.7	0.10	0.14	0.06	0.09		4.0	0.9	0.13	0.19	0.10	0.15	
	max		82.3	18.5	2.64	3.62	1.63	2.37		48.1	10.8	1.55	2.42	1.21	1.76	
Thornel 75	$\bar{x}$	31.3	87.0	20.8	2.90	4.21	1.77	2.56	23.1	36.0	8.1	1.16	1.68	0.84	1.21	48.4
(UC-307)	σ		8.0	1.8	0.24	0.35	0.14	0.21		16.9	3.8	0.55	0.79	0.32	0.47	
	max		98.6	22.2	3.10	4.50	1.83	2.76		57.0	12.8	1.83	2.65	1.32	1.92	
HMG 50	$\bar{x}$	41.0	78.6	17.9	1.94	2.82	1.05	1.52	26.4	34.8	7.6	0.85	1.24	0.60	0.87	57.2
	σ		3.6	0.8	0.09	0.13	0.05	0.07		3.6	0.8	0.09	0.13	0.06	0.09	
	max		82.6	18.6	2.02	2.93	1.09	1.58		37.8	8.5	0.95	1.39	0.67	0.97	
Mod I	$\bar{x}$	42.9	540	121.4	1.12	1.62	0.55	0.80	31.3	185	41.5	0.38	0.55	0.25	0.36	45.0
	σ		12.5	28.1	0.26	0.37	0.13	0.19		17	3.9	0.04	0.05	0.02	0.03	
	max		755	170	1.57	2.06	0.78	1.12		209	47	0.43	0.63	0.28	0.41	
Mod II	$\bar{x}$	47.8	948	213	1.87	2.72	0.83	1.21	36.0	512	115	1.00	1.46	0.59	0.86	72.0
	σ		104	23	0.20	0.29	0.09	0.13		53	12	0.10	0.15	0.06	0.09	
	max		1075	242	2.12	3.10	0.95	1.37		552	124	1.08	1.58	0.64	0.93	
FTIC-1000	$\bar{x}$	46.9	55.6	12.5	0.73	1.08	0.34	0.49	35.0	30.2	6.8	0.40	0.59	0.25	0.36	73.5
	σ		1.4	3.1	0.18	0.27	0.08	0.12		11.1	2.5	0.15	0.20	0.09	0.13	
	max		77.0	17.3	1.01	1.50	0.47	0.68		42.5	9.6	0.58	0.83	0.35	0.51	
Celanese	$\bar{x}$	21.4	31.1	7.0	1.40	2.04	0.99	1.44	25.2	13.3	3.0	0.61	0.89	0.39	0.56	38.8
GY 70	σ		4.5	1.0	0.20	0.29	0.14	0.20		4.0	0.9	0.18	0.27	0.12	0.17	
	max		33.2	8.0	1.60	2.33	1.14	1.65		17.8	4.0	0.83	1.09	0.52	0.75	
Thornel	$\bar{x}$	31.2	126	28.4	2.76	4.01	1.72	2.50	19.3	16.9	3.8	0.36	0.53	0.29	0.42	16.8
400	σ		14	3.2	0.31	0.45	0.19	0.28		7.5	1.7	0.16	0.24	0.13	0.19	
	max		136	30.6	2.96	4.33	1.86	2.70		25.6	6.0	0.57	0.84	0.45	0.66	

(a) $\bar{x}$ = average, σ = standard deviation, max = maximum value

TABLE XVII. - SCREENING OF CANDIDATE FIBERS WITH SC-1008

Fiber	Function(a)	Cured to 450°K							Pyrolyzed to 1273°K							% of As Cured Value
		% Matrix	Tensile Force		Tensile Stress				% Matrix	Tensile Force		Tensile Stress				
					From Fiber Area		From Fiber + Matrix					From Fiber Area		From Fiber + Matrix		
			N	lb	$n/m^2 \times 10^9$	$psi \times 10^5$	$n/m^2 \times 10^9$	$psi \times 10^5$		N	lb	$n/m^2 \times 10^9$	$psi \times 10^5$	$n/m^2 \times 10^9$	$psi \times 10^5$	
Thornel 75	$\bar{x}$	55.9	78.0	17.7	2.52	3.66	0.84	1.22	49.1	45.8	10.3	1.47	2.13	0.62	0.90	74
(PVA)	σ		9.8	2.2	0.32	0.44	0.11	0.16		8.5	1.9	0.13	0.28	0.08	0.12	
	Max		85.5	19.2	2.63	3.97	0.91	1.32		52.5	11.8	1.68	2.44	0.71	1.03	
Thornel 75	$\bar{x}$	61.2	88.1	19.8	2.76	4.01	0.82	1.19	36.4	42.0	9.45	1.32	1.91	0.74	1.08	91
(UC-307)	σ		14.2	3.2	0.45	0.65	0.13	0.19		3.2	0.73	0.10	0.15	0.06	0.08	
	Max		104.5	23.5	3.16	4.57	0.97	1.41		45.5	10.2	1.43	2.06	0.80	1.17	
HMG-50	$\bar{x}$	46.1	80.2	18.0	2.02	2.93	0.90	1.31	49.7	32.6	7.33	0.82	1.19	0.36	0.52	40
	σ		4.0	0.9	0.10	0.15	0.05	0.07		3.5	0.78	0.09	0.13	0.04	0.06	
	Max		84.5	19.0	2.13	3.09	0.95	1.38		36.3	8.15	0.91	1.32	0.40	0.58	
Mod I	$\bar{x}$	62.6	775	174	1.60	2.32	0.37	0.54	51.5	321	72.2	0.66	0.96	0.28	0.40	74
	σ		50.5	11.6	0.11	0.15	0.03	0.04		37	8.32	0.08	0.12	0.03	0.05	
	Max		829	186	1.71	2.48	0.40	0.58		339	76.0	0.70	1.02	0.30	0.42	
FTIC-1000	$\bar{x}$	57.0	66.4	14.9	0.88	1.28	0.30	0.44	45.2	32.0	7.2	0.43	0.62	0.21	0.30	69
	σ		11.1	2.5	0.17	0.21	0.05	0.07		12.5	2.8	0.17	0.24	0.08	0.12	
	Max		80.1	18.0	1.06	1.55	0.36	0.53		50.3	11.3	0.68	0.98	0.33	0.47	
Celanese	$\bar{x}$	34.1	32.9	7.4	1.50	2.16	0.80	1.16	24.6	19.2	4.3	0.86	1.25	0.58	0.84	72.5
GY-70	σ		4.0	0.9	0.18	0.26	0.10	0.14		4	0.9	0.18	0.26	0.12	0.18	
	Max		36.6	8.2	1.66	2.40	0.89	1.29		22.2	5.0	1.00	1.46	0.68	0.98	
Thornel 400	$\bar{x}$	45.1	142	31.9	3.11	4.51	1.41	2.04	36.4	17.8	4.0	0.39	0.57	0.22	0.32	15.7
	σ		4.0	0.9	0.85	1.27	0.40	0.57		3.6	0.8	0.08	0.11	0.04	0.06	
	Max		140.5	32.9	3.21	4.65	1.45	2.10		20.5	4.6	0.45	0.65	0.25	0.37	
Mod II	$\bar{x}$	62.4	88.5	199	1.75	2.54	0.50	0.72	50.1	625	140.2	1.23	1.79	0.53	0.77	107
	σ		8.5	19	0.18	0.25	0.05	0.07		9.6	21.6	0.19	0.27	0.08	0.12	
	Max		100.5	226	1.99	2.88	0.57	0.82		756	170	1.49	2.18	0.65	0.94	

(a) $\bar{x}$ = average, σ = standard deviation, Max = maximum value

TABLE XVIII. - SCREENING OF CANDIDATE FIBERS WITH VARCUM

Fiber	Function(a)	Cured							Pyrolyzed							% of As-Cured Value
		% Matrix	Tensile Force		Tensile Stress				% Matrix	Tensile Force		Tensile Stress				
					From Fiber Area		From Fiber + Matrix					From Fiber Area		From Fiber + Matrix		
			N	lb	$n/m^2 \times 10^9$	$psi \times 10^5$	$n/m^2 \times 10^9$	$psi \times 10^5$		N	lb	$n/m^2 \times 10^9$	$psi \times 10^5$	$n/m^2 \times 10^9$	$psi \times 10^5$	
Thornel 75	$\bar{x}$	65.6	84.5	19.0	2.71	3.93	0.717	1.04	52	34.7	7.8	1.11	1.61	0.48	0.70	67.0
(PVA)	σ		1.65	0.4	0.05	0.07	0.017	0.02		10.1	2.3	0.32	0.47	0.14	0.20	
	Max		87.0	19.5	2.79	4.04	0.737	1.07		41.5	9.3	1.32	1.92	0.57	0.84	
HMG	$\bar{x}$	Resin Rich	67.6	15.2	1.71	2.48	–	–	Resin Rich	26.7	6.0	0.67	0.97	Resin Rich		–
	σ		1.65	0.4	0.04	0.06	–	–		3.8	0.9	0.10	0.14			
	Max		70.0	15.7	1.77	2.56	–	–		31.2	7.0	0.78	0.13			
Thornel 75s	$\bar{x}$	56.8	85.4	19.2	2.68	3.89	1.08	1.56	53	24.0	5.4	0.75	1.09	0.33	0.48	30.8
(UC-307)	σ		6.72	1.5	0.21	0.31	0.08	0.12		11.7	2.6	0.37	0.53	0.16	0.23	
	Max		89.5	20.2	2.82	4.20	1.14	1.64		33.8	7.6	1.06	1.54	0.46	0.68	
Thornel 400	$\bar{x}$	53.1	130.8	29.4	2.87	4.16	1.33	1.93	47	9.8	2.2	0.21	0.31	0.14	0.20	10.4
	σ		7.65	1.8	0.17	0.25	0.08	0.12		3.3	0.7	0.07	0.10	0.05	0.07	
	Max		143.5	32.2	3.04	4.56	1.46	2.11		13.4	3.0	0.29	0.42	0.19	0.27	
Mod I	$\bar{x}$	65.9	681.0	153.0	1.41	2.04	0.39	0.56	53	359.4	80.8	0.74	1.08	0.32	0.46	83.3
	σ		126.3	28.4	0.26	0.38	0.07	0.10		101.9	22.9	0.21	0.30	0.09	0.13	
	Max		890.0	200	1.85	2.57	0.51	0.73		472	106	0.97	1.42	0.42	0.60	
Mod II	$\bar{x}$	67.9	992.0	223.0	1.96	2.84	0.50	0.73	54	737.5	165.8	1.45	2.11	0.64	0.93	127
	σ		49.8	11.2	0.10	0.14	0.03	0.04		78.3	17.6	0.15	0.22	0.07	0.10	
	Max		1042	234.0	2.04	2.98	0.53	0.77		833	187.0	1.64	2.38	0.72	1.05	
FTIC 1000	$\bar{x}$	68.9	68.9	15.5	0.92	1.34	0.23	0.34	58	24.9	5.6	0.33	0.48	0.13	0.19	56.0
	σ		15.1	3.4	0.20	0.29	0.05	0.07		8.0	1.8	0.11	0.16	0.04	0.06	
	Max		89.5	19.9	1.07	1.72	0.30	0.45		31.2	7.0	0.41	0.60	0.16	0.24	
Celanese	$\bar{x}$	43.0	32.0	7.2	1.45	2.10	0.67	0.97	36		Samples too brittle to test					
	σ		2.4	0.54	0.11	0.16	0.05	0.07								
	Max		34.3	7.8	1.57	2.28	0.73	1.05								

(a) $\bar{x}$ = average, σ = standard deviation, Max = maximum value

3.5.2 Process Optimization

Based on these screening results, Thornel 75 fibers and GW-173 resin precursor were chosen for a more intensive study. The variability of results obtained with Thornel 75 (PVA and UC-307) in 60- and 70-percent-solvent/GW-173 indicated the need of further work to determine the effect of solvent concentration and fiber finish on the composite monofilament properties. Resin solutions of GW-173 in 60-, 70-, 75-, and 80-percent methanol were prepared, and specimens of Thornel 75 with PVA and UC-307 were pregged, cured, and pyrolyzed to 1273°K.

The tensile strength of the resulting pyrolyzed monofilaments is shown in Table XIX. The highest composite tensile strength of 1.34×10^9 N/m^2 (1.95×10^5 psi) was obtained with Thornel 75 and UC-307 in 80-percent-solvent/GW-173. However, observations by scanning electron microscopy indicated that the 80-percent solution did not provide sufficient matrix and that the fiber was highly friable. No statistical evidence was found that indicates an overall preference for either surface finish. An analysis of the tensile data and of the scanning electron microscopy observations suggested that the optimum system, for further work in the program, was Thornel 75 (PVA) pregged with a 70-percent-solvent/GW-173 resin. The maximum value observed, tensile strength $= 1.74 \times 10^9$ N/m^2 (2.55×10^5 psi),* Row 3, Table XIX, was obtained with this system and the composite was more coherent and less friable.

Optical and scanning electron microscopy observations of the pyrolyzed composite monofilament have shown that the low and/or erratic tensile strength values can be associated with four different causes: pyrolysis cracking, poor fiber penetration, variation in matrix precursor concentration, and voids within the matrix.

To reduce pyrolysis cracking, a series of double heat-treatment and re-impregnation experiments were tried. Results are tabulated in Table XX. In a single pyrolysis run to 1273°K (row 5), the maximum tensile load observed was 48.1 N (10.8 lb), corresponding to a tensile stress of 1.12×10^9 N/m^2 (1.63×10^5 psi). Moderate improvements in tensile load ($\sim$ 10 percent)were obtained by various double pyrolysis and pregging procedures. However, such improvements did not correspond to a higher tensile stress because the matrix volume fraction and the cross-sectional area had increased substantially. For example in specimens pyrolyzed to 973° K, repregged with GW-173, and pyrolyzed again to 973° K, the maximum tensile load was 51.5 N (11.6 lb) with a percent matrix of 38.2,and the composite tensile stress was only 0.86×10^9 N/m^2 (1.24×10^5 psi). One such sample is shown in Figure 16. Some of the fibers are loosely held. The matrix generated from the second impregnation appears to be attached primarily at the periphery of the fiber. There are, however, good regions of matrix bonding (Figure 17), as well as regions of poor fiber-matrix bonding (Figure 18).

Another pyrolyzed sample, examined in cross section, shows that the matrix generated during the second impregnation (regions marked as in Figure 19), bridges large pyrolysis cracks but does not form an even film or blunt the preexisting pyrolysis cracks. It was concluded that double pyrolysis and prepregging give only marginal improvement in properties.

A resistance-heated hot-melt approach using solvent-free GW-173 was evaluated in an attempt to reduce void and bubble formation caused by the entrapment of volatiles. The

---

*Corrected for fiber matrix cross-sectional area only. [The corresponding composite value was 1.29×10^9 N/m^2 (1.87×10^5 psi)].

TABLE XIX. - TENSILE PROPERTIES OF PYROLYZED COMPOSITE MONOFILAMENT AS A FUNCTION OF RESIN AND SOLVENT CONCENTRATION[a]

Fiber	% Solution	Function (b)	Tensile Force		Tensile Stress			
					Fiber Area		Fiber + Matrix	
			n	lbs	$n/m^2 \times 10^9$	$psi \times 10^4$	$n/m^2 \times 10^9$	$psi \times 10^4$
Th-75 PVA	80	$\bar{x}$	47.6	10.7	1.52	22.1	1.24	18.0
		σ	1.8	0.4	0.06	0.8	0.05	0.7
Th-75 PVA	75	$\bar{x}$	39.6	8.9	1.27	18.4	0.99	14.4
		σ	4.9	1.1	0.16	2.3	0.12	1.8
Th-75 PVA	70	$\bar{x}$	50.3	11.3	1.60	23.3	1.19	17.2
		σ	4.5	1.0	0.14	2.1	0.10	1.5
Th-75 PVA	60	$\bar{x}$	48.7	10.95	1.56	22.6	0.99	14.4
		σ	2.3	0.5	0.07	1.1	0.05	0.7
Th-75 UC-307	80	$\bar{x}$	46.7	10.5	1.50	21.7	1.34	19.5
		σ	5.0	1.1	0.16	2.3	0.15	2.1
Th-75 UC-307	75	$\bar{x}$	39.6	8.9	1.24	18.0	0.99	14.4
		σ	9.3	2.1	0.30	4.3	0.23	3.4
Th-75 UC-307	70	$\bar{x}$	47.6	10.7	1.50	21.7	1.18	17.1
		σ	5.3	1.2	0.17	2.4	0.13	1.9
Th-75 UC-307	60	$\bar{x}$	49.8	11.2	1.57	22.8	1.20	17.4
		σ	1.8	0.4	0.06	0.8	0.04	0.6

a - GW-173 precursor
b - $\bar{x}$ = average; σ = standard deviation

TABLE XX. - MONOFILAMENT IMPROVEMENT STUDIES

Monofilament Constituents	Condition	(%) Matrix	Function(a)	Tensile Load		Tensile Stress (Fiber Area)		Tensile Stress (Fiber + Matrix)	
				N	lb	$n/m^2 \times 10^9$	$psi \times 10^5$	$n/m^2 \times 10^9$	$psi \times 10^5$
Thornel 75 in 70% GW-173 solution	Cured to 673°K Repregged with GW-173 Pyrolysed to 1273°K	38.1 57.2 44.7	– $\bar{x}$ σ max. value	b – 35.6 12.9 46.2	b – 8.0 2.9 10.4	b – 1.14 0.41 1.48	b – 1.65 0.60 2.25	b – 0.57 0.21 0.75	b – 0.82 0.30 1.07
Thornel 75 in 70% GW-173 solution	Pyrolyzed to 673°K Repregged with GW-173 Pyrolyzed to 1273°K Repregged with GW-173 Pyrolyzed to 1173°K	38.1 57.2 44.7 c –	$\bar{x}$ σ max. value	46.7 7.7 51.1	10.5 1.73 11.5	1.50 0.25 1.64	2.17 0.36 2.38	b	b
Thornel 75 in 70% GW-173 solution	Pyrolyzed to 973°K Repregged with GW-173 Pyrolyzed to 973°K	31.2 45.7 38.2	– – $\bar{x}$ σ max. value	b – 32.5 12.0 51.5	b – 7.3 2.7 11.6	b – 1.04 0.39 1.65	b – 1.51 0.56 2.4	b – 0.54 0.20 0.86	b – 0.78 0.29 1.24
Thornel 75 in 70% GW-173 solution	Pyrolyzed to 1273°K Repregged with GW-173 Pyrolyzed to 1173°K	17.7 – –	$\bar{x}$ σ max. value	48.0 10.5 52.5	10.8 2.4 11.8	1.54 0.34 1.68	2.23 0.49 2.42	b	b
Thornel 75 in 70% GW-173 solution	Single pyrolysis to 1273°K	17.7	$\bar{x}$ σ max. value	42.7 4.0 48.1	9.6 0.9 10.8	1.37 0.13 1.54	1.99 0.18 2.22	1.07 0.10 1.12	1.56 0.15 1.63
Thornel 75 in GW-173 no solvent	Hot-melt, resistance-heated prepreg to 453°K; pyrolyzed to 1273°K	c	$\bar{x}$ σ max. value	40.0 6.9 49.5	9.0 1.6 11.1	1.28 0.22 1.58	1.86 0.32 2.30	b	b

(a) $\bar{x}$ = mean, σ = standard deviation
(b) Samples too resin rich to report

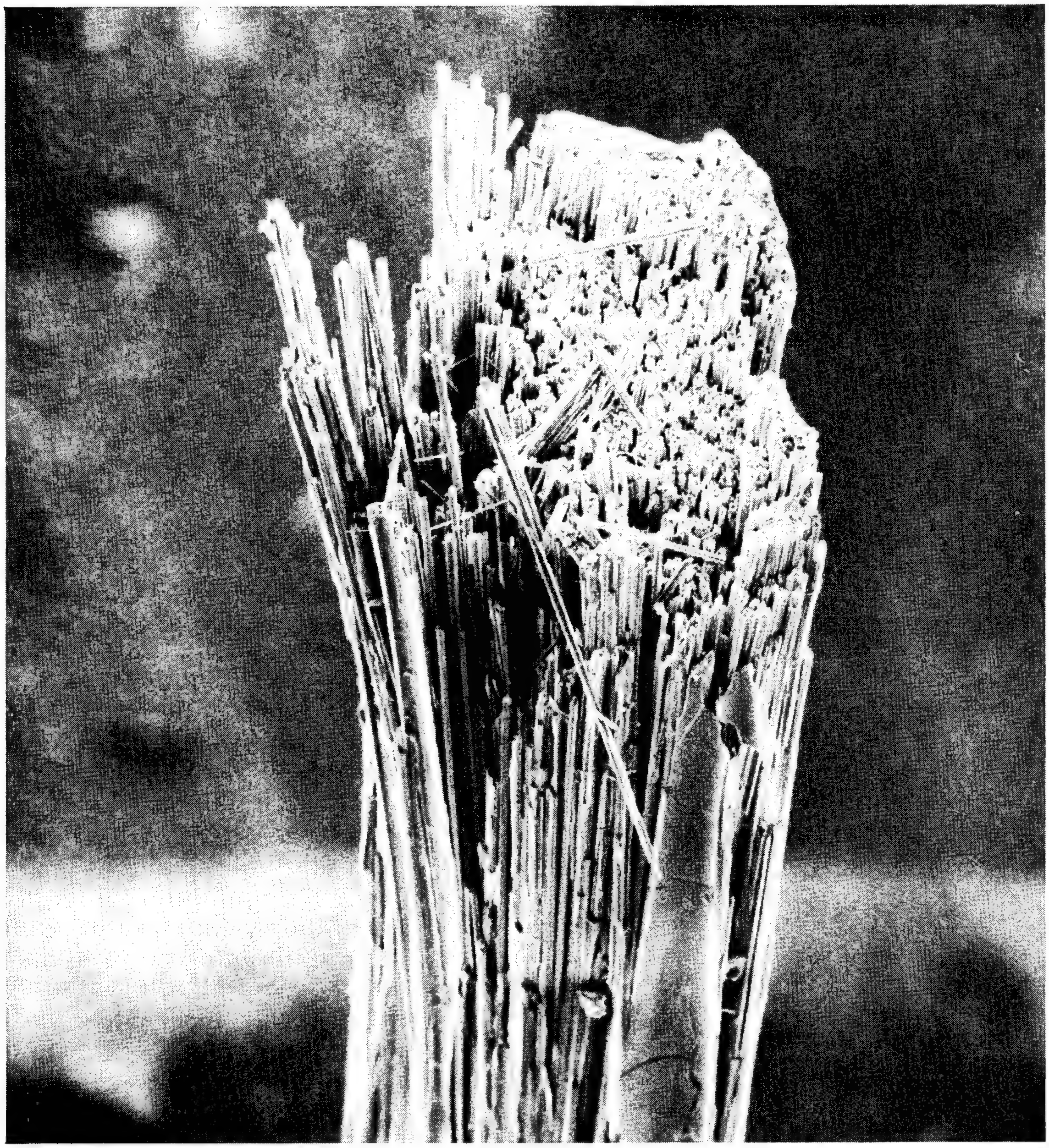

200×

Figure 16. - Sample 7 – Thornel 75 in GW-173, Pyrolyzed to 973°K, Repregged and Pyrolyzed to 973°K. Composite tensile strength = 0.86×10^9 N/m^2

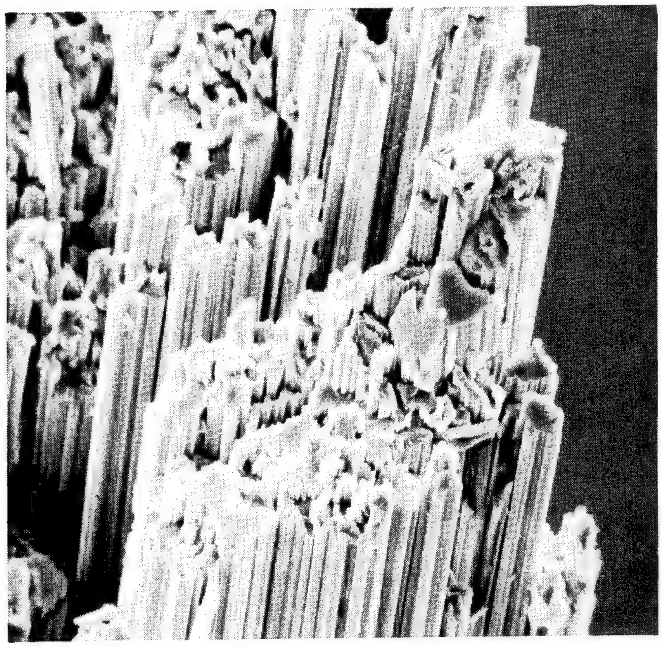

1000×

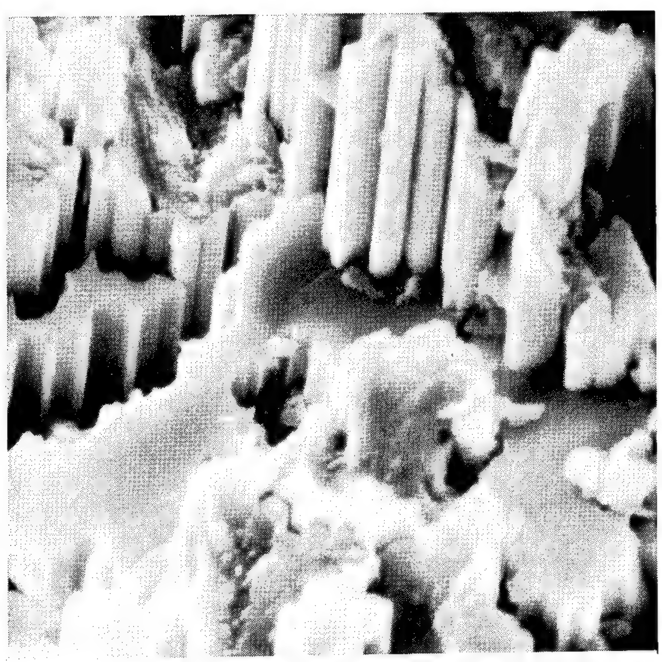

5000×

Figure 17. - Sample 7 – Fracture Surface, Region of Good Fiber-Matrix Bonding. Tensile strength = 0.86×10^9 N/m^2

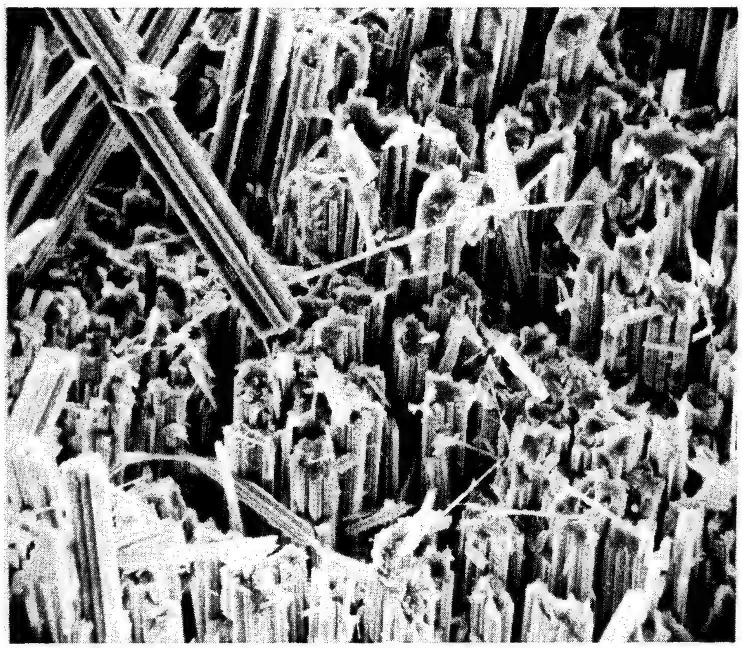

1000×

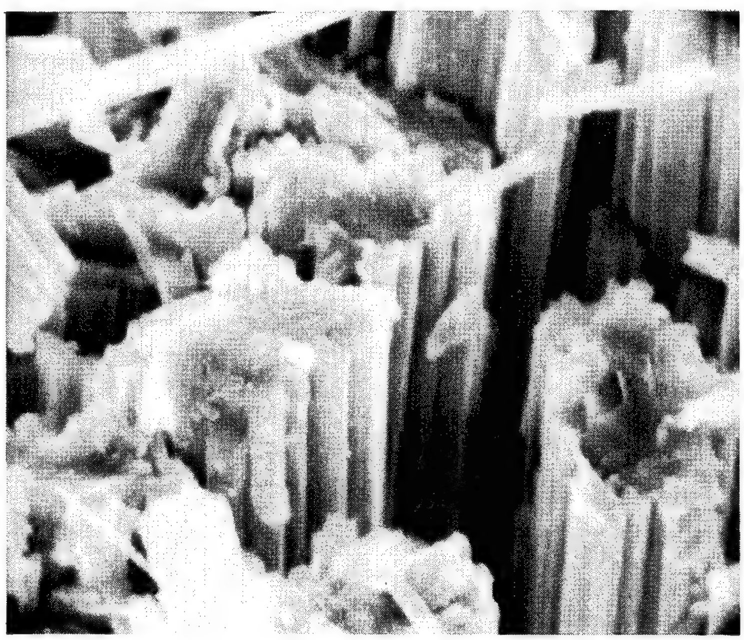

5000×

Figure 18. - Sample 7 – Fracture Surface, Region of Poor Fiber-Matrix Bonding. Tensile strength = 0.86×10^9 N/m^2

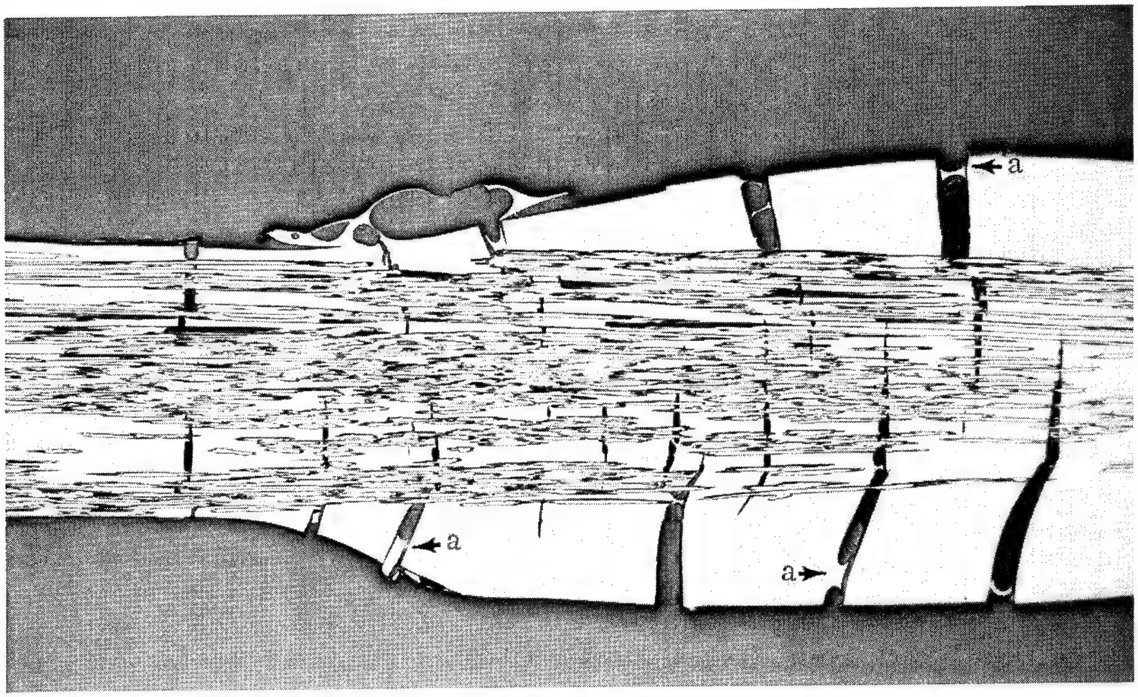

75×

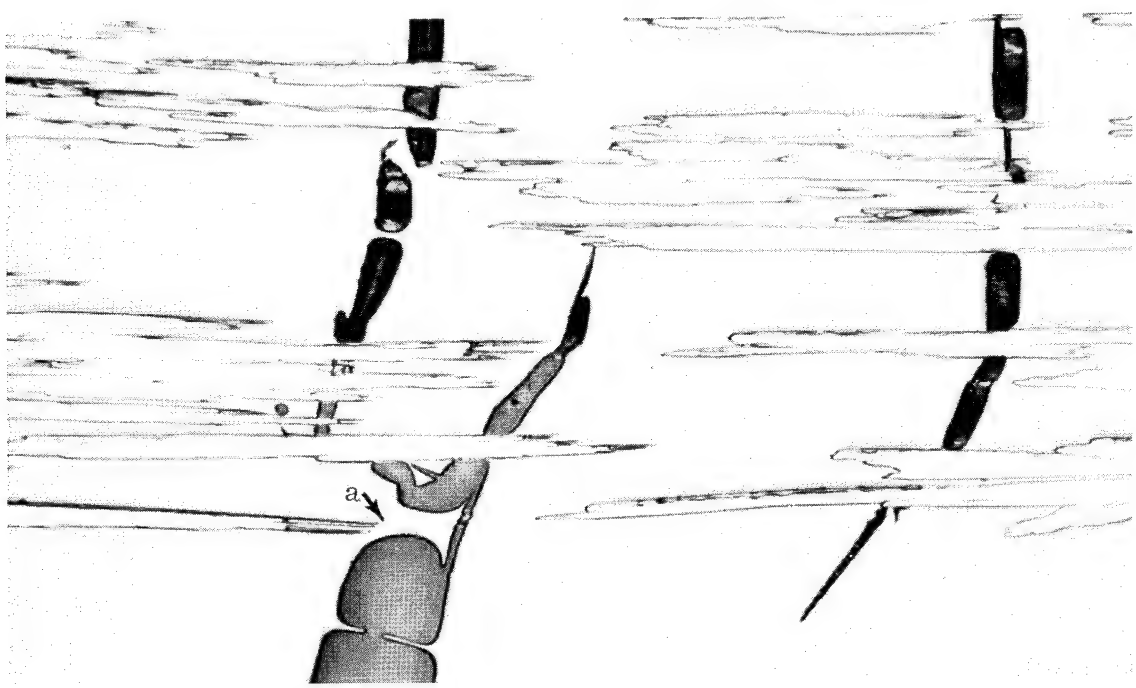

500×

Figure 19. - Sample 8 – Thornel 75 in GW-173, Pyrolyzed to 1273° K, Repregged and Pyrolyzed to 1173° K, Longitudinal Cross Section, Untested Monofilament

improvement in the tensile load was only marginal (Table XX, row 6), and beading was not eliminated (Figure 20). However, large pyrolysis cracks found in matrix-rich surface beads were not translated into large cracks normal to the fiber axis within the fiber bundle. Refinement of this technique to eliminate surface beading might result in some improvement.

It was concluded that neither double pyrolysis and prepregging nor the hot-melt resistance-preg procedure offered any advantage over the solvent-controlled pregging conventional pyrolysis procedure used in the screening tests.

To develop further understanding of pyrolysis interactions in the Thornel-75/GW-173 system, a study was initiated to determine the properties of carbon composite monofilaments as a function of pyrolysis temperature. Monofilament properties were measured after both cure and pyrolysis to temperatures ranging from 673°K (400° C) to 1273°K 1000°C). Results are plotted in Figure 21. Best results were obtained at 673° K (400° C), when the weight loss is only 20 percent. The greatest decrease in monofilament properties occurs between 673° K and 973° K, during which time the weight loss has reached 38 percent. Results are tabulated in detail in Table XXI. There is a decrease in tensile load with increasing heat-treatment temperature, and a decrease in tensile stress when calculated on the basis of fiber area alone. When corrected for the total area, the apparent strength retention increases between 973° K and 1,273°K because shrinkage of the matrix results in a smaller volume fraction of matrix.

Similar effects were observed with Hitco 50 and Modmor I (Table XXII), except that the apparent fiber degradation was more severe.

This degradation in monofilament properties does not result from degradation of the fiber properties, but as a result of cracks forming in the matrix during pyrolysis. Scanning electron microscopy shows that the monofilament surface is crack free after a high temperature cure to 673° K. Cracks start developing at 743°K (470°C) and become more severe as the pyrolysis temperature is increased.

That the apparent degradation observed does not result from degradation of the fiber, but from cracking of the matrix, is indicated by the experiments described in Table XXIII. Degradation of fiber properties as a result of heat treatment alone does not occur with Thornel 75, as indicated by comparing samples 1 and 2. Some degradation (14 percent) occurs when Hitco 50 is similarly heat-treated.

When Thornel 75 is pyrolyzed, the apparent strength retention is only 53 percent. However, if such pyrolyzed fiber is repregged with epoxy (sample 4) to measure the true fiber strength, the retention is 81.5 percent. This suggests that the poor properties observed in pyrolyzed materials result from degradation of matrix properties and possibly fiber-matrix debonding.

The influence of pyrolysis cracking on the tensile strength was studied in detail by scanning electron microscopy. The fracture surface of a sample of Thornel 75 in GW-173, which was heat-treated to 673°K, is shown in Figure 22. There are no external circumferential pyrolysis cracks. One longitudinal crack exists, but this appears to be definitely associated with the fracture of the monofilament, which failed

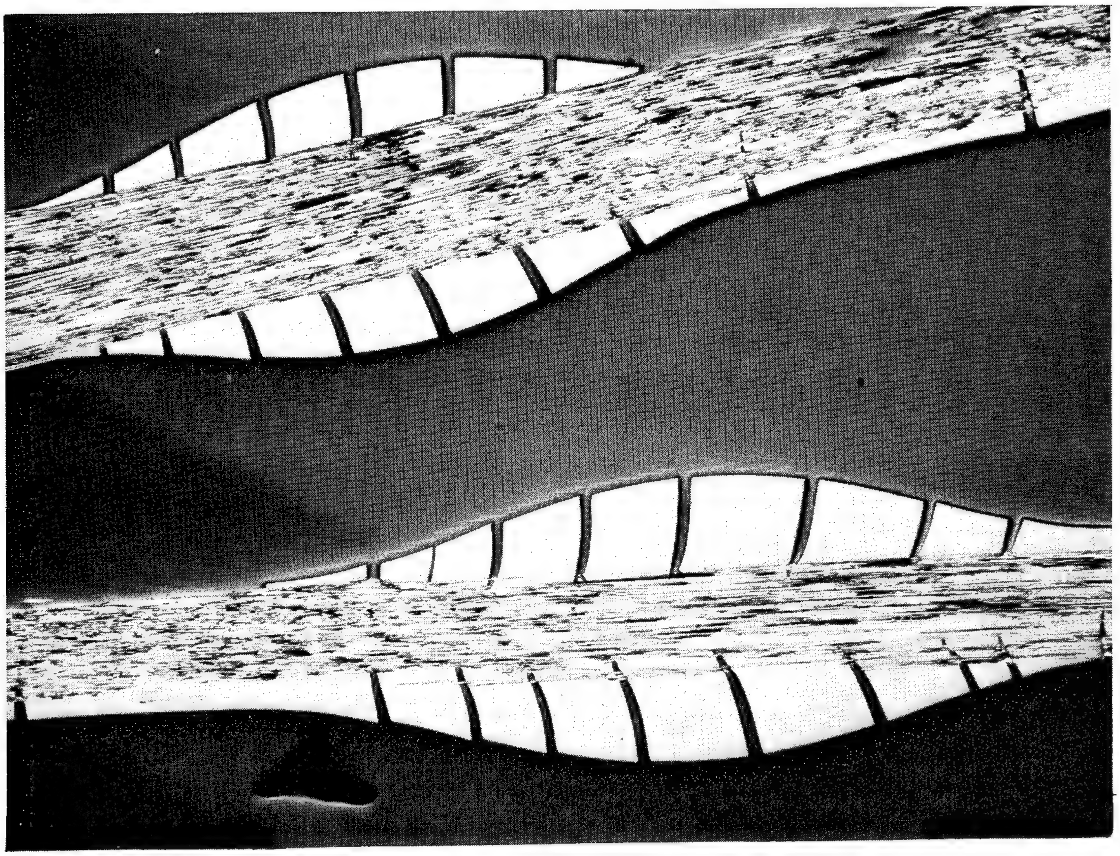

40×

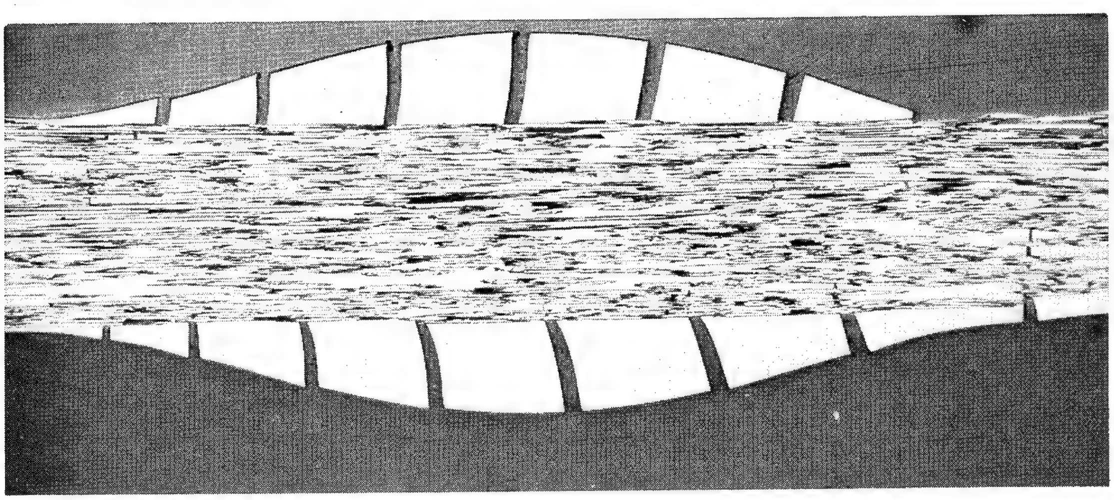

75×

Figure 20. - Sample 9 – Thornel 75 in GW-173, Hot Melt Pregged at 453°K, Pyrolyzed at 1273°K

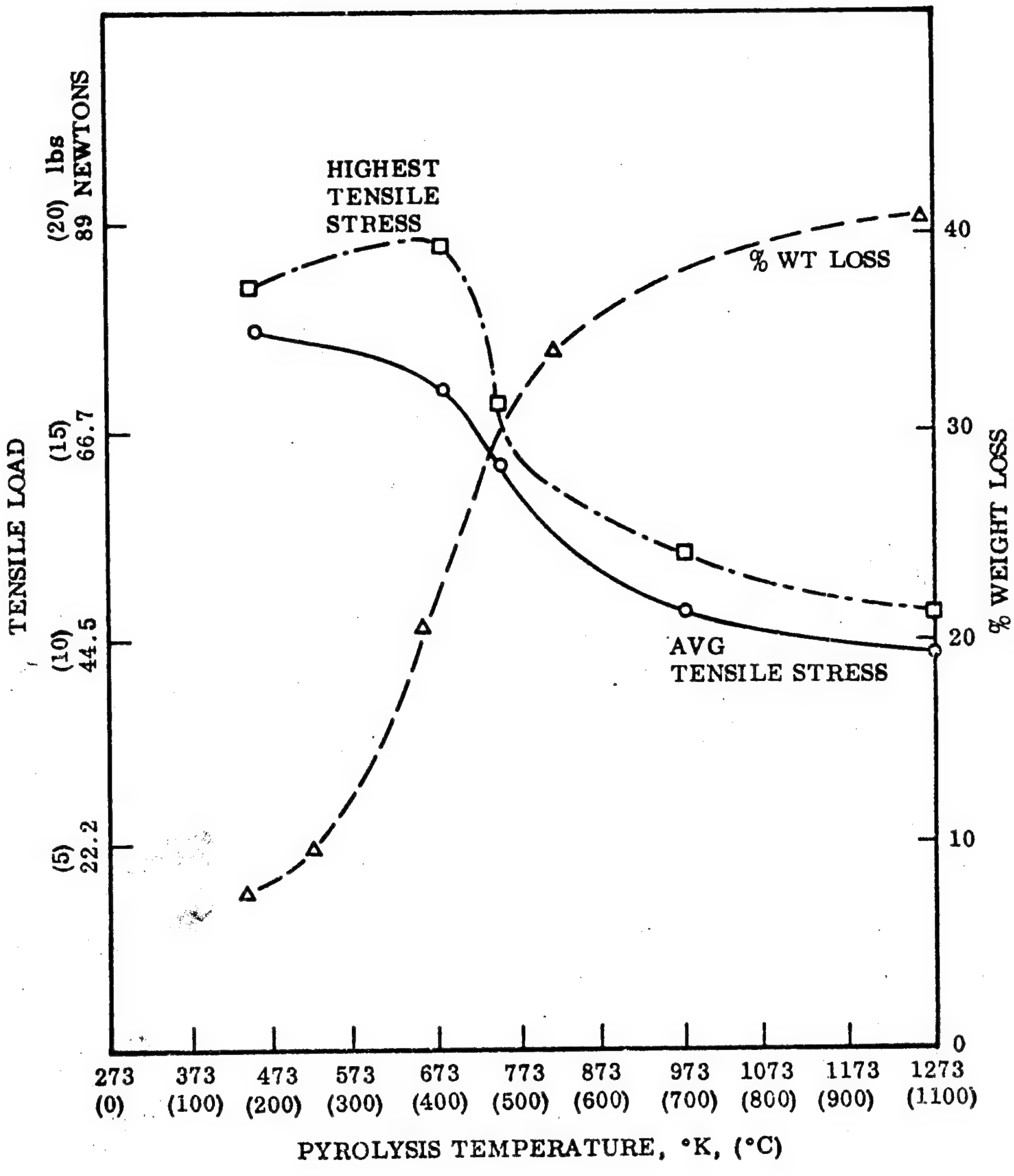

Figure 21. - Composite Monofilament Properties As a Function of Pyrolysis Temperature (Thornel 75 in GW-173)

TABLE XXI. - EFFECT OF PYROLYSIS TEMPERATURE ON MONOFILAMENT PROPERTIES
(Thornel 75 in 70-Percent GW-173)

Pyrolysis Temperature		Function (a)	Tensile Load		Tensile Stress (Fiber Area)		% Matrix	Tensile Stress (Fiber + Matrix)		% Of As Cured Data
°K	°C		Newtons	lbs	$n/m^2 \times 10^9$	$psi \times 10^5$		$n/m^2 \times 10^{+9}$	$psi \times 10^{+5}$	
450	177	$\overline{x}$	76.5	17.4	2.48	3.60[b]	29.9	1.54	2.23	–
		σ	3.1	0.7	0.09	0.14	–	0.07	0.09	–
		$\sigma/\sqrt{n}$	1.3	0.3	0.02	0.06	–	0.03	0.04	–
673	400	$\overline{x}$	71.1	16.0	2.28	3.30	38.1	1.16	1.68	75
		σ	16.9	3.8	0.54	0.78	–	0.28	0.40	–
		$\sigma/\sqrt{n}$	6.2	1.4	0.20	0.29	–	0.11	0.15	–
743	470	$\overline{x}$	62.8	14.1	2.01	2.91	39.7	1.00	1.45	65
		σ	5.8	1.3	0.17	0.27	–	0.09	0.13	–
		$\sigma/\sqrt{n}$	1.8	0.4	0.06	0.08	–	0.03	0.04	–
973	700	$\overline{x}$	48.6	10.7	1.52	2.21	31.2	0.931	1.35	60
		σ	9.0	2.1	0.30	0.44	–	0.186	0.27	–
		$\sigma/\sqrt{n}$	3.6	0.8	0.12	0.17	–	0.069	0.10	–
1273	1000	$\overline{x}$	42.7	9.6	1.37	1.99	17.7	1.07	1.56	69
		σ	4.0	0.9	0.13	0.18	–	0.10	0.15	–
		$\sigma/\sqrt{n}$	1.8	0.4	0.06	0.08	–	0.04	0.06	–

a – Functions – $\overline{x}$ = mean, σ = standard deviation, $\sigma/\sqrt{n}$ = standard error.

TABLE XXII.- EFFECT OF HEAT TREATMENT TEMPERATURE ON MONOFILAMENT PROPERTIES (Hitco 50 And Mod I In 50-Percent GW-173)

Constituents	Heat Treatment Temperature		Function[a]	Tensile Load		Tensile Stress (Fiber Area)		% Matrix	Tensile Stress		% of As Cured Data
	°K	°C		Newtons	lbs	$n/m^2 \times 10^9$	psi $\times 10^5$		$n/m^2 \times 10^9$	psi $\times 10^5$	
Hitco 50 in 70% GW-173	450	177	$\overline{x}$	79.6	17.9	1.94	2.82	41.0	–	1.52	–
			σ	3.6	0.8	.07	0.13	–	–	.07	–
			$\sigma/\sqrt{n}$	1.3	0.3	.03	0.05	–	–	0.03	–
Hitco 50 in 70% GW-173	973	700	$\overline{x}$	40.1	9.02	1.01	1.47	38.7	.553	0.802	52.8
			σ	1.9	.43	0.05	0.07	–	0.03	0.038	–
			$\sigma/\sqrt{n}$	0.8	0.18	0.02	0.03	–	0.01	0.016	–
Hitco 50 in 70% GW-173	1273	1000	$\overline{x}$	33.8	7.6	0.86	1.24	26.4	0.603	0.874	57.5
			σ	3.6	0.8	0.09	0.13	–	0.063	0.092	–
			$\sigma/\sqrt{n}$	1.3	0.3	0.03	0.05	–	0.024	0.039	–
Mod I in 70% GW-173	450	177	$\overline{x}$	540	121.4	1.12	1.62	42.9	0.553	0.802	–
			σ	125	28.1	0.26	0.37	–	0.127	0.185	–
			$\sigma/\sqrt{n}$	55.6	12.5	0.12	0.16	–	0.055	0.080	–
Mod I in 70% GW-173	673	400	$\overline{x}$	699	157.2	1.44	2.09	47.6	0.632	0.917	114
			σ	120	26.9	0.25	0.36	–	0.108	0.157	–
			$\sigma/\sqrt{n}$	48.9	11.0	0.10	0.15	–	0.044	0.064	–
Mod I in 70% GW-173	973	700	$\overline{x}$	477	107.2	0.986	1.43	44.8	0.472	0.689	86
			σ	35.6	8.0	0.073	0.11	–	0.035	0.051	–
			$\sigma/\sqrt{n}$	16.0	3.6	0.033	0.05	–	0.016	0.023	–
Mod I in 70%	1273	1000	$\overline{x}$	184.6	41.5	0.380	0.551	31.3	0.249	0.361	45
			σ	2.7	0.6	0.007	0.010	–	0.005	0.007	–
			$\sigma/\sqrt{n}$	1.8	0.4	0.003	0.004	–	0.002	0.003	–

a – Functions – $\overline{x}$ = mean, σ = standard deviation, $\sigma/\sqrt{n}$ = standard error.

TABLE XXIII. - FIBER DEGRADATION DURING HEAT TREATMENT

Sample Number and Description	Function	Tensile Load		Tensile Stress (Fiber Area)		% Retention
		Newtons	lbs	$n/m^2 \times 10^9$	$psi \times 10^5$	
1. Thornel 75 (As Received)	$\overline{x}$	84.5	19.0	2.7	3.9	–
	σ	8.0	1.8	0.2	0.4	–
	$\sigma/\sqrt{n}$	2.8	0.63	0.1	0.1	–
2. Thornel 75, heat-treated to 1273° K, in vacuum, no matrix	$\overline{x}$	86.2	19.4	2.8	4.0	102
	σ	4.0	0.9	0.1	0.2	–
	$\sigma/\sqrt{n}$	1.8	0.4	0.05	0.1	–
3. Thornel 75, in GW-173, pyrolysed to 1273° K	$\overline{x}$	35.1	7.9	1.13	1.64	53
	σ	17.4	3.9	0.54	0.78	–
	$\sigma/\sqrt{n}$	6.7	1.5	0.21	0.31	–
4. Thornel 75, same as sample 3, but repregged with epoxy-815	$\overline{x}$	67.5	15.4	2.19	3.18	81.5
	σ	8.7	1.95	0.28	0.40	–
	$\sigma/\sqrt{n}$	3.6	0.80	0.12	0.17	–
						–
5. Hitco 50 (As Received)	$\overline{x}$	85.5	19.2	2.16	3.13	–
	σ	11.2	2.4	0.27	0.39	–
	$\sigma/\sqrt{n}$	3.1	0.7	0.08	0.11	–
6. Hitco 50, same condition as sample 2	$\overline{x}$	73.8	16.6	1.86	2.7	86
	σ	6.7	1.15	0.13	0.2	
	$\sigma/\sqrt{n}$	2.2	0.5	0.05	0.1	

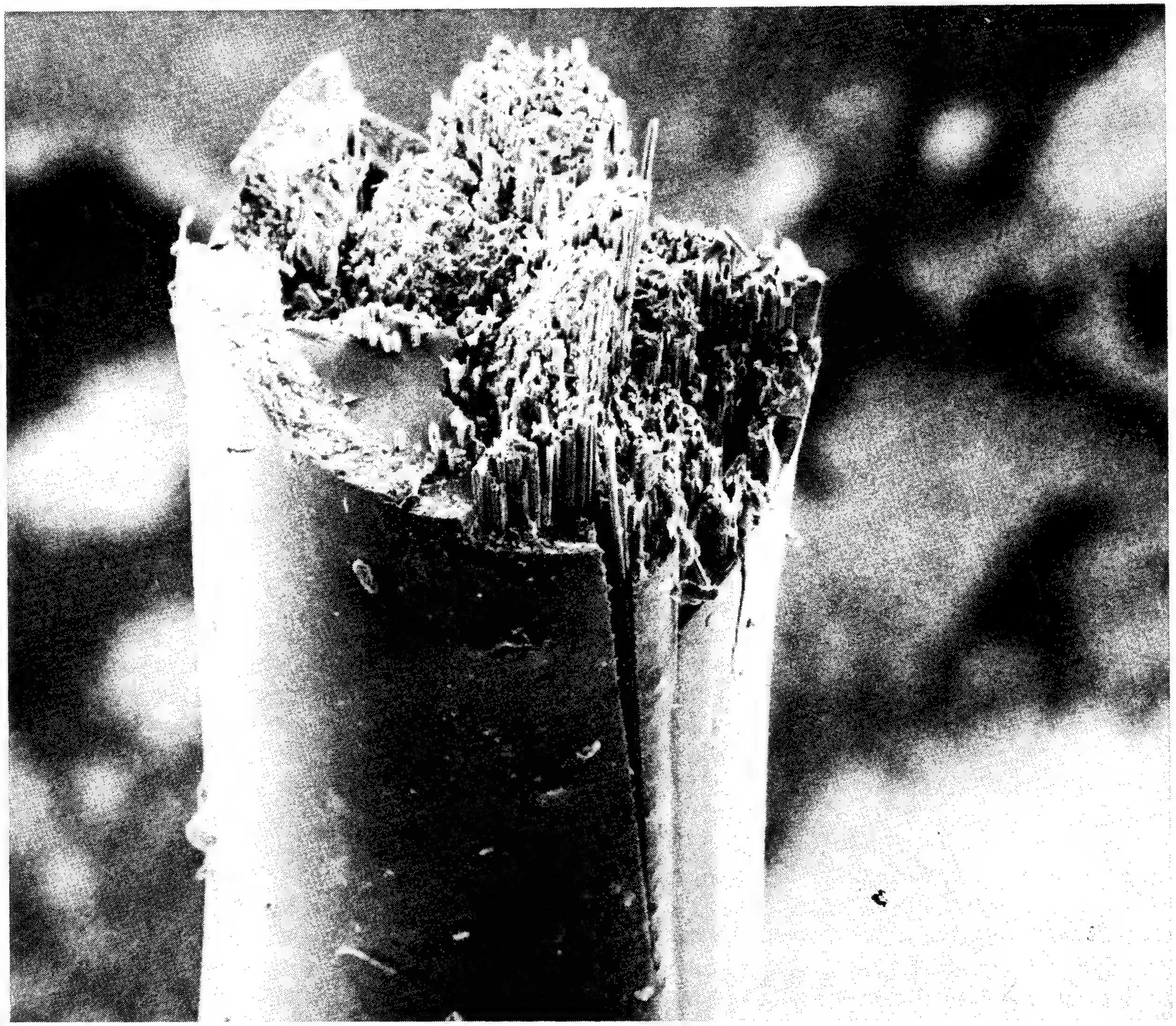

200×

Figure 22. - Sample 1 – Thornel 75 in GW-173, Postcured to 673° K, Composite Tensile Stress = 1.44×10^9 N/m^2. Maximum value observed after pyrolysis to 673° K (Row 2, Table XXI)

at a fiber tensile stress of 1.44×10^9 N/m^2 (2.08×10^5 psi).* Close examination of the fracture surface (Figure 23) indicates a fairly good bond between fiber and matrix and the absence of pyrolysis cracks. After pyrolysis to 743° K, a 30-percent weight loss has occurred and the monofilament bundle is no longer matrix rich (Figures 24 and 25). The fracture surface consists primarily of fibers with small fragments of matrix adhering to it (Figure 25), which indicates excellent fiber-matrix bonding. This sample failed at 1.09×10^9 N/m^2 (1.57×10^5 psi).* Another sample pyrolyzed to the same temperature (743°K) had excessive circumferential pyrolysis cracking (Figure 26) and failed at a fiber tensile stress of 0.86×10^9 N/m^2 (1.25×10^5 psi).*

After pyrolysis to 1273° K, monofilament degradation can be severe. Sample 4 is a representative monofilament with a tensile strength of 0.97×10^9 N/m^2 (1.41×10^5 psi), in which fibers are loosely bonded and held (Figure 27), and the fiber-matrix bonding is not good. Extensive pyrolysis cracking occurs both parallel and normal to the monofilament axis (Figure 28). However, in a "good" fiber, maximum tensile strength is 1.17×10^9 N/m^2(1.71×10^5 psi);*degradation is less severe. Sample 5 is representative of such a monofilament (Figures 29 and 30). Pyrolysis cracking is much less severe and there is excellent bonding between fiber and matrix (Figure 30). The fiber bundle is well impregnated and no interior regions are resin poor.

The tensile strength (corrected for matrix cross-section area) increases between 973 and 1273° K because volume shrinkage of the matrix results in a reduced cross-section area.

The effect of pyrolysis cracking may also be studied by examining the longitudinal axis of a carbon-carbon monofilament. A sample which was heat-treated to 673° K is shown in Figure 31). There is no cracking in the matrix in regions away from the fracture surface. This sample failed at 1.41×10^9 N/m^2 (2.04×10^5 psi)*and fracture was initiated in the matrix. After heat-treatment to 743° K, pyrolysis cracking perpendicular to the fiber axis had been initiated (Figure 32), and the composite fiber tensile strength dropped to 1.09×10^9 N/m^2 (1.58×10^5 psi). *

As indicated previously, the hypotheses that the apparent degradation of properties does not result from degradation of the fiber properties but by degradation of the matrix was shown by taking a sample which had been pyrolyzed to 1273° K and repregging it with epoxy. The resultant composite (Figure 33) had a fiber tensile strength of 2.19×10^9 N/m^2 (3.18×10^5 psi).** Examination of the fracture surface (Figure 34) indicates that there is excellent bonding between the fiber and matrix with small fragments of matrix adhering to the fiber surface.

To summarize this study, degradation of monofilament properties with pyrolysis temperature is associated with shrinkage of the matrix and consequent pyrolysis cracking. Variation in monofilament properties at a given pyrolysis temperature is apparently associated with variation in matrix impregnation, excessive pyrolysis cracking, and/or poor fiber-matrix bonding in localized regions.

---

*Calculated on the basis of fiber plus matrix cross-sectional area. Unless otherwise indicated, samples are representative of individual data points used in tabulating Table XXI.

**Calculated on the basis of fiber cross-sectional area only, representative of samples of Type 4 (Table XXIII).

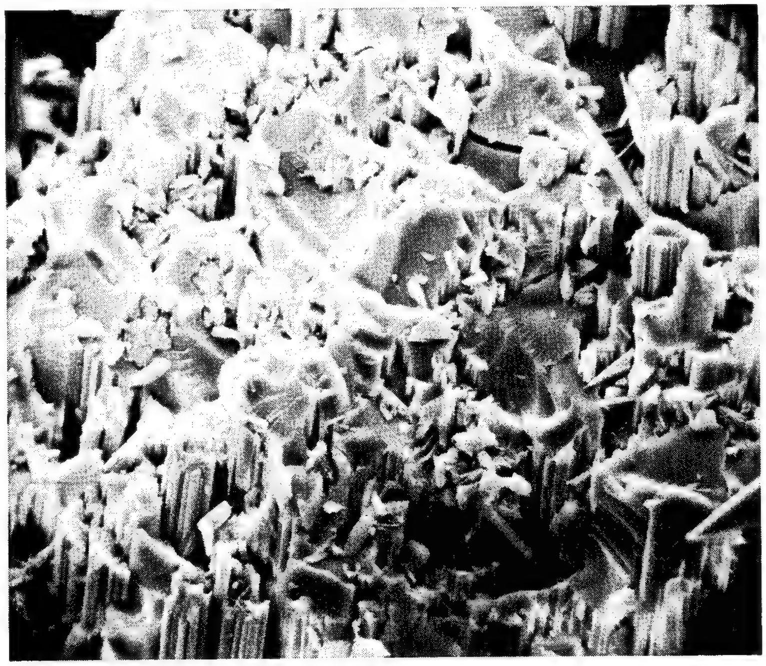

1000×

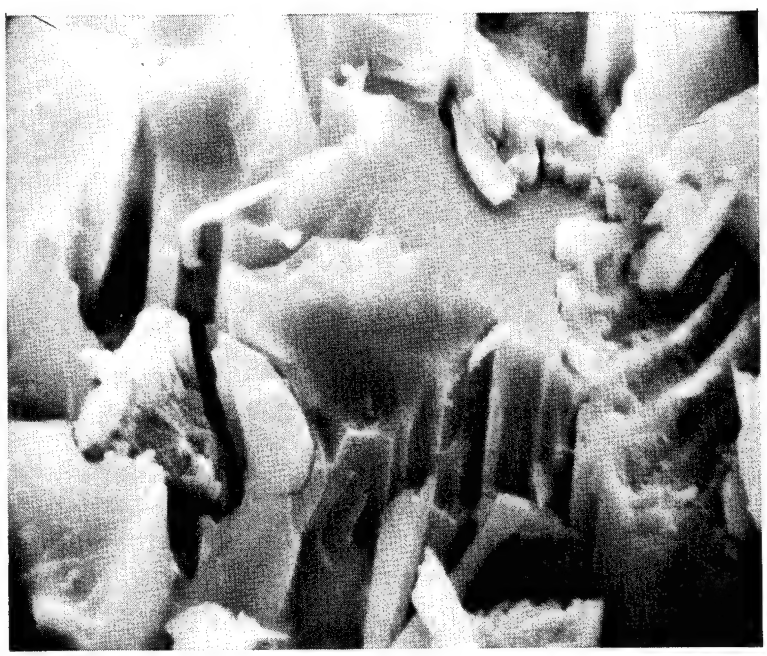

5000×

Figure 23. - Sample 1 – Fracture Surface, Postcured to 673°K. Maximum composite tensile strength = 1.44×10^9 N/m^2 (Row 2, Table XXI)

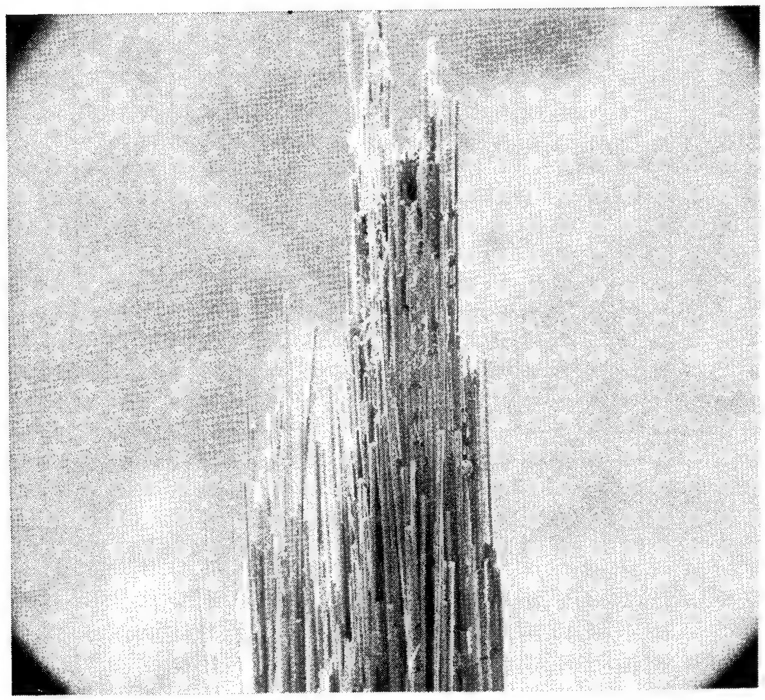

110×

Figure 24. - Sample 2 – Thornel 75 in GW-173, Pyrolyzed to 743°K. Composite tensile strength = 1.1×10^9 N/M^2, maximum value observed at this heat-treatment condition (Row 3, Table XXI)

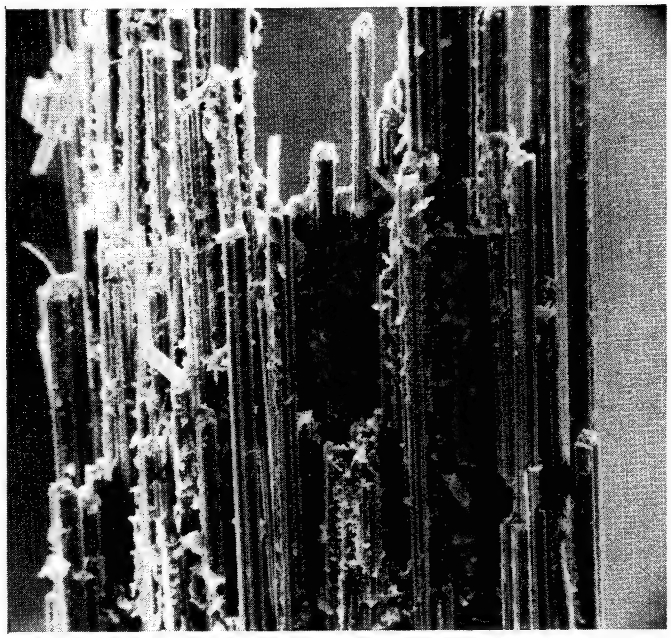

550×

2200×

Figure 25. - Sample 2 – Fracture Surface, Pyrolyzed to 743°K. Maximum composite tensile strength = 1.1×10^9 N/m^2 (Row 3, Table XXI)

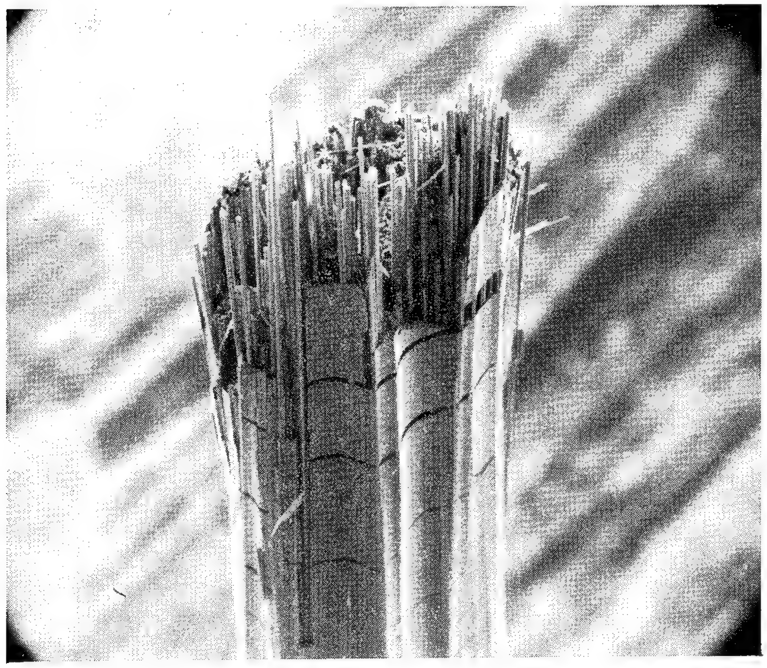

110×

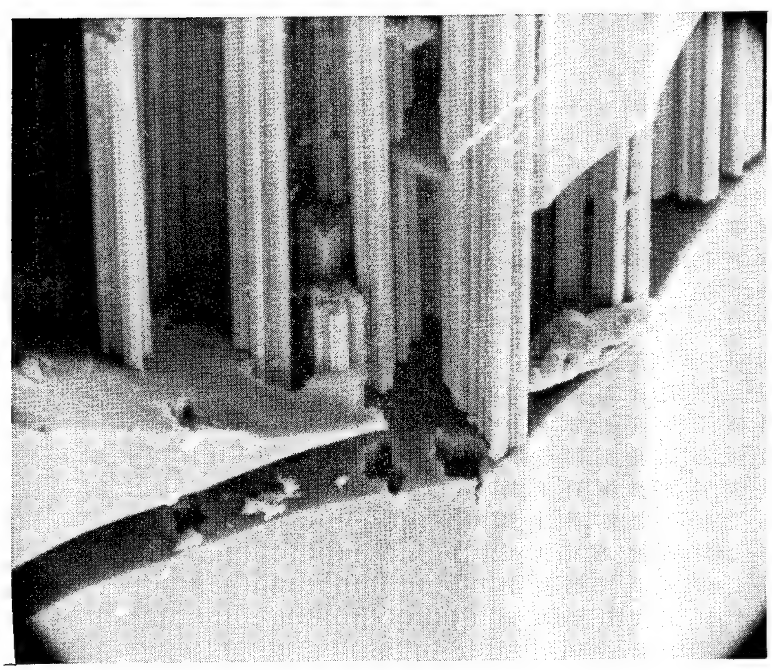

1100×

Figure 26. - Sample 3 – Pyrolyzed to 743° K With Excessive Pyrolysis Cracking. Composite tensile stress = 0.86×10^9 N/m^2

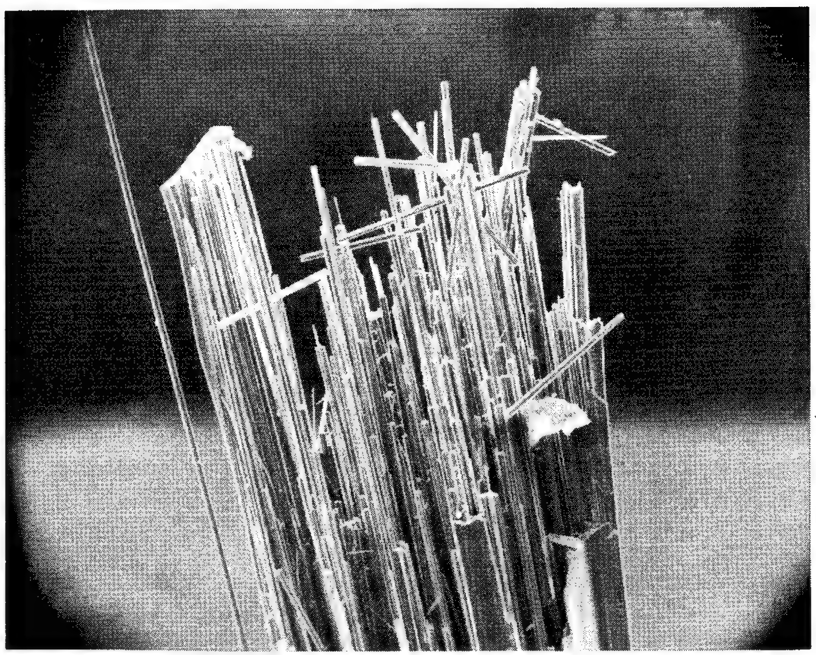

130×

1900×

Figure 27. - Sample 4 – Representative of Low-Strength Monofilament, Thornel 75 in GW-173, Pyrolyzed to 1273°K. Individual monofilament failed at composite tensile strength = 0.97×10^9 N/m^2

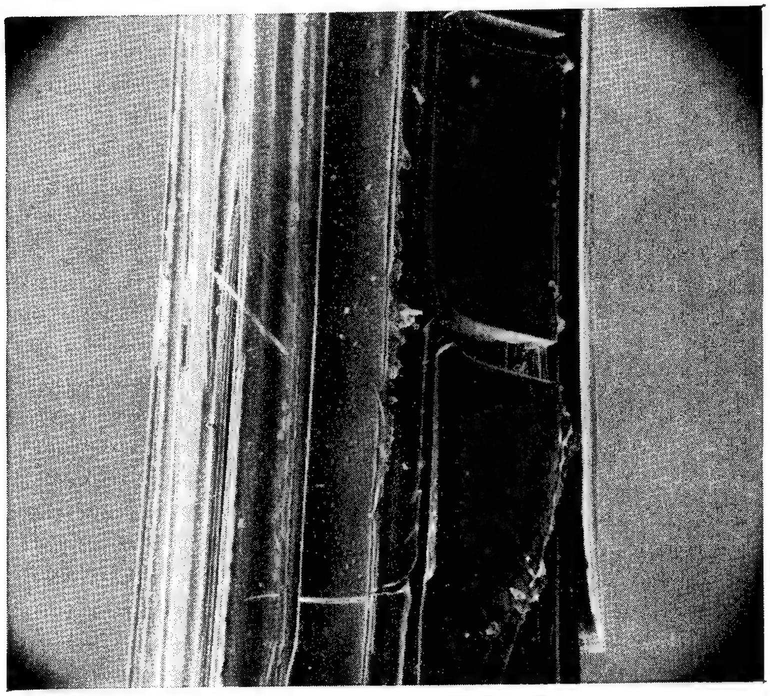

190×

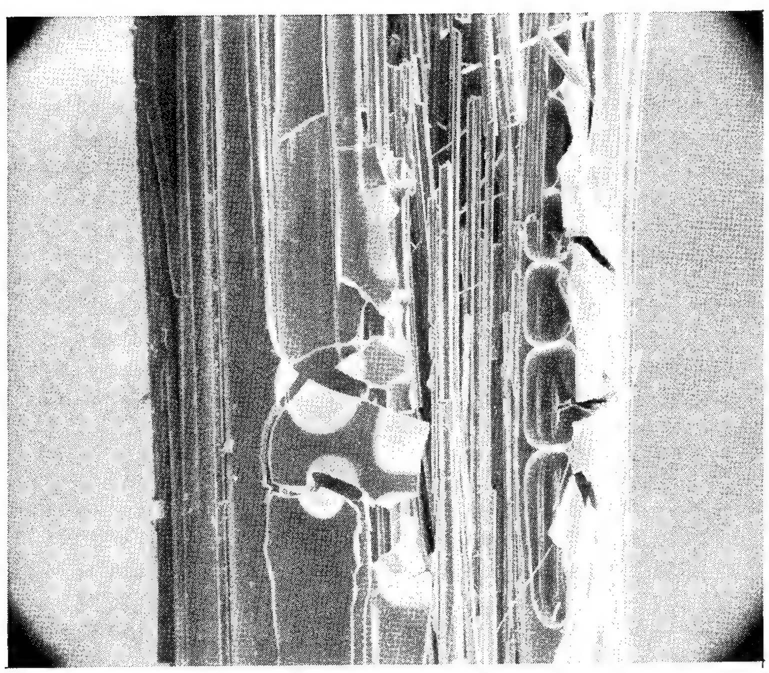

190×

Figure 28. - Sample 4 — Pyrolysis Cracking. Composite tensile strength = 0.97×10^9 N/m^2

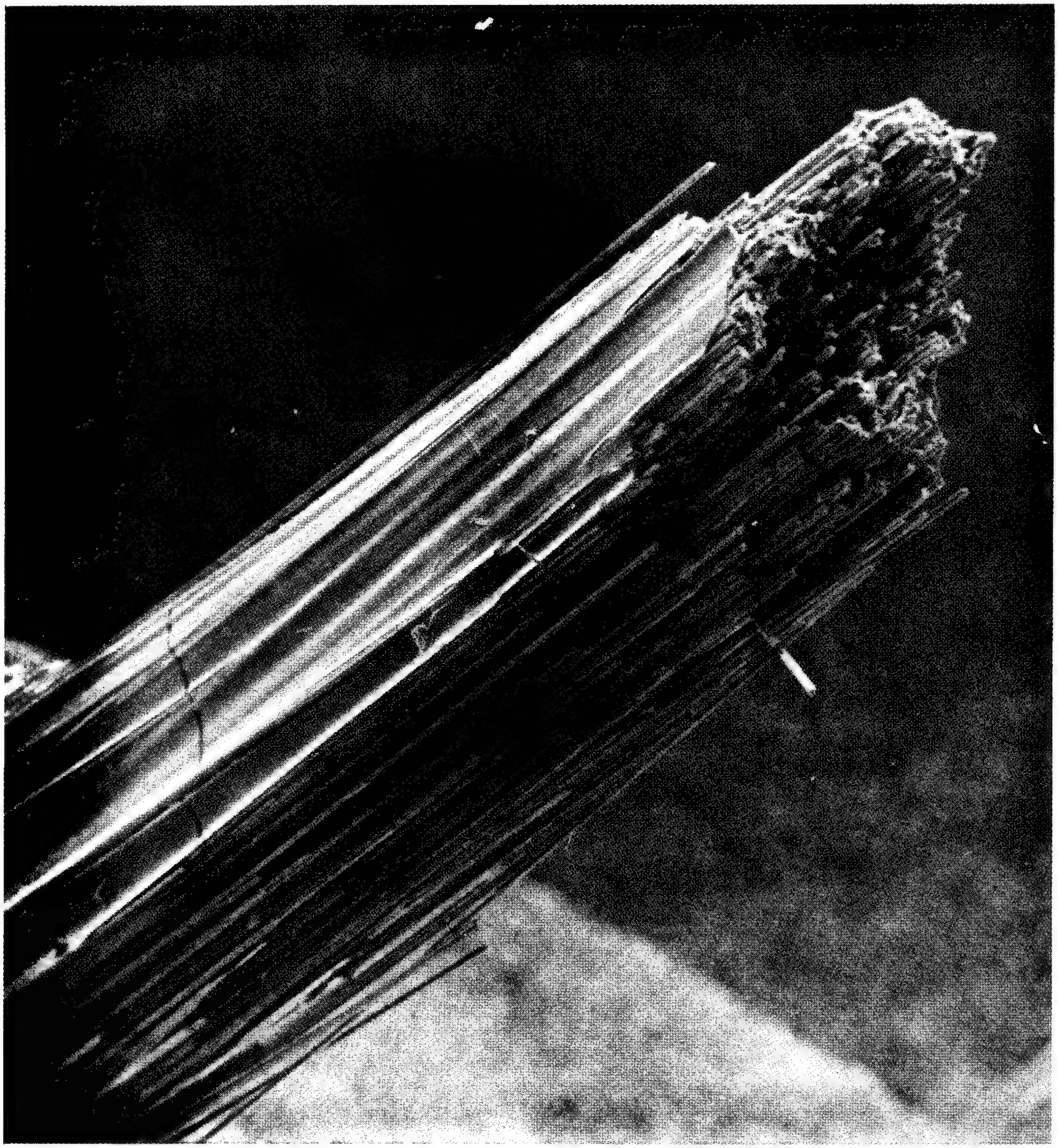

200×

Figure 29. - Sample 5 – Representative of Higher-Strength Monofilament, Thornel 75 in GW-173, Pyrolyzed to 1273° K. Maximum composite tensile strength = 1.17×10^9 N/m^2 (Row 5, Table XXI)

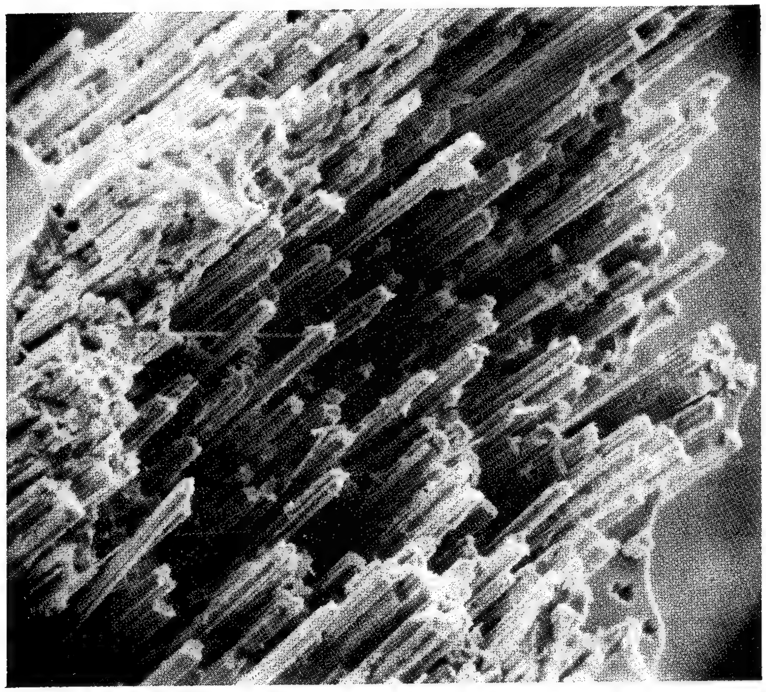

500×

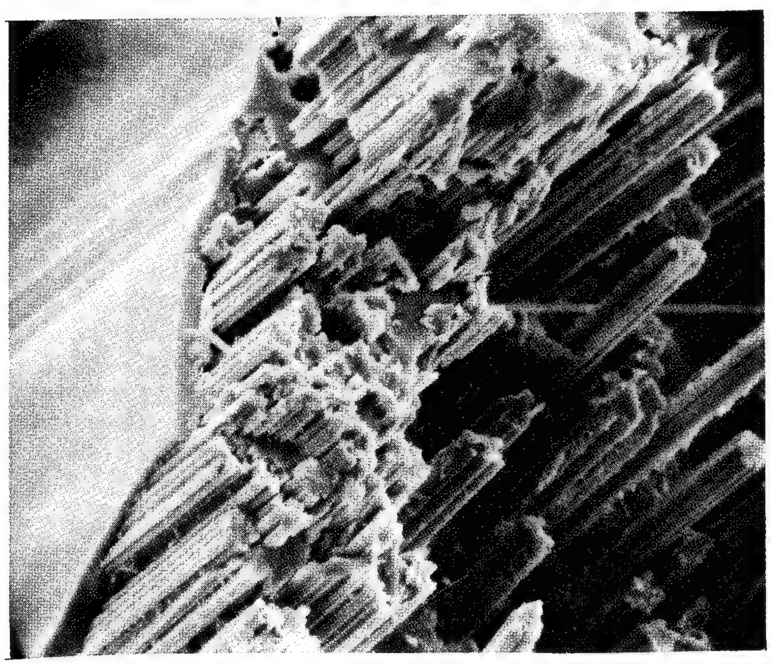

1000×

Figure 30. - Sample 5 – Fracture Surface. Composite Tensile strength = 1.17×10^9 N/m^2

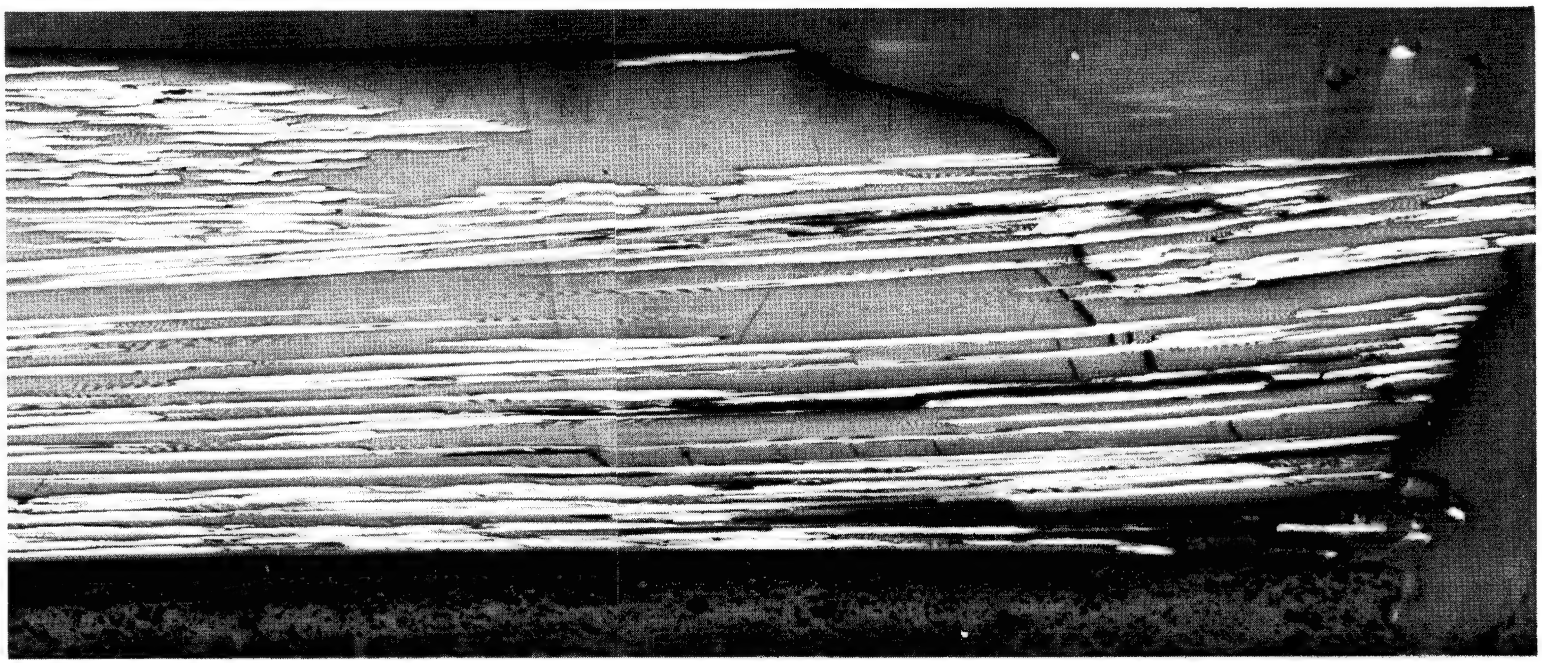

200×

Figure 31. - Longitudinal Cross Section of Thornel 75 in GW-173 Heat-Treated to 673° K. Composite tensile strength = 1.41×10^9 N/m^2 (individual value)

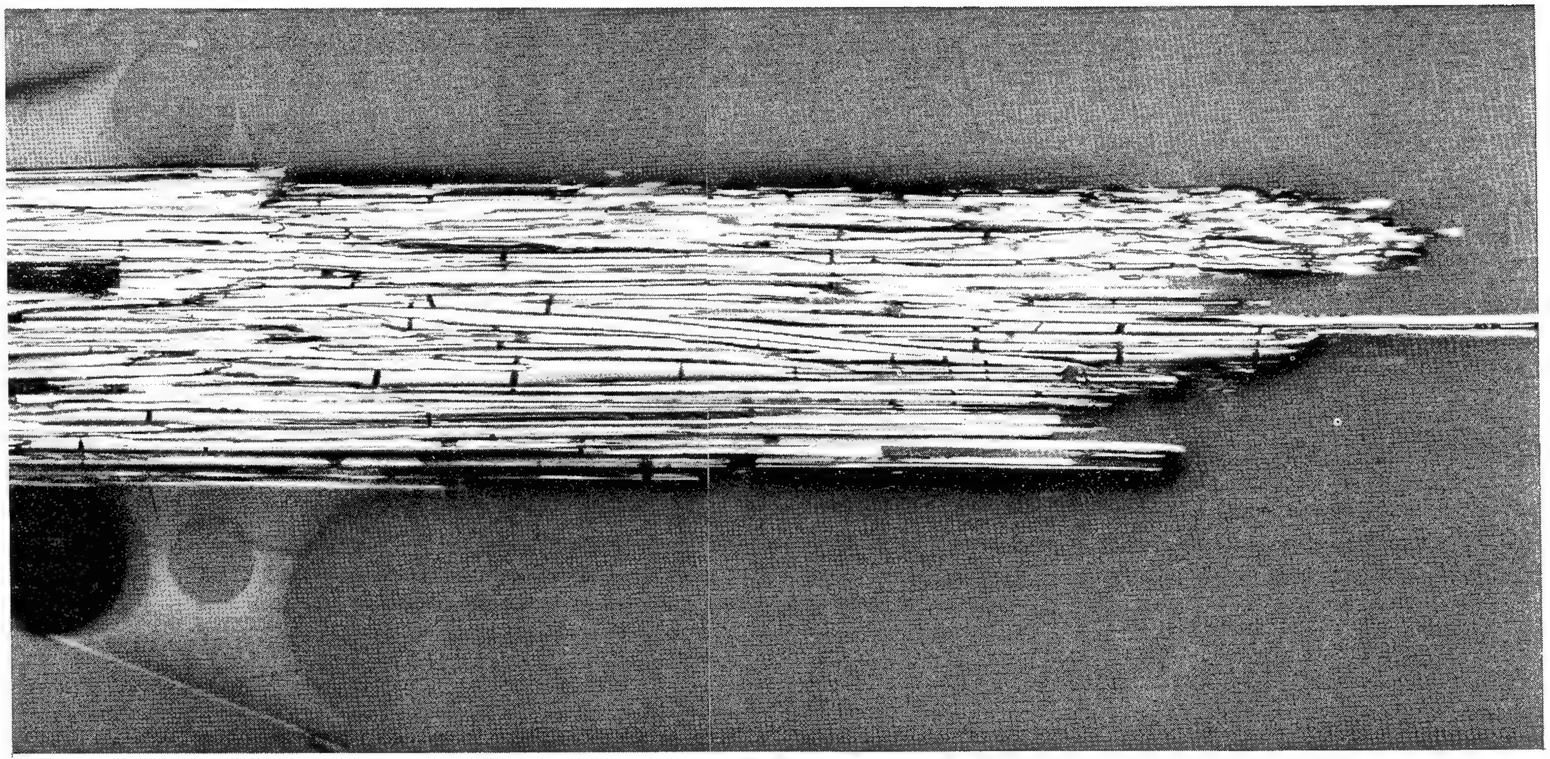

100×

Figure 32. - Pyrolysis Cracking Observed in a Thornel 75/GW-173 Monofilament Heat-Treated to 743° K. Composite tensile strength = 1.09×10^9 N/m^2

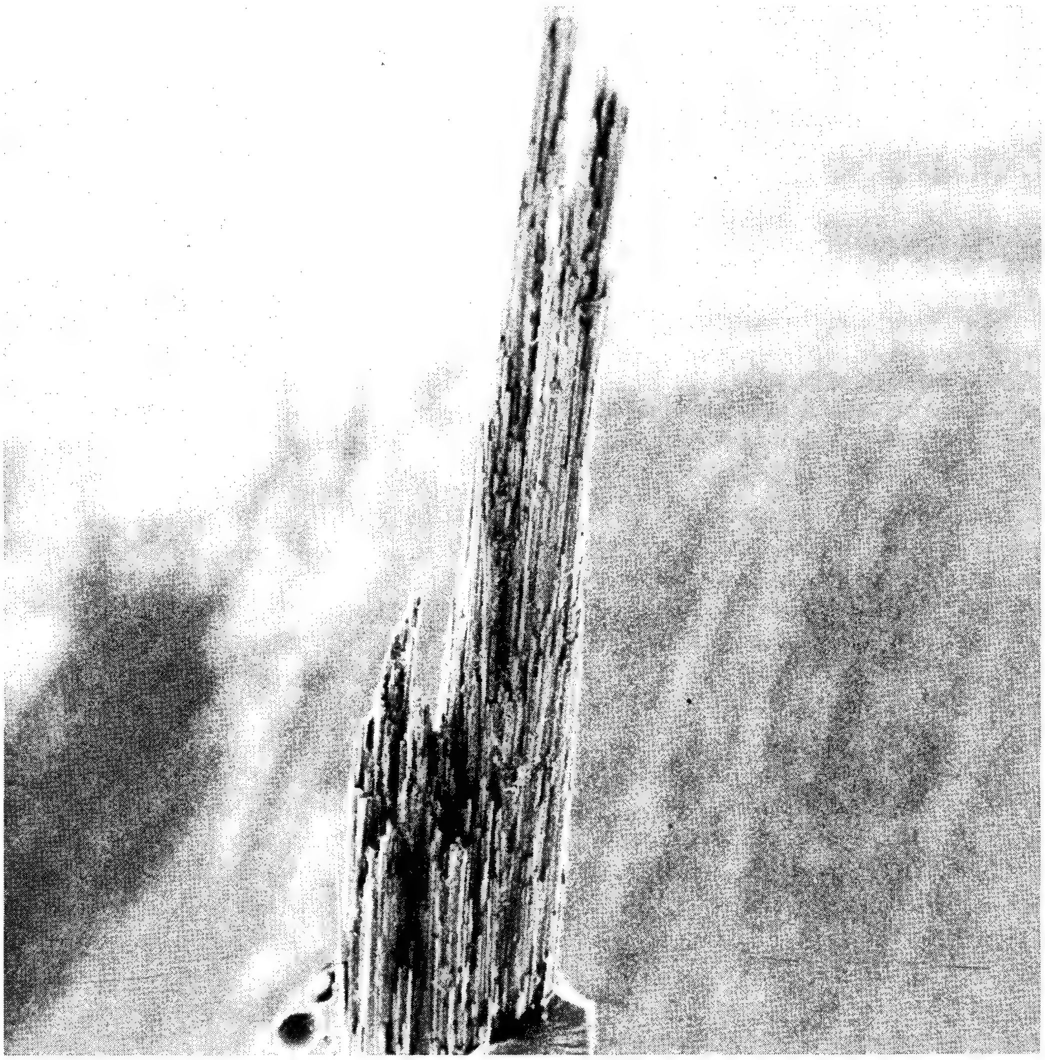

100×

Figure 33. - Sample 6 – Thornel 75 in GW-173, Pyrolyzed to 1273°K, Repregged With Epoxy. Fiber tensile stress = 2.19×10^9 N/m^2 (Sample Type 4, Table XXIII)

1000×

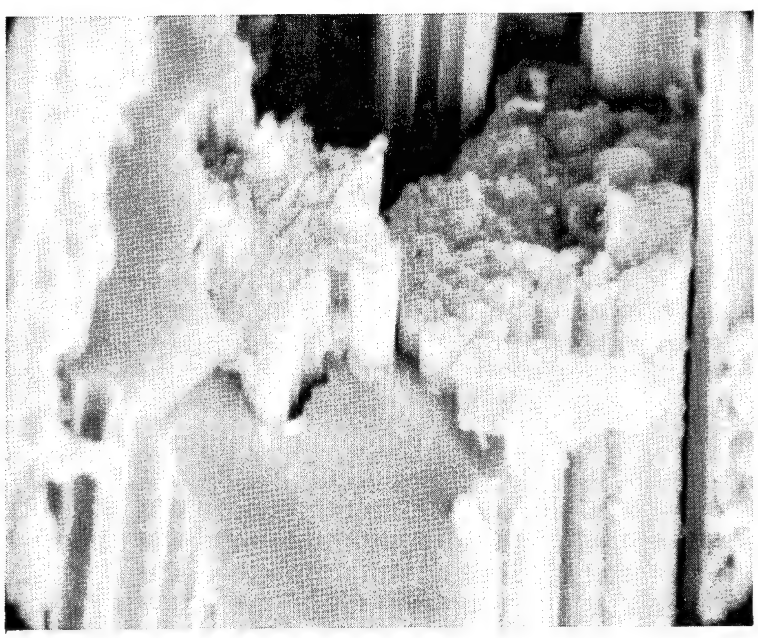

5000×

Figure 34. - Fracture Surface, Pyrolyzed to 1273°K, Repregged With Epoxy. Fiber tensile stress = 2.19×10^9 N/m^2 (Sample Type 4, Table XXIII)

3.6 ADVANCED CONCEPTS

Preliminary studies were conducted in the latter part of the program to develop advanced concepts which would reduce the problems associated with matrix discontinuity, interfacial bonding, and low strain-to-failure. Two approaches were investigated: a higher strain-to-failure matrix derived from resin modified with coal tar pitch, and fiber/matrix copyrolysis.

3.6.1 Pitch-Modified Resin

Mackay and Courtney (Ref. 21) performed work with a coal tar pitch, PR-275, which reacts with phenol-formaldehyde resins. The addition of 20- to 30-percent pitch to a phenol-formaldehyde resin upon pyrolysis reportedly produced a significantly higher char yield and a graphitizable carbon. Following procedures described by Mackay and Courtney, a thermosetting resin was prepared with 20 percent by weight of PR-275 (a coal tar pitch) in GW-173.

A viscosity sufficiently low for pregging operations was obtained by the addition of 30 percent (by volume) of tetrahydrofuran solvent. Sample specimens were prepared by casting and curing the resin in an aluminum dish. This material was then removed from the aluminum dish, sectioned, pyrolyzed, and heat-treated to determine the following thermogravimetric data:

Heating Cycle	Weight Loss
8.6×10^4-sec cure @ 350°K	Solvent loss and resin set
6.5×10^4-sec post-cure @ 473°K	6%
473°K to 1273°K in 26×10^4 sec	39%
1273°K to 2273°K in 17.3×10^4 sec	6%

The work by Mackay and Courtney indicates a 74-percent char yield for pyrolysis from 473°K to 1113°K. In comparison, we have demonstrated a 61-percent char yield for pyrolysis 160°K higher to 1273°K. A 13-percent weight loss from 1113°K to 1273°K must be associated with sulfur or similar species since only hydrogen has sufficient bond energy to remain in the system at this temperature range. After heat treatment to 2273°K, the carbon is uniformly black and hard.

To determine the graphitizability, a specimen of 20-percent PR-275 in GW-173 was pyrolyzed and heat-treated to 2773°K for 15 min. X-ray diffraction determined an interlayer spacing (d_{002}) of 3.49×10^{-10} m and peak half-width ($B_{1/2}$) of 0.075 rad (4.3 deg). These values are only slightly lower than $d = 3.56 \times 10^{-10}$ m and $B_{1/2} = 0.087$ rad (5.0 deg) for glass-like carbon produced from GW-173 precursor resin heat-treated to the same condition.

Composite specimens of Thornel 75 (PVA) pregged with the 20-percent pitch resin system were prepared by the batch process, oven-cured to 473°K and pyrolyzed to 1273°K. The pyrolyzed specimens were then heat-treated to higher temperatures

prior to determining tensile strength. The composite properties after curing, pyrolysis, and high-temperature heat treatment are summarized in Table XXIV, and tensile strength versus heat treatment is shown graphically in Figure 35. The fiber-matrix volume fractions reported are actual measured values which indicate a small batch-to-batch variation but, in general, agree. A maximum composite strength of 1.12×10^9 N/m^2 (1.63×10^5 psi) was developed after 2273°K heat treatment. This is 73 percent above the strength after 1273°K heat treatment. Analysis of the monofilament by a scanning electron microscope reveals numerous cracks and fissures in the matrix after each level of heat treatment, which indicates that the addition of coal-tar pitch (20 to 30 percent) did not reduce pyrolysis cracking.

3.6.2 Copyrolysis Studies

In the copyrolysis approach, precursors for high-strength fibers such as polyacrylontrile (PAN) are subjected to an intermediate processing step to set the fiber structure. Then the fibers are pregged with suitable matrix precursor, and both are pyrolyzed together to a temperature selected to develop optimum composite properties. The advantage of this method is that both fiber and matrix shrink together and pyrolysis cracks can be minimized or avoided totally. PAN fiber is particularly amenable to this approach because it forms a ladder polymer, and some of the preferred orientation necessary to develop high strength and modulus develops during spinning of the fiber and the first thermal treatment, which is oxidation. In a cross-linked polymer such as cellulose, preferred orientation can be accomplished only by hot-stretching during the graphitization process. Successful utilization of this concept requires a full understanding of changes which occur in the fiber and matrix during pyrolysis. PAN fiber was chosen for all study work since extensive stretching facilities are not required. Matrix systems analyzed were GW-173, GW-173 modified by PR-275 coal tar pitch, and PAN.

The feasibility of the copyrolysis procedure was demonstrated using PAN fiber and GW-173, a modified phenol-formaldehyde. Linear shrinkage, indicated in Figure 36, shows that the shrinkage parameters of the resin and matrix reach the same value at 1273°K (1000°C) provided the 8-percent shrinkage during oxidation is included. At this temperature total shrinkages of PAN and GW-173 appear to be very close, and during pyrolysis the shrinkage in PAN is slightly smaller than that in GW-173. Evaluation of weight loss (Figure 37) indicates that a plateau has not been reached with PAN after heat treatment to 1273°K (1000°C). X-ray diffraction analysis (Table XXV) of the copyrolyzed monofilaments heat treated to 2273°K (2000°C) indicates that the degree of graphitization of the fibers is the same for the cases of fiber initially heat treated to 973°K (700°C) and 1273°K (1000°C).

The effect of heat treatment on oxidized bare PAN fiber tensile strength was determined and is summarized in Figure 38. The bare fiber was pyrolyzed at a 100°K/hr heating rate in an inert argon atmosphere. Since a much slower pyrolysis heating rate of 13°K/hr is required for the GW-173 matrix, specimens of bare oxidized PAN were also pyrolyzed at the slower heating rate. Bare fiber properties after 1273°K pyrolysis are compared in Table XXVI.

TABLE XXIV. - TENSILE STRENGTH OF THORNEL 75 WITH 20-PERCENT PR-275 IN GW-173 AS A FUNCTION OF HEAT TREATMENT

Maximum Heat Treat Temperature		Fiber/Matrix Volume Ratio	Function (a)	Tensile Force		Tensile Strength			
						Fiber Area		Fiber + Matrix	
°K	°C			n	lb	$n/m^2 \times 10^9$	$psi \times 10^5$	$n/m^2 \times 10^9$	$psi \times 10^5$
450	177	29/71	$\bar{x}$	89.8	20.2	2.86	4.16	0.83	1.21
			σ	3.1	0.7	0.10	0.15	0.03	0.04
1273	1000	40/60	$\bar{x}$	50.7	11.4	1.63	2.36	0.65	0.94
			σ	1.8	0.4	0.06	0.08	0.02	0.03
1673	1400	48/52	$\bar{x}$	42.3	9.5	1.36	1.97	0.66	0.95
			σ	5.8	1.3	0.18	0.26	0.09	0.13
1973	1700	51/49	$\bar{x}$	36.9	8.3	1.19	1.72	0.60	0.87
			σ	16.9	3.8	0.54	0.79	0.28	0.40
2273	2000	59/41	$\bar{x}$	59.5	13.4	1.91	2.77	1.12	1.63
			σ	6.2	1.4	0.21	0.30	0.12	0.17
2773	2500	44/56	$\bar{x}$	61.8	13.9	1.98	2.87	0.87	1.26
			σ	2.7	0.6	0.09	0.13	0.04	0.06
3073	2800	47/53	$\bar{x}$	45.4	10.2	1.46	2.12	0.68	0.99
				13.8	3.1	0.44	0.64	0.21	0.30

(a) $\bar{x}$ = arithmetic average
σ = Standard Deviation

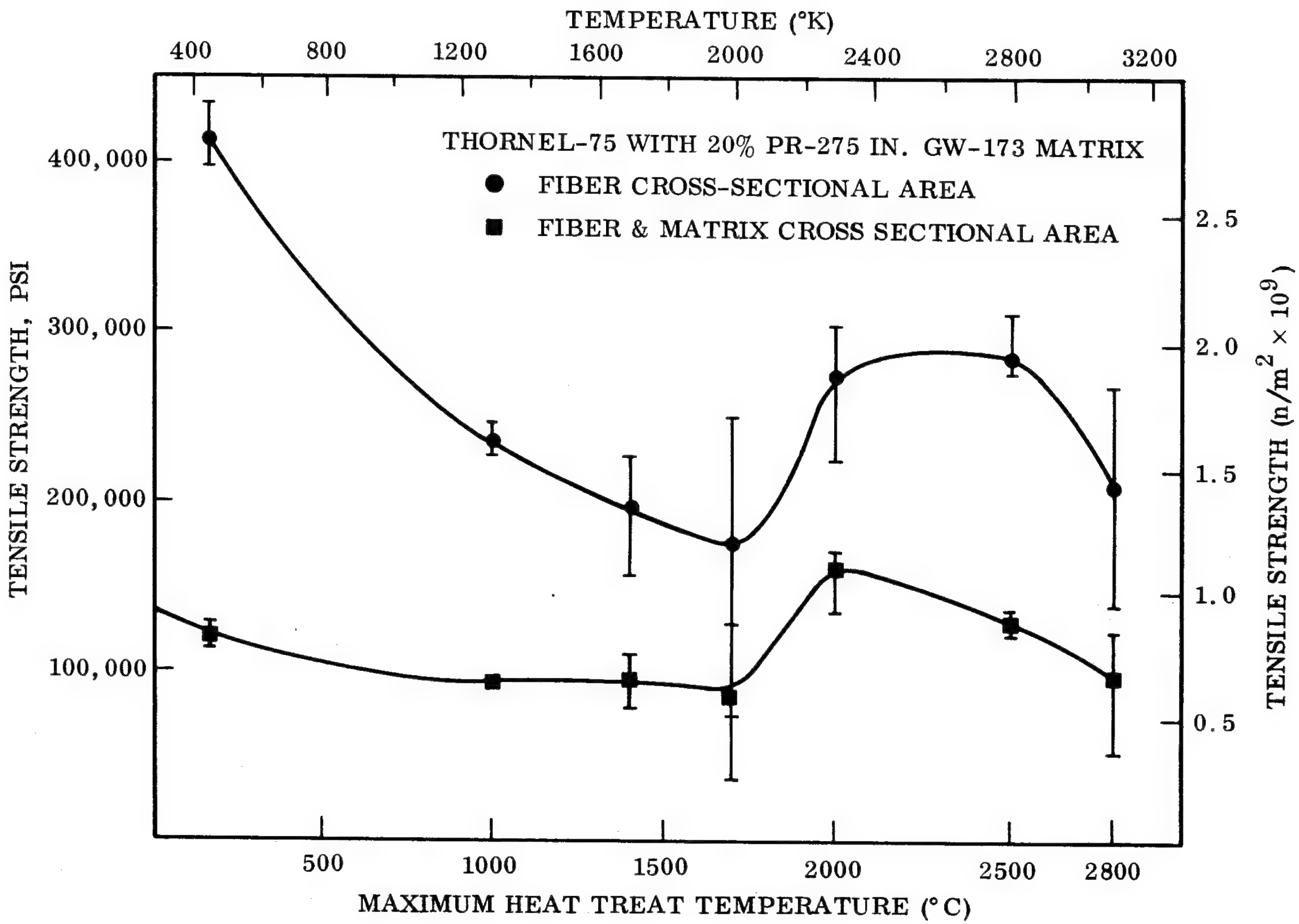

Figure 35. - Tensile Strength of Composite Monofilaments

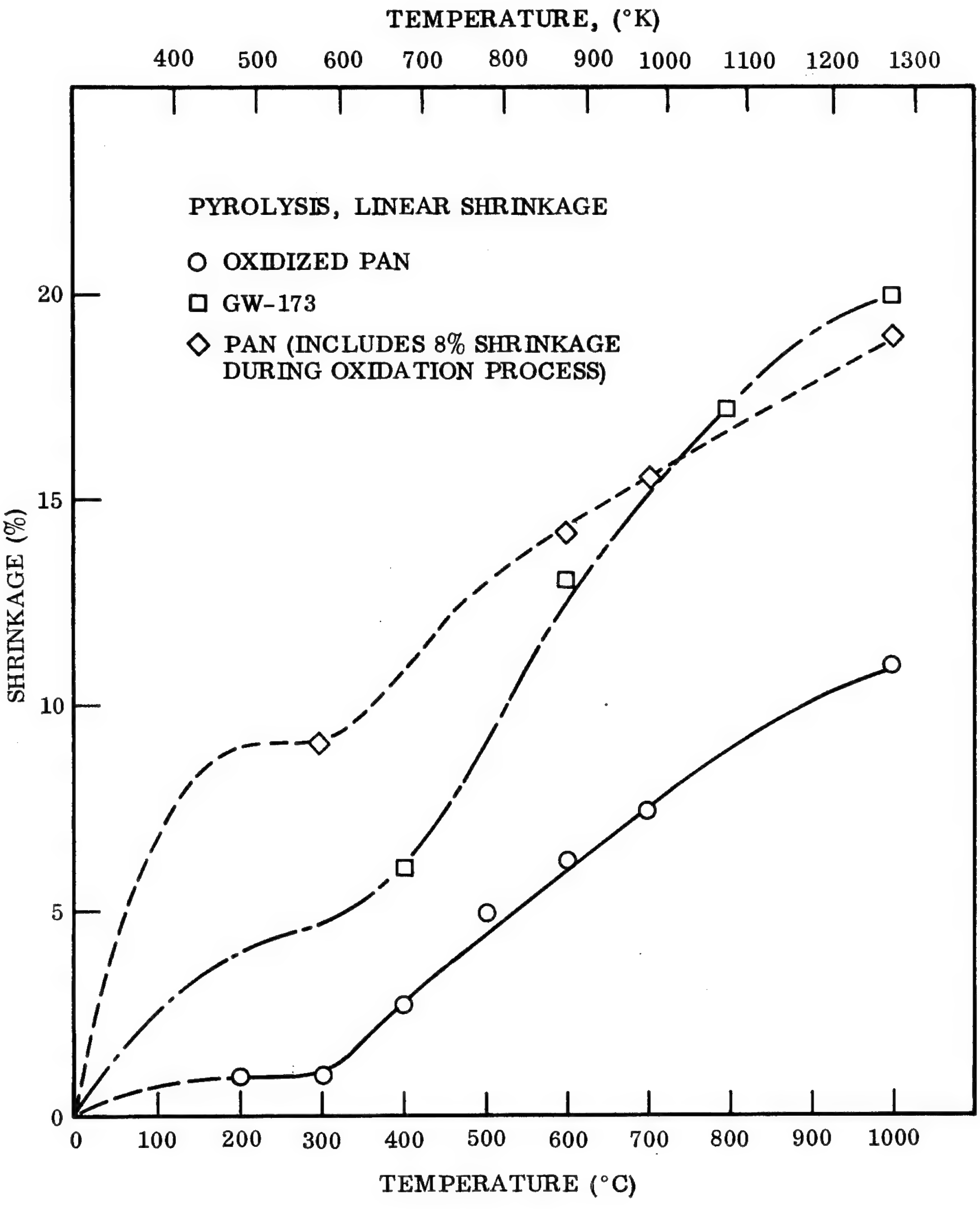

Figure 36. - Shrinkage of PAN and GW-173 When Subjected to Various Temperatures

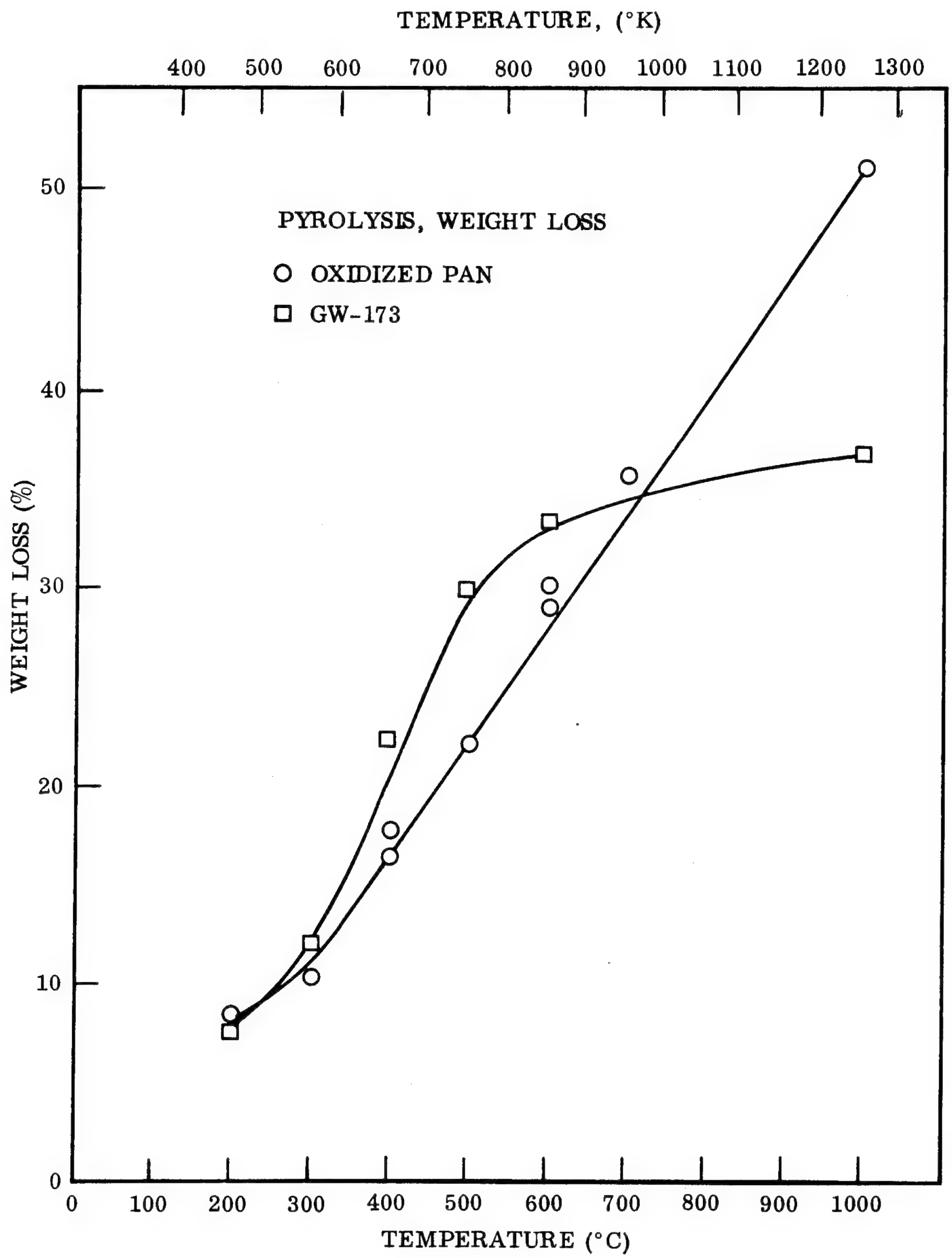

Figure 37. - Weight Loss of PAN and GW-173 When Subjected to Various Temperatures

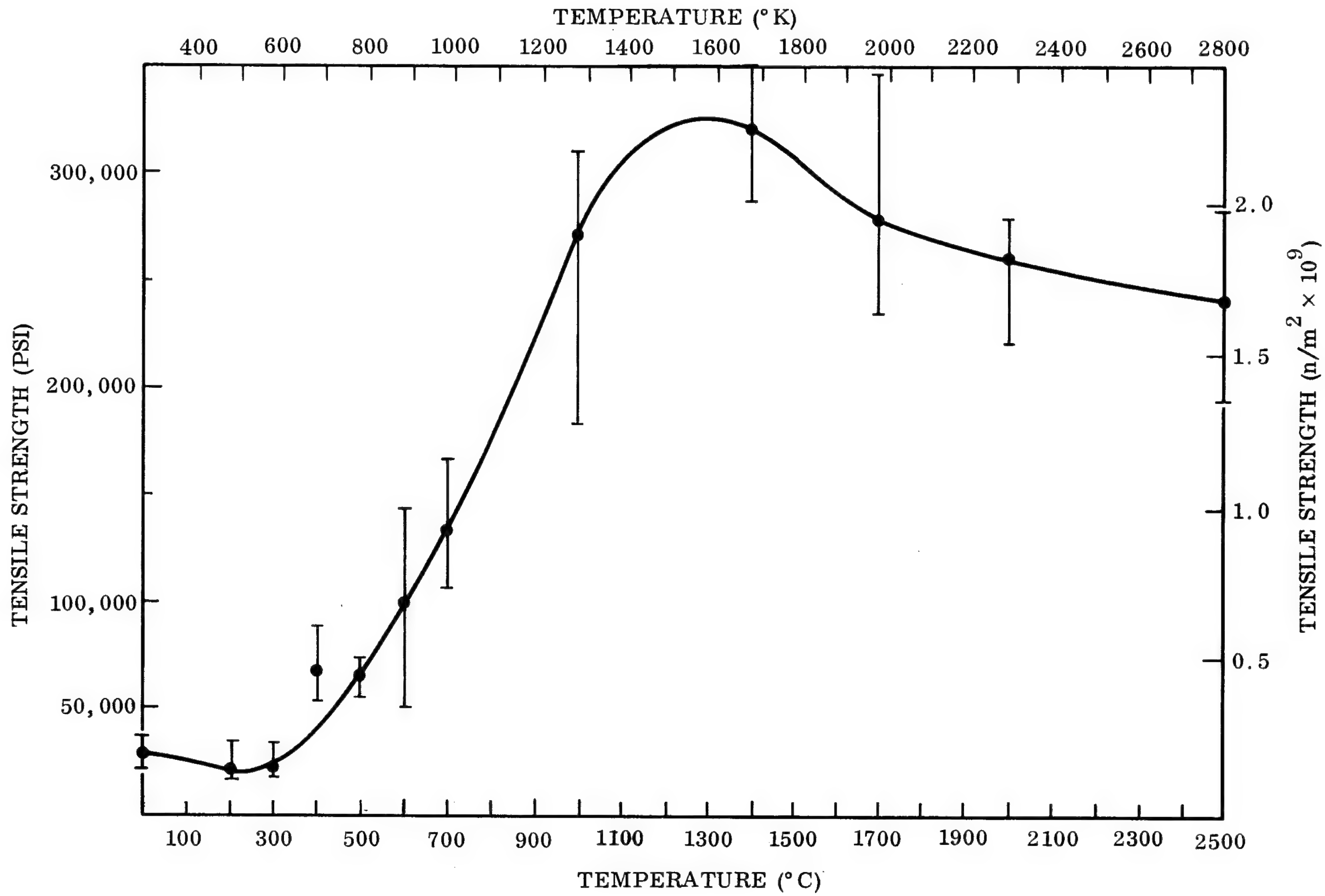

Figure 38. - Tensile Strength of Bare Oxidized PAN Fibers After Heat Treatment

TABLE XXV. - X-RAY DIFFRACTION ANALYSIS OF COPYROLYSIS OF GW-173 WITH OXIDIZED PAN

Sample Designation	Fiber Heat Treatment		Final Heat Treatment of Composite		d Spacing $m \times 10^{10}$	Peak Half-Width	
	°K	°C	°K	°C		rad	deg
CP-310	573	300	1273	1000	3.63	0.123	7.1
CP-710	973	700	1273	1000	3.60	0.117	6.7
CP-1010	1273	1000	1273	1000	3.48	0.075	4.3
CP-320	573	300	2273	2000	3.52	0.072	4.1
CP-720	973	700	2273	2000	3.45	0.059	3.4
CP-1020	1273	1000	2273	2000	3.45	0.061	3.5
Mod I	–	–	1273	1000	3.43	0.035	2.0
Thornel 75	–	–	1273	1000	3.42	0.061	3.5

TABLE XXVI. - BARE FIBER PROPERTIES AFTER PYROLYSIS AT 1273°K

Property	Heating Rate	
	Slow, 13°K/hr	Fast, 100°K/hr
Tensile Modulus, N/m^2(psi)	17.9×10^{10} (26×10^6)	18.6×10^{10} (27×10^6)
Ultimate Tensile, N/m^2(psi)	13.0×10^8 (18.8×10^4)	17.5×10^8 (25.5×10^4)
Strain-to-Failure, %	0.72	1.0

The modulus values are in close agreement with lower ultimate tensile and strain-to-failure values for the slower heating rate. However, these lower values resulted from a longer specimen gage length and incremental load application with sustained loading over a 15-min total test period. The close agreement in modulus indicates that the development of the fiber structure during pyrolysis to 1273°K is insensitive to heating rates from 13°K/hr to 100°K/hr.

In addition, the tensile strength, fiber density, and cross-section areas were measured on oxidized PAN fiber at stages during pyrolysis (Table XXVII).

Copyrolysis results with oxidized PAN and GW-173 are summarized in Table XXVIII. The highest composite strength of 0.51×10^9 N/m^2 (74,000 psi) was developed with fibers pre-heat-treated to 1273°K. The 1273°K pre-heat-treated fiber is a set fiber structure which does not fit in with the copyrolysis approach but does offer a tensile value which should be achievable by the copyrolysis approach. Composite monofilaments made with fibers pre-heat-treated up to 1273°K did exhibit a substantial reduction in matrix voids and fractures (Figures 39 and 40).

TABLE XXVII. - PROPERTIES OF LMSC-PRODUCED CARBON FIBER

PAN Fiber Heat-Treat Condition	Specific Gravity, gm/cc	Cross-Section Area		Weight per Length of Bundle	
		in.^{2}	m^2	gm/in.	kg/m
As Received	1.18	22.0×10^{-4}	14.2×10^{-7}	42.6×10^{-3}	16.8×10^{-2}
Oxidized	1.52	15.9×10^{-4}	10.3×10^{-7}	39.8×10^{-3}	15.7×10^{-2}
473°K	1.56	14.4×10^{-4}	9.3×10^{-7}	36.8×10^{-3}	14.5×10^{-2}
573°K	1.56	13.8×10^{-4}	8.9×10^{-7}	35.3×10^{-3}	13.9×10^{-2}
673°K	1.55	13.3×10^{-4}	8.6×10^{-7}	33.8×10^{-3}	13.3×10^{-2}
773°K	1.61	12.1×10^{-4}	7.8×10^{-7}	31.8×10^{-3}	12.5×10^{-2}
873°K	1.67	10.9×10^{-4}	7.0×10^{-7}	29.9×10^{-3}	11.8×10^{-2}
973°K	1.70	10.0×10^{-4}	6.5×10^{-7}	27.9×10^{-3}	11.0×10^{-2}
1273°K	1.75	7.26×10^{-4}	4.7×10^{-7}	20.8×10^{-3}	8.2×10^{-2}

The high-temperaturefiber pretreatment (1273°K) followed by further heat-treatment to 2273°K was thought to lead to the possibility of formation of pyrolyses cracks, since such fiber pretreatment did not take full advantage of fiber shrinkage characteristics. Consequently, use of low-temperature fiber pretreatment (less than 1273°K) followed by composite heat-treatment no greater than 1273°K was explored further. The highest composite tensile strength that had been obtained using this approach was 1.3×10^8 N/m^2 (19,000 psi), with a fiber pretreatment of 673°K (Row 4, Table XXVIII).

To further investigate pre-heat-treatment in this range, fiber specimens were conditioned to 673°K, 723°K, and 773°K. The standard copyrolysis heating rate was reduced from 13°K/hr to 5°K/hr, and a 24-hr hold was instituted at 753°K. Vacuum was applied up to 753°K and the remainder of the pyrolysis cycle was conducted under an argon inert atmosphere. The extended cycle and application of vacuum induces the polymer disassociation to occur at a lower temperature. At 753°K the GW-173 matrix develops a maximum open-pore structure and is sufficiently soft to relieve stress associated with shrinkage. The composite tensile strengths before and after pyrolysis are summarized in Tables XXIX and XXX. The highest composite tensile strength of 1.05 N/m^2 $\times 10^8$ (15,200 psi) was achieved with 723°K heat-treated fiber. When results are compared with previous results, this approach does not appear to offer any significant advantage.

Additional copyrolysis specimens were prepared with GW-173 and PR-275-modified GW-173 resin, and with 1273°K heat-treated PAN fibers. These specimens were copyrolyzed to 1273°K, then subjected to incremental heat treatments up to 2273°K.

TABLE XXVIII. - TENSILE PROPERTIES OF COPYROLYSIS MONOFILAMENTS
(Oxidized PAN in GW-173)

Fiber Heat-Treatment Condition (°K)	Function[a]	Cured to 450°K: Tensile Strength		Cured to 450°K: Strain-to Failure	Cured to 450°K: Elastic Modulus		Pyrolysed to 1273°K: Tensile Strength, Fiber		Pyrolysed to 1273°K: Tensile Strength, Fiber + Matrix		Heat Treated to 2273°K: Tensile Strength, Fiber		Heat Treated to 2273°K: Tensile Strength, Fiber + Matrix		Heat Treated to 2273°K: Strain-to Failure
		($n/m2 \times 10^8$)	($psi \times 10^4$)	(%)	($n/m^2 \times 10^{10}$)	($psi \times 10^6$)	($n/m^2 \times 10^8$)	($psi \times 10^4$)	($n/m^2 \times 10^8$)	($psi \times 10^4$	($n/m^2 \times 10^8$)	($psi \times 10^4$)	($n/m^2 \times 10^8$)	($psi \times 10^4$)	(%)
Oxidized PAN	$\bar{x}$	1.9	2.7	0.9	2.1	3.1	–	–	–	–	–	–	–	–	–
	σ	0.4	0.6												
473	$\bar{x}$	1.5	2.2	1.0	1.5	2.2	3.1	4.5	1.2	1.7	3.2	4.7	1.2	1.7	0.1
	σ	0.6	0.8				0.2	0.3	0.1	0.1	1.2	1.8	0.5	0.7	–
573	$\bar{x}$	1.5	2.2	–	–	–	1.5	2.2	0.6	0.9	1.8	2.6	0.7	1.0	–
	σ	0.5	0.7				1.2	1.7	0.5	0.7	1.4	2.0	0.6	0.8	–
673	$\bar{x}$	4.5	6.6	1.1	4.1	6.0	3.0	4.4	1.3	1.9	3.6	5.2	1.7	2.4	0.1
		1.0	1.4				1.8	2.6	0.8	1.1	1.0	1.5	0.5	0.7	
773	x	4.5	6.6	1.0	4.6	6.6	1.17	1.7	0.6	0.8	3.2	4.7	1.6	2.3	0.1
	σ	0.5	0.7				0.55	0.8	0.3	0.4	0.7	1.0	0.3	0.5	–
873	$\bar{x}$	6.8	9.9	1.4	5.2	7.5	1.24	1.8	0.6	0.8	1.8	2.6	1.0	1.4	0.24
	σ	2.2	3.2				0.62	0.9	0.3	0.5	0.9	1.3	0.5	0.7	–
973	$\bar{x}$	9.9	14.3	–	–	–	1.8	2.6	1.0	1.4	1.3[b]	1.9[b]	0.7	1.0[b]	–
	σ	1.7	2.4				1.7	2.4	0.9	1.3					
1273	$\bar{x}$	17.5	25.5	1.0	18.6	27.0	3.8	5.5	2.8	4.1	6.9	9.9	5.1	7.4	0.23
	σ	2.9	4.2				1.2	1.7	0.9	1.3	1.5	2.1	1.1	1.6	
2273	$\bar{x}$	11.2	16.3	0.45	24.8	36.0	–	–	–	–	–	–	–	–	–
	σ	1.8	2.6												

a - $\bar{x}$ = arithmetic average
σ = standard deviation

b - single value only

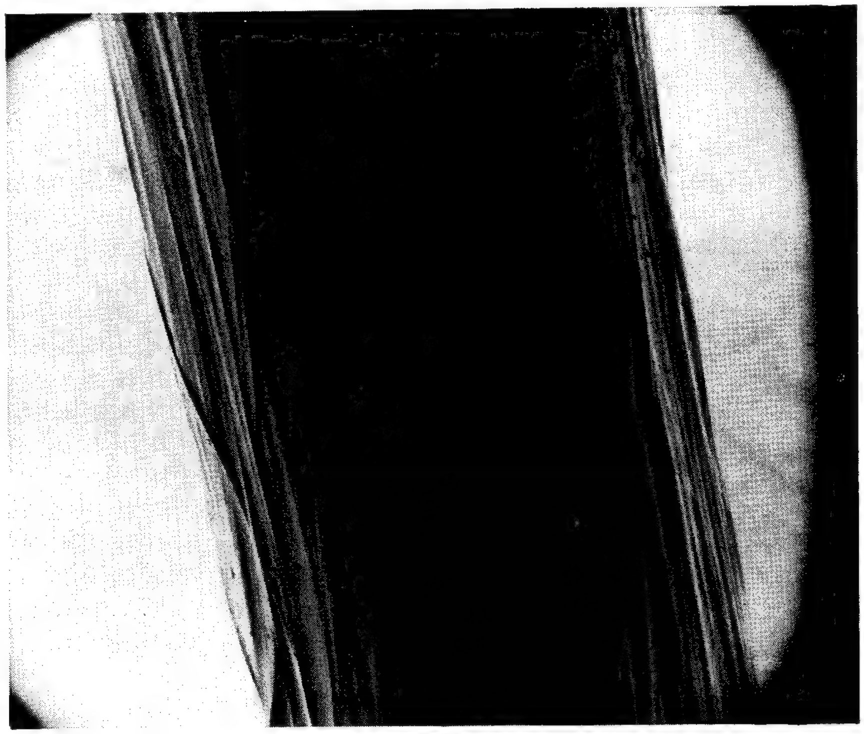

200—1000 45×

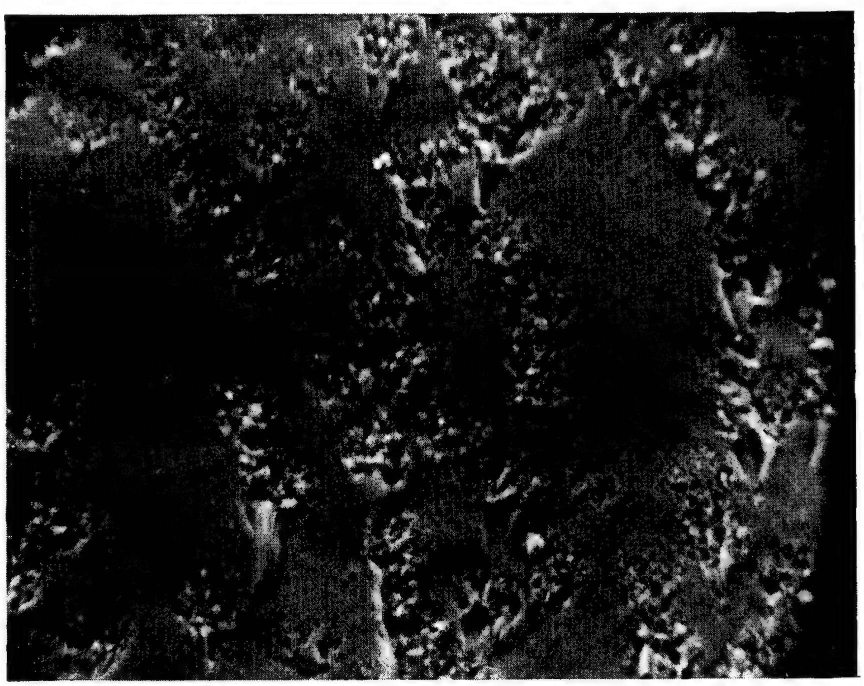

200—1000 1000×

Figure 39. - Monofilament Copyrolyzed to 1273°K. Oxidized PAN fibers previously heat treated to 473°K

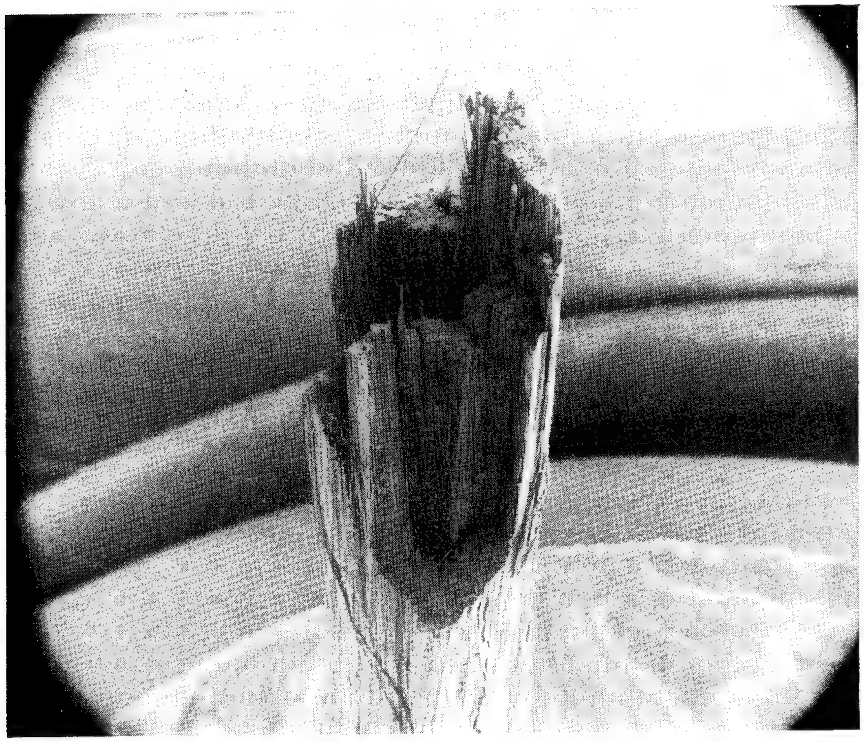

1000—1000 20×

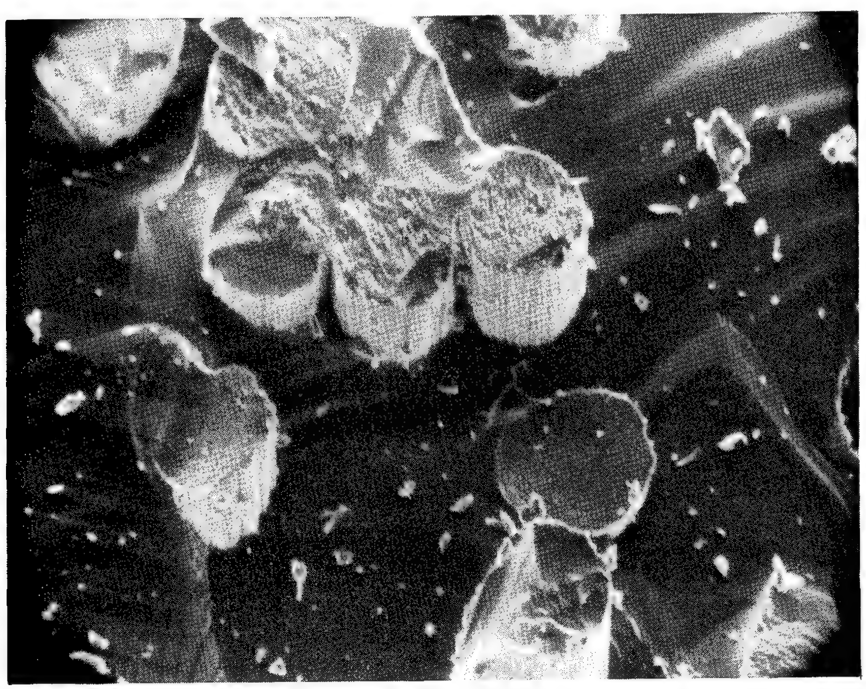

1000—1000 2000×

Figure 40. - Monofilament Copyrolyzed to 1273°K. Oxidized PAN fibers previously heat treated to 1273°K

Tensile strength and volume fractions are summarized in Table XXXI. The highest composite strength (based on total monofilament cross-section area) was 5.17×10^7 N/ m^2 (75,000 psi), obtained with GW-173 matrix and a final heat treatment to 2273°K. This result correlates well with the bare fiber strength (Figure 38), which shows a maximum strength after 1673°K, and represents the best copyrolysis data obtained to date.

The third matrix precursor evaluated for copyrolysis was PAN monomer in solution. A solution of 20 percent (by weight) of PAN in dimethylformaline (DMF) was prepared and used to preg oxidized PAN fiber in the conventional manner. The composite thus produced, PAN/PAN, should be compatible during pyrolysis. For this technique to be effective, the DMF solvent must not attack the fiber during the pregging operation. To analyze this aspect, specimens of oxidized PAN were pregged and air-dried to 450°K, then tensile-tested. These PAN/PAN specimens developed a strength of 0.166×10^9 N/m^2 (24,100 psi), which compares favorably with the bare fiber strength (Figure 38) of 0.186×10^9 N/m^2 (27,000 psi), indicating a minimal solvent effect on the oxidized PAN fiber.

Specimens of oxidized PAN were heat-treated to 673° K and 973° K to preset the fiber structure. These specimens and oxidized PAN were then pregged with a solution of 20-percent PAN in DMF. One-half of each batch was then subjected to pyrolysis with oxidation; the remaining specimens were subjected to pyrolysis without oxidation. This approach provided data to analyze the effect of fiber pre-heat-treatment and matrix oxidation. The data are summarized in Table XXXII. The highest tensile strength was developed with a 973° K fiber pretreatment and with no oxidation during pyrolysis. The effectiveness of matrix oxidation is clearly shown by the matrix volume fraction values for all specimens. The char yield for unoxidized PAN matrix is generally 50 percent less than for the oxidized matrix.

During copyrolyses, the PAN fibers retained their integrity and showed the development of some preferred orientation, a basic structural characteristic associated with high mechanical properties in bare carbon fibers. However, this structure was not developed fully and, as a result, properties were lower than anticipated. Most of the copyrolyzed monofilaments showed, however, the matrix continuity that was expected with the absence of pyrolysis cracks.

The results on fiber tensile strength given in Table XXVIII are lower than estimated. Also they do not show a relationship with the initial fiber heat treatments, which would allow an interpretation of the findings. For the case of the initial fiber heat treatment of 1273°K (Table XXXI), results show reasonably good agreement with predicted strength,indicating the potential of the process. It remains to be explained why fiber strength is not improved by the high-temperature heat treatments.

However, the results of copyrolysis experiments have yielded sufficient evidence to prove the possibility of the process for manufacturing high-strength and modulus carbon-carbon composite monofilaments having matrix continuity. More experimental work is required to investigate the influence of different process variables to achieve the optimum processing conditions.

TABLE XXIX. - TENSILE STRENGTH OF OXIDIZED PAN WITH GW-173 MATRIX RESIN-CURED TO 450°K

Fiber Pre-heat Treatment		Function (a)	Tensile Load		Tensile Stress (Fiber Area)		Fiber/ Matrix Ratio	Tensile Stress (Fiber and Matrix)	
°K	°C		n	lb_f	$n/m^2 \times 10^7$	$psi \times 10^3$		$n/m^2 \times 10^7$	$psi \times 10^3$
673	400	$\bar{x}$	107.2	24.1	12.5	18.1	63/37	7.9	11.4
		σ	36.0	8.1	4.2	6.1	—	2.6	3.8
723	450	$\bar{x}$	170.8	38.4	20.8	30.2	61/39	12.8	18.6
		σ	49.8	11.2	6.1	8.8	—	3.8	5.5
773	500	$\bar{x}$	272.7	61.3	34.9	50.6	62/38	21.7	31.5
		σ	105.0	23.6	13.4	19.4	—	6.9	10.0

(a) $\bar{x}$ = Arithmetic Mean
σ = Standard Deviation

TABLE XXX. - TENSILE STRENGTH OF OXIDIZED PAN WITH GW-173 MATRIX-EXTENDED PYROLYSIS CYCLE TO 1273°K

Fiber Pre-heat Treatment		Function (a)	Tensile Load		Tensile Stress (Fiber Area)		Fiber/ Matrix Ratio	Tensile Stress (Fiber and Matrix)		% of Predicted Strength (b)
°K	°C		n	lb_f	$n/m^2 \times 10^7$	$psi \times 10^3$		$n/m^2 \times 10^7$	$psi \times 10^3$	
673	400	$\bar{x}$	47.6	10.7	10.1	14.7	62/38	6.3	9.1	14
		σ	31.1	7.0	6.6	9.6	—	4.1	6.0	—
723	450	$\bar{x}$	85.4	19.2	18.2	26.4	58/42	10.5	15.2	26
		σ	46.7	10.5	10.0	14.5	—	5.7	8.3	—
773	500	$\bar{x}$	81.0	18.2	17.3	25.1	59/41	10.2	14.8	25
		σ	41.4	9.3	8.9	12.9	—	5.2	7.6	—

(a) $\bar{x}$ Arithmetic Mean
σ Standard Deviation

(b) Based on efficiency factor of 0.40; predicted fiber strength — 70.4×10^7 n/m^2 (102,000 psi)

TABLE XXXI. - TENSILE STRENGTH OF COMPOSITE MONOFILAMENT[(a)]

Monofilament Heat Treatment		Matrix Precursor	Function (b)	Tensile Load		Tensile Stress Fiber Area		Fiber/ Matrix Ratio	Tensile Stress Fiber and Matrix		% of Predicted Strength (c)
°K	°C			n	lb_f	$n/m^2 \times 10^7$	$psi \times 10^3$		$n/m^2 \times 10^7$	$psi \times 10^3$	
1273	1000	GW-173	$\bar{x}$	201.0	45.2	42.9	62.2	54/46	23.3	33.9	61
			σ	33.4	7.5	7.1	10.3	—	3.9	5.6	—
1673	1400	GW-173	$\bar{x}$	352.7	79.3	75.2	109.0	57/43	43.0	62.4	71
			σ	45.4	10.2	9.6	13.9	—	5.6	8.1	—
1973	1700	GW-173	$\bar{x}$	270.4	60.8	57.7	83.7	53/47	30.6	44.4	52
			σ	91.6	20.6	19.5	28.3	—	10.3	15.0	—
2273	2000	GW-173	$\bar{x}$	328.7	73.9	70.3	102.0	59/41	41.4	60.1	55
			σ	82.3	18.5	17.6	25.5	—	10.3	15.0	
1273	1000	20% PR-275/ GW-173	$\bar{x}$	242.5	54.6	51.8	75.2	56/44	26.9	39.1	74
			σ	57.8	13.0	12.3	17.9	—	6.4	9.3	—
1673	1400	20% PR-275/ GW-173	$\bar{x}$	205.9	46.3	43.9	63.7	57/43	25.0	36.2	41
			σ	59.6	13.4	12.8	18.6		7.2	10.4	
1973	1700	20% PR-275/ GW-173	$\bar{x}$	262.0	58.9	56.0	81.2	53/47	29.8	43.2	50
			σ	32.0	7.2	7.3	10.6		3.6	5.2	
2273	2000	20% PR-275/ GW-173	$\bar{x}$	264.7	59.5	56.5	82.0	59/41	34.2	49.6	44
			σ	39.1	8.8	8.3	12.0		5.1	7.4	

a - Oxidized PAN Fiber Heat Treated to 1273°K

b - $\bar{x}$ Arithmetic Mean

σ Standard Deviation

c - The predicted strength calculated as $\sigma_f = E_f \times \epsilon_m$, where E_f is the fiber's elastic modulus (Ref. 21) and $\epsilon_m = 0.41$, the strain-to-failure of the matrix.

TABLE XXXII. - TENSILE STRENGTH OF OXIDIZED PAN WITH PAN MATRIX-PYROLYZED TO 1273°K

Fiber Pre-heat Treatment		Matrix Pyrolysis Cycle	Function (a)	Tensile Load		Tensile Stress Fiber Area		Fiber/Matrix Ratio	Tensile Stress Fiber and Matrix	
°K	°C			n	lb_f	$n/m^2 \times 10^7$	$psi \times 10^3$		$n/m^2 \times 10^7$	$psi \times 10^3$
543	270	Oxidizing to 543°K	$\bar{x}$	65.8	14.8	13.8	20.0	54/46	7.4	10.8
			σ	29.8	6.7	6.3	9.1		3.4	4.9
543	270	Inert Atmosphere	$\bar{x}$	54.7	12.3	11.7	16.9	81/19	10.6	15.4
			σ	11.1	2.5	2.4	3.5		2.2	3.2
673	400	Oxidizing to 511°K	$\bar{x}$	34.2	7.7	7.3	10.6	88.12	6.4	9.3
			σ	10.2	2.3	2.2	3.2		1.9	2.8
673	400	Inert Atmosphere	$\bar{x}$	36.5	8.2	7.8	11.3	94/6	7.3	10.6
			σ	16.5	3.7	3.4	5.0		3.2	4.7
973	700	Oxidizing to 511°K	$\bar{x}$	49.4	11.1	10.6	15.3	81/19	8.5	12.3
			σ	8.0	1.8	1.7	2.5		1.4	2.0
973	700	Inert Atmosphere	$\bar{x}$	90.7	20.4	19.4	28.1	90/10	17.4	25.2
			σ	14.2	3.2	3.0	4.4		2.8	4.0

(a) $\bar{x}$ Arithmetic Mean
σ Standard Deviation

Section 4

GENERAL DISCUSSION

An evaluation of all proposed fiber-matrix monofilament systems has demonstrated that the best mechanical properties are obtained with the combination of Thornel 75 and GW-173 matrix precursors. This carbon monofilament system has shown an average composite tensile strength of 1.34×10^9 N/m^2 (1.95×10^5 psi) or a fiber tensile strength of 1.50×10^9 N/m (2.17×10^5 psi). These results are very close to the original program objective to produce a monofilament with 1.38×10^9 N/m (2.0×10^5 psi) tensile strength. To obtain high mechanical strength it was important to provide optimum fiber wetting and minimum matrix volume fraction contingent with a complete bundle encapsulation. The batch impregnation technique using 70 percent methanol/ 30 percent GW-173 solution met these requirements.

Good fiber-matrix interface and matrix continuity are unfortunately incompatible with the pyrolysis process. Because of the differential shrinkage, occurring during pyrolysis between the fibers and the pyrolyzing resin, cracks have to form to accommodate the changes in matrix volume. At the very last stages of pyrolysis the matrix shrinkage continues and, if cracks do not form, it will remain in a state of internal tension. Both internal stresses built up during processing and pyrolysis cracks decrease the strain-to-failure of the carbon matrix, consequently diminishing the possibilities of obtaining all the potential reinforcement offered by the stiff and strong carbon fibers. This is the case in reinforced brittle materials since the strength of the composite is dependent on the lower strain-to-failure of the matrix. Good interfacial bonding means that upon deformation the condition of equal strains prevails. Figure 41 shows schematically the stress-strain behavior of several fibers and the glass-like carbon derived from GW-173. The vertical dotted line represents the strain at which the pyrolyzed GW-173 fails. Its intersection with the deformation curves of the fibers indicates (on the equal strains concept) the maximum obtainable fiber strength in a composite with a carbonized GW-173 matrix. Matrix flaws, like cracks or internal stresses, reduce the matrix strain-to-failure and, therefore, the dotted line is displaced toward the left. This results in a lower fiber stress contribution and consequently a lower strength composite. An average of 0.41 percent strain-to-failure was measured for glass-like GW-173 carbon matrix (Table IV in Section 3). If the composite fails at this strain it becomes evident that full utilization of the fiber strength cannot be achieved (Fig. 41). Thornel 75 and Thornel 400 are the extreme cases of fiber-strength utilization – in the first case 83 percent and in the second case 30 percent of the ultimate strength of the fibers.

Table XXXIII summarizes the experimental results of several composites made with the indicated fibers in GW-173. Predicted values of each composite with the carbonized GW-173 are also included; these values were calculated in the following manner. An

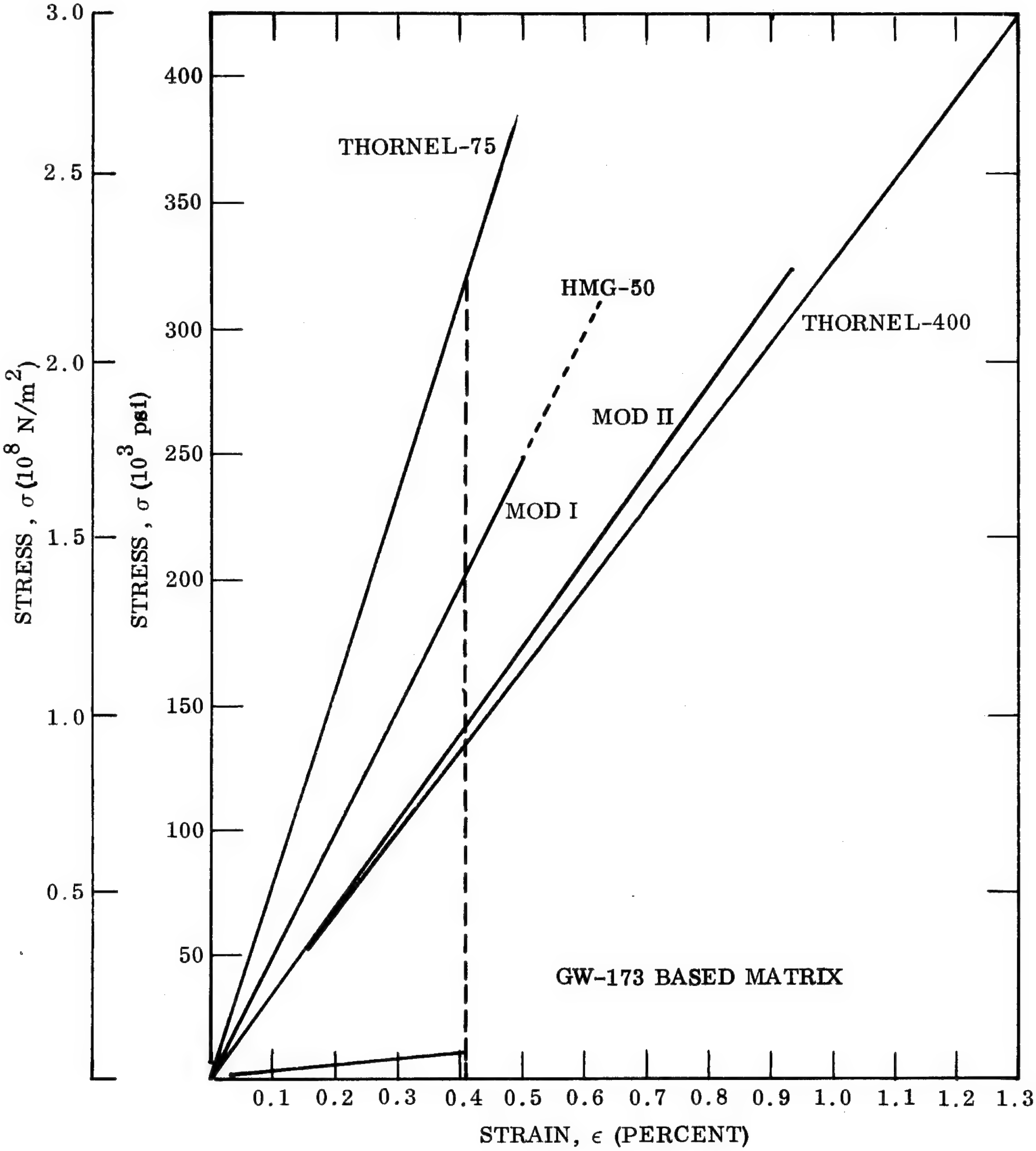

Figure 41. - Stress-Strain Relationship of Candidate Fibers and Matrix

TABLE XXXIII. - UTILIZATION OF FIBER TENSILE PROPERTIES[a]

Fiber	Function[b]	Tensile Stress of Cured Fiber (c)		Tensile Stress of Pyrolyzed Fiber (c)		ϵ_f, %	Efficiency Factor (d) ϵ_m/ϵ_f	Predicted Tensile Strength(e)		% of Predicted Value
		$N/m^2 \times 10^9$	psi $\times 10^5$	$N/m^2 \times 10^9$	psi $\times 10^5$			$N/m^2 \times 10^9$	psi $\times 10^5$	
Thornel 75	$\bar{x}$	2.48	3.60	1.60	2.33	0.50	0.82	2.03	2.95	79
(PVA)	Max.	2.64	3.62	1.78	2.58			2.16	2.97	87
Thornel 75	$\bar{x}$	2.90	4.21	1.50	2.17	0.50	0.82	2.38	3.45	63
(UC-307)	Max.	3.10	4.50	1.65	2.39			2.54	3.69	67
HMG-50	$\bar{x}$	1.94	2.82	0.85	1.24	0.62	0.66	1.28	1.86	66
	Max.	2.02	2.93	0.95	1.39			1.33	1.93	72
Mod I	$\bar{x}$	1.12	1.62	0.38	0.55	0.50	0.82	0.92	1.33	41
	Max.	1.57	2.06	0.43	0.63			1.29	1.69	37
Mod II	$\bar{x}$	1.87	2.72	1.00	1.46	0.93	0.44	0.82	1.20	122
	Max.	2.12	3.10	1.08	1.58			0.93	1.36	116
FTIC-1000	$\bar{x}$	0.73	1.08	0.40	0.59	0.66	0.62	0.45	0.67	88
	Max.	1.01	1.50	0.58	0.83			0.63	0.93	89
Celanese GY-70	$\bar{x}$	1.40	2.04	0.61	0.89	0.44	0.93	1.30	1.90	47
	Max.	1.60	2.33	0.83	1.09			1.49	2.17	50
Thornel 400	$\bar{x}$	2.76	4.01	0.36	0.53	1.30	0.32	0.88	1.26	42
	Max.	2.96	4.33	0.57	0.84			0.95	1.36	62

(a) Matrix is GW-173 precursor resin.

(b) $\overline{X}$ = avg , max = maximum value.

(c) Corrected for fiber cross sectional area only.

(d) $E = \epsilon_m/\epsilon_f$ where ϵ_m = matrix tensile strain = 0.41 , ϵ_f = Nominal fiber tensile strain.

(e) $\sigma_T = \sigma_f \times$ where σ_f = fiber tensile stress measured in as-cured monofilament.

efficiency factor E was computed from the ratio of the matrix, $\varepsilon_m = 0.41$, to the fiber strain-to-failure, ϵ_f. The predicted tensile strength σ_T is given by the product of σ_f, the fiber strength (taken as the as-cured monofilament strength), and the factor E. A percent of predicted value is calculated by dividing the measured monofilament strength by the predicted strength. These percentages indicate the departure from the calculated ideal mechanical strength behavior and are reasonable for all systems. Table XXXIII shows, as expected, that the best results are obtained with high modulus (which corresponds to low strain-to-failure) fibers.

The presence of cracks at discrete intervals in the carbon matrix exposed the reinforcing fibers which, unfortunately, precludes the use of these monofilaments as reinforcement for metals or alloys. In the crack areas the bare fibers will be exposed to the metallic matrix, thereby invalidating the benefits of the large diameter monofilament. Two procedures have been suggested to improve the properties and characteristics of the composite monofilaments — matrix improvement studies to increase the matrix strain-to-failure and copyrolysis to eliminate pyrolysis cracking.

As indicated previously, matrix strain-to-failure is a key factor in obtaining optimum composite properties. It has been found that to obtain the optimum mechanical properties in carbon-carbon composites, it is necessary that the matrix strain-to-failure matches that of the fiber. Otherwise, failure occurs at the strain at which the fiber or matrix reaches its maximum allowable stress (Fig. 41). If the strain-to-failure of the matrix is less than that of the reinforcing fiber, then the potential strengthening effect of fibers is not realized.

In the current program, evaluation was performed only with matrix precursors that are readily available and that adapt readily to a prepreg process. It has been found that matrices generated from phenolics, furfuryl alcohol, and related thermosetting resins form, upon pyrolysis, glass-like carbon that has a relatively low strain-to-failure. Consequently, it is necessary to develop advanced matrices that have a higher strain-to-failure. Carbonaceous materials that have exhibited a higher strain-to-failure are those generated from ladder polymers such as polyacrylonitrile and soft pitches that can be graphitized.

Potential matrix precursors can be placed into five categories: (1) cross-linking polymers such as phenol-formaldehyde, (2) mixture of two polymers with similar decomposition temperatures resulting in a high degree of cross-linkage during post-cure, (3) polymers that are linear (such as p-polyphenylene) or form ladder chains under specialized processing condition (such as polyacrylonitrile), and (4) soft-pitches.

Potential candidates are listed in Table XXXIV. To obtain baseline information, phenol-formaldehyde should be varied to obtain various degrees of cross-linking.

Linear or ladder polymers are of interest because they can be graphitized and have, in the case of polyacrylonitriles, been used to develop carbon fibers with more than

TABLE XXXIV. - POTENTIAL MATRIX PRECURSORS

Matrix Type	Type	Comment
Phenol-formaldehyde	–	Baseline information
Polyphenylene	Monsanto 1711	Char yield = 70 – 75 w/o graphitizing Linear polymer  (Ref. 23)
Polyacrylonitrile	Dupont experimental	Forms anisotropic product with a high strain-to-failure Forms ladder polymer upon oxidative degradation (Ref. 22) 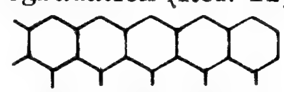 CN CN CN CN CN
Cyclized rubber	Reichold Goodyear	Forms ladder polymer 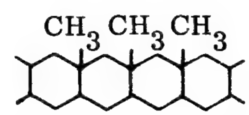
Resin-pitch systems	3M	Cross-linking pitch forms high char yield (75%) graphitizing pitch with phenolic resins and furfuryl alcohol. C-C composites have 85 – 120% of original strength values (Ref. 20)
Isotruxene	Oak Ridge Natl. Lab, or AFML	Air-cured isotruxene – 83% char yield graphitizing, d = 3.35 (Ref. 26)
Ashland petroleum pitch No. 240	Asbury graphite	Forms mesophase graphite (Ref. 27)

1 percent strain-to-failure (Ref. 22). Polyphenylene is a high char former that also can be graphitized (Ref. 23).

Resin pitch systems are suggested because they can be graphitized readily, and they show potential for developing a high strain-to-failure. The 3M resin-pitch system is representative of the utilization of two polymers to achieve a high degree of cross-linking with a consequent char yield greater than that predicted from the char yields of the individual components (Ref. 20).

It is desirable to make a systematic evaluation of the effect of varying the molecular weight and degree of cross-linking on matrix and composite properties. One way of studying this effect is to use solvent extraction techniques such as those described by McNeil and Wood (Refs. 24, 25) in which successively more complex molecular weights are extracted as follows:

- Crystalloid fraction, soluble in petroleum ether or hexane
  MW = 200 to 395
- Resinoid fraction, insoluble in petroleum ether but soluble in benzene
  MW = 400 to 600
- C_2 fraction, insoluble in benzene, but soluble in quinoline
  MW = 1000 to 1500
- C_1 fraction, insoluble in quinoline
  MW = 1800 to 2600

The properties of matrices generated from increasingly complex pitches may thus be determined, and such fractions can be used in prepregging studies to relate precursor molecular weight to composite properties.

Isutruxene is a synthetic pitch derived from indene (Ref. 26), the properties of which can be varied by air oxidation. A highly graphitic structure and very high char yield can be obtained in this manner. Mesophase forming pitches in which spherical crystallites are formed during a molten phase (Ref. 27) should also be studied to relate such structure to that of the final product.

As has been indicated briefly, a key problem in producing high-strength in carbon composite monofilaments is the presence of pyrolysis cracks that reduce composite strengths. A conventional approach to minimizing such cracks is the use of high char formers and redensification techniques such as reimpregnation. High-char resins are ordinarily difficult to process as their viscosity is too great. Reimpregnation has been found not to yield improved properties because the additional resin coats the outside of the fiber bundle and does not fill the pyrolysis cracks completely.

In the copyrolysis approach, precursors for high-strength fibers such as (PAN) polyacrylonitrile are subjected to an intermediate processing step (to set the fiber structure) and pregged with suitable matrix precursor, and then both are pyrolyzed together to a heat-treatment temperature selected to develop optimum composite properties.

The advantage of this method is that both fiber and matrix shrink together so that pyrolysis cracks can be minimized or avoided totally. Polyacrylonitrile is particularly amenable to this approach because it forms a ladder polymer, and the preferred orientation necessary for high strength, and modulus develops during spinning of the fiber and the first thermal treatment, which results in oxidation. In a cross-linked polymer such as cellulose, preferred orientation can only be accomplished by hot-stretching during the graphitization process.

The feasibility of the copyrolysis procedure has been demonstrated using polyacrylonitrile* and GW-173, a modified phenol-formaldehyde. The linear shrinkage that occurs shows that the shrinkage parameters of the resin and matrix reach the same value at 1273°K provided the 8 percent shrinkage during oxidation is included. At this temperature, total shrinkages of PAN and GW-173 appear to be very close, and during pyrolysis the shrinkage in the PAN favorably exceeds that of the GW-173. Evaluation of weight loss indicates that a plateau has not been reached with the PAN after heat treatment to 1273°K, and x-ray diffraction analysis of copyrolyzed monofilaments heat treated to 2273°K show that PAN fibers initially treated to 973° and 1273°K develop the same degree of graphitization.

Mechanical testing of copyrolysis monofilaments show definitive reinforcing action. However, further work is required to enhance the formation of the fiber structure, which will result in much higher tensile strength. Additional precursor fibers and matrices should be studied to optimize this approach.

---

*Courtelle wet-spun polymer.

Section 5

CONCLUSIONS

Current studies have shown that large diameter carbon-composite monofilaments can be produced by the technique of pregging high-strength carbon yarn or tows with organic resins and then pyrolyzing to form a carbon-carbon composite monofilament. The best results obtained to date have been with Thornel 75 in GW-173, a modified phenol-formaldehyde. Maximum properties obtained have been a tensile stress of 1.34×10^9 N/m^2 (1.95×10^5 psi), a tensile strain of 0.28 percent, and a modulus of elasticity of 45×10^{10} N/m^2 (65×10^6 psi) in a composite containing 87 percent fiber.

It has been found that there are two factors that limit the properties of the composite monofilament. The first is development of pyrolysis cracking due to differential shrinkage, which also puts the remaining matrix in tension and seriously reduces the matrix strain-to-failure and, consequently, the composite tensile strength. Pyrolysis cracking would also be detrimental if such monofilaments were to be used in metal matrix composites because they expose fiber surfaces to the metal. The second factor is the inherently low strain-to-failure of matrices produced from resins such as phenol-formaldehyde, furfuryl alcohol, and most resins readily available and processable as prepregging resins. These factors suggest two areas for additional research and development – i.e., copyrolysis to eliminate pyrolysis cracking and matrix improvement studies to improve strain-to-failure.

Preliminary studies have demonstrated the feasibility of composite processing by copyrolysis. In this technique both fibers and matrix are pyrolyzed simultaneously. This fabrication method has produced composites with excellent fiber-matrix interface and no pyrolysis cracks. It is recommended that additional work be continued in these areas.

REFERENCES

1. Lockheed Missiles & Space Company, High Temperature Reactions in the Solid State, Report 6-78-68-10, Palo Alto, Calif., Mar 1968

2. -----, High Temperature Reactions in the Solid State, Report N-47-68-1, Palo Alto, Calif., Jul 1968

3. Philco Ford Corp., Aeroneutronics Division, Large Diameter Graphite/Carbon Composite Filament Development, by N. E. Quackenbush, NASA CR-72769, Newport Beach, Calif., 24 Jul 1970

4. E. Fitzer and W. Shafer, "The Effect of Crosslinking on the Formation of Glass-Like Carbons From Thermosetting Resins," Carbon, Vol. 8, 1970, pp. 353–364

5. K. Ouchi, "Infra-Red Study of Structural Changes During the Pyrolysis of Phenol-Formaldehyde Resins," Carbon, Vol. 4, 1966, pp. 59–66

6. W. Bradshaw, P. C. Pinoli, and R. Lindberg, "The Mechanical Behavior of LMSC Glass-Like Carbon During Its Formation and Heat-Treatment," paper presented at AIME meeting, Cleveland, Ohio, Oct 1970

7. Lockheed Missiles & Space Company, LMSC Glass-Like Carbon, Report 6-78-69-33, Palo Alto, Calif., Aug 1969

8. A. S. Thomas, Inc., Processing Parameters of Pyrolyzed Reinforced Plastics, Phase I, Final Report, M-67-3, prepared for LMSC under Contract N000 3066-C-0186, Cupertino, Calif., Jun 1968

9. Philco-Ford Corp., Aeroneutronics Division, Investigation of Graphite Filament Reinforced Epoxies, Final Report, by R. C. Novak, U-4379, Navy Contract N00 19-67-C-0354, Newport Beach, Calif., May 1968

10. Defense Metals Information Center, A Review of Glass-Like Carbons, by S. Yamada, AD 668463, Columbus, Ohio, Apr 1968

11. W. G. Bradshaw, "Mechanical and Thermal Properties of Glass-Like Carbons," Proceedings of the Continuum Aspects of Graphite Design, Gatlinburg, Tenn., 9–12 Nov 1970, sponsored by the Atomic Energy Commission

12. W. Bradshaw, "Mechanical Behavior of Carbon-Carbon Composites as a Function of Degree of Graphitization," paper presented at AIME meeting, Cleveland, Ohio, Oct 1970

13. W. G. Bradshaw, "LMSC Carbon/Carbon Research and Development," paper presented at 17th Refractory Composites Working Group Meeting, NASA-Langley, Langley, Va., 16–18 Jun 1970

14. Lockheed-Georgia Company, Surface Treatment, by A. Cunningham, D-02-2333

15. J. W. Johnson, "Factors Affecting the Tensile Strength of Carbon-Graphite Fibers," Polymer Preprints, Vol. 9, No. 2, papers presented at American Chemical Society meeting, Atlantic City, N. J., Sep 1968, p. 1316

16. Union Carbide Corporation in Association With Case Institute of Technology, Integrated Research in Carbon Composite Materials, Part 1, AFML-TR-66-310, Wright-Patterson AFB, Ohio, Oct 1966

17. U.S. Air Force, Investigation and Chemical Nature of the Surface of Recently Developed Fibers, by M. A. DeCrescente, D. A. Scola, and C. S. Brooks, AFML-TR-67-218, Part 1

18. H. M. Ezekiel, "The Direct Graphitization of Polymer Yarns," Abstracts, Vol. 31, No. 1, papers presented at 161st Meeting of American Chemical Society, Div. of Organic Coatings and Plastics Chemistry, Los Angeles, Calif., March – April, 1971, pp. 415–425

19. McDonnell Douglas Astronautics Co., Investigation of the Properties of Carbon-Carbon Composites and Their Relationship to Non-Destructive Test Measurements, Part II, by J. S. Evangelides, R. A. Meyer, and J. E. Zimmer, AFML-TR-70-213, Santa Monica, Calif., Aug 1971

20 H. A. Mackay and R. L. Courtney, "Resin-Pitch Systems for Carbon-Char Composites," Modern Plastics, Aug 1968, pp. 147–150

21. R. Moreton, W. Watt, and W. Johnson, "Carbon Fibres of High Strength and High Breaking Strain," Nature, Feb 1967, p. 690

22. O. Vohler et al., "New Forms of Carbon," Angew.Chem. Internat. Edit., Vol. 7, No. 6, 1970, pp. 414–425

23. D. O. Newling and E. J. Walker, "High-Performance 'Graphitized' Carbon-Carbon Fibers," paper presented at International Conference on Carbon Fibers, Their Composites and Applications, London, 1971

24. D. McNeil and L. J. Wood, "The Use of Coal Tar Pitch as an Electrode Binder," Industrial Carbon and Graphite, Society of Chemical Industry, London, 1958, pp. 162–172 (papers read at the conference held in London, 24 to 26 Sep 1957)

25. Enclyclopedia of Polymer Science and Technology, Vol. 2, ed. H. F. Mark, N. B. Gaylord, and N. M. Bikales, Interscience, 1965, p. 404

26. Oak Ridge, Y-12 Plant, Properties of Carbon Derived From Indene Compounds, by W. E Smith et al., Y-1790, Oak Ridge, Tenn., 15 Sep 1971

27. D. Rester, "NOL Synthetic Precursor Programs," paper presented at REVMAT Review Meeting, White Oaks, Md., 9 to 10 May 1972

1. Report No.	2. Government Accession No.	3. Recipient's Catalog No.
CR-120973		

4. Title and Subtitle	5. Report Date
DEVELOPMENT OF MANUFACTURING PROCESS FOR LARGE-DIAMETER COMPOSITE MONOFILAMENTS BY PYROLYSIS OF RESIN-IMPREGNATED CARBON-FIBER BUNDLES	1 October 1972
	6. Performing Organization Code
7. Author(s)	8. Performing Organization Report No.
W. G. Bradshaw, P. C. Pinoli, and A. E. Vidoz	LMSC-D309742
	10. Work Unit No.
9. Performing Organization Name and Address	
Lockheed Palo Alto Research Laboratory 3251 Hanover Street Palo Alto, California 94304	11. Contract or Grant No. NAS 3-15552
	13. Type of Report and Period Covered
12. Sponsoring Agency Name and Address	Contractor Report – Final
National Aeronautics and Space Administration Washington, D.C. 20546	14. Sponsoring Agency Code

15. Supplementary Notes

Project Manager, David L. McDanels, Materials & Structures Division, NASA Lewis Research Center, Cleveland, Ohio

16. Abstract

Large-diameter carbon-carbon-composite monofilaments were produced from the pyrolysis of organic precursor resins reinforced with high-strength carbon fibers. The mechanical properties were measured before and after pyrolysis and the results were correlated with the properties of the constituents. The composite resulting from the combination of Thornel 75 and GW-173 resin precursor produced the highest tensile strength. The importance of matching strain-to-failure of fibers and matrix to obtain all the potential reinforcement of fibers is discussed. Methods are described to reduce, within the carbonaceous matrix, pyrolysis flaws which tend to reduce the composite strength. Preliminary studies are described which demonstrated the feasibility of fiber-matrix copyrolysis to alleviate matrix cracking and provide an improved matrix-fiber interfacial bonding.

17. Key Words (Suggested by Author(s))	18. Distribution Statement
Carbon, Monofilaments, Composites, Fibers, Metal Matrix, Glass-Like Carbon	Unclassified - unlimited

19. Security Classif. (of this report)	20. Security Classif. (of this page)	21. No. of Pages	22. Price*
Unclassified	Unclassified		$3.00

* For sale by the National Technical Information Service, Springfield, Virginia 22151

NASA-C-168 (Rev. 6-71)